

## Meeting the Cool Neighbors. IX. The Luminosity Function of M7–L8 Ultracool Dwarfs in the Field

Kelle L. Cruz<sup>1,2,3,4</sup>, I. Neill Reid<sup>3,4,5</sup>, J. Davy Kirkpatrick<sup>6</sup>, Adam J. Burgasser<sup>7</sup>, James Liebert<sup>3,8</sup>, Adam R. Solomon<sup>1,9,10</sup>, Sarah J. Schmidt<sup>1,11,12</sup>, Peter R. Allen<sup>3,13</sup>, Suzanne L. Hawley<sup>12</sup>, and Kevin R. Covey<sup>12</sup>

### ABSTRACT

---

<sup>1</sup>Department of Astrophysics, American Museum of Natural History, Central Park West at 79th Street, New York, NY 10024;

kelle@amnh.org

<sup>2</sup>NSF Astronomy and Astrophysics Postdoctoral Fellow

<sup>3</sup>Visiting Astronomer, Kitt Peak National Observatory, National Optical Astronomy Observatory, which is operated by the Association of Universities for Research in Astronomy, Inc. (AURA) under cooperative agreement with the National Science Foundation.

<sup>4</sup>Visiting Astronomer, Cerro Tololo Inter-American Observatory, National Optical Astronomy Observatories, which are operated by the Association of Universities for Research in Astronomy, under contract with the National Science Foundation.

<sup>5</sup>Space Telescope Science Institute, 3700 San Martin Drive, Baltimore, MD 21218

<sup>6</sup>Infrared Processing and Analysis Center, MS 100-22, California Institute of Technology, Pasadena, CA 91125

<sup>7</sup>Massachusetts Institute of Technology, Kavli Institute for Astrophysics and Space Research, Building 37, Room 664B, 77 Massachusetts Avenue, Cambridge, MA 02139

<sup>8</sup>Department of Astronomy and Steward Observatory, University of Arizona, Tucson, AZ 85721

<sup>9</sup>John F. Kennedy High School, 3000 Bellmore Avenue, Bellmore, NY 11710

<sup>10</sup>Department of Astronomy, Yale University, P.O. Box 208101, New Haven, CT 06520

<sup>11</sup>Department of Physics and Astronomy, Barnard College, Columbia University, 3009 Broadway, New York, NY 10027

<sup>12</sup>Department of Astronomy, University of Washington, Box 351580, Seattle, WA 98195

<sup>13</sup>Department of Astronomy and Astrophysics, Pennsylvania State University, 525 Davey Lab, University Park, PA 16802

We present a 20-pc, volume-limited sample of M7–L8 dwarfs created through spectroscopic follow-up of sources selected from the Two Micron All Sky Survey (2MASS) Second Incremental Release Point Source Catalog. In this paper, we present optical spectroscopy of 198 candidate nearby ultracool dwarfs, including 12 late-M and L dwarfs likely to be within 20 pc of the Sun and 94 more distant late-type dwarfs. We have also identified five ultracool dwarfs with spectral signatures of low-gravity. Combining these data with previous results, we define a sample of 99 ultracool dwarfs in 91 systems within 20 pc. These are used to estimate the  $J$ - and  $K$ -band luminosity functions for dwarfs with optical spectral types between M7 and L8 ( $10.5 < M_J < 15$ ,  $9.5 < M_{K_S} < 13$ ). We find a space density of  $4.9 \times 10^{-3} \text{ pc}^{-3}$  for late-M dwarfs (M7–M9.5) and a lower limit of  $3.8 \times 10^{-3} \text{ pc}^{-3}$  for L dwarfs.

*Subject headings:* Galaxy: stellar content — solar neighborhood — stars: late-type stars: low-mass, brown dwarfs — stars: luminosity function, mass function

## 1. Introduction

Over the last several years, we have been using the Two Micron All Sky Survey (2MASS, Skrutskie et al. 2006) to carry out a census of late-type dwarfs in the vicinity of the Sun. In particular, we have undertaken the first comprehensive survey of ultracool M and L dwarfs in the immediate Solar Neighborhood (Cruz et al. 2003, hereafter Paper V). This population of cool, low-luminosity dwarfs includes both very low-mass stars and substellar-mass brown dwarfs (Chabrier & Baraffe 2000; Burrows et al. 2001).

One of the primary aims of our program is the derivation of the luminosity function (the number of objects as a function of absolute magnitude) across the hydrogen-burning limit. The local field luminosity function has been well measured for objects as cool as late-M dwarfs (Reid et al. 2002a), but studies probing to fainter magnitudes have been limited by poor statistics and low sensitivity (Reid et al. 1999; Kirkpatrick et al. 1999, 2000; Gizis et al. 2000; Burgasser 2002). Pushing to lower luminosities and larger volumes is crucial to measuring the contribution of brown dwarfs to the local space density.

The initial results from our program to create a statistically well-defined sample of nearby ultracool dwarfs were presented in Paper V. In that paper, we described how we constructed a sample of 630 candidate nearby late-M and L dwarfs from the 2MASS Second Incremental Data Release Point Source Catalog, designated the “2MU2” sample. We also presented follow-up spectroscopic observations of a subset of the ultracool candidates. In

this paper, we present the remainder of the far-red optical spectroscopic observations and combine these results with previous observations to construct the  $J$ - and  $K_S$ -band luminosity functions. These data include many newly discovered late-type dwarfs, including twelve additions to the core “20-pc 2MU2” sample of M7–L8 dwarfs estimated to be within 20 parsecs and used to measure the luminosity function.

This is the ninth paper in the series and follows directly from Paper V. The first three papers and Papers VII and VIII (Reid & Cruz 2002; Reid et al. 2002b; Cruz & Reid 2002; Reid et al. 2003a, 2004) concentrate on proper-motion selected K and M dwarfs. Paper IV (Reid et al. 2003b) describes the discovery of 2MASS J18353790+3259545, an M8.5 dwarf within 6 pc of the Sun (which is included in the present analysis). Results from a search for ultracool dwarfs lying close to the Galactic Plane are presented in Reid (2003, Paper VI).

Here, we build on Paper V and present the remainder of the far-red optical spectroscopic follow-up of the 2MU2 sample and derive the  $J$ - and  $K_S$ -band luminosity functions based on objects estimated to be within 20 pc. In § 2 we overview the characteristics of the 2MU2 sample including its creation and follow-up status. Spectroscopic observations from seven telescopes over sixteen runs are described in § 3. The results of the spectroscopy and the methods used to estimate spectral types, absolute magnitudes, and distances are in § 4. Interesting individual objects are presented in § 5. In § 6 we examine the completeness of the 20-pc 2MU2 sample and derive the luminosity function. Finally, we discuss these results in § 7 and briefly summarize our findings in § 8.

## 2. The 2MU2 Sample

The creation of the 2MU2 sample is meticulously discussed in Paper V; however, we briefly summarize the selection criteria and procedures here, making particular note of the minor changes that have since been applied. Eleven million point sources were selected from the 2MASS Second Incremental Data Release Point Source Catalog (PSC) with  $|b| > 10^\circ$ ,  $(J - K_S) > 1.0$ , and  $J < 16.5$ . The sample was narrowed to 1672 objects using optical and near-infrared color-color and color-magnitude criteria<sup>1</sup>, and excluding sources with positional coincidence with star formation regions (e.g., Taurus, Orion), high star density regions (e.g., LMC, M31), and other reddening regions (listed in Paper V, Table 3). Below we discuss the further reduction of the sample to 630 objects, and the follow-up status of the 518 candidates requiring additional observations.

---

<sup>1</sup>Paper V incorrectly stated the slope of the  $J, (J - K_S)$  selection criterion as 1.5 where the correct value is 3. The line is plotted correctly in Figure 1 of Paper V.

## 2.1. Narrowing and Refining the Sample

As discussed in Paper V, 588 of the 1672 sources in the 2MU2 sample have  $J \leq 9$ . Those bright sources were considered separately in the appendix of Paper V, and they include no new, nearby late-type dwarfs. Ninety-nine of the remaining 1084 candidates were eliminated based either on previous observations listed in the SIMBAD database<sup>2</sup> (24), positional coincidence with known interstellar clouds (41), or near-infrared colors consistent with mid-type M dwarfs (34 tagged “bland”). We have eliminated a further 355 stars based on the following criteria:

Visual inspection.— We originally identified 211 sources in Paper V as either artifacts or as being associated with large galaxies or globular clusters. A further eight sources have been added to this list, giving a total of 219 sources eliminated.

$(F - J)/(J - K_S)$ .— We cross-referenced the sample against the HST Guide Star Catalog v2.2 (Morrison et al. 2001), and used the photographic  $F$ -band (red) magnitudes to eliminate 137 sources as too blue in  $(F - J)$ . However, one object, 2MASS J07003664+3157266, proved to be matched incorrectly. Observations by Thorstensen & Kirkpatrick (2003) show that this object is a nearby L dwarf, and it is included in the present sample. We have double-checked the remaining 136  $(F - J)$  rejectees, paying particular attention to outliers in the  $(J - H)/(H - K_S)$  plane. No additional ultracool candidates were recovered.

Of the remaining 630 ultracool candidates, 112 objects were already known as nearby, late-type dwarfs at the time of publication of Paper V, thus leaving 518 sources requiring follow-up observations.

## 2.2. Follow-up Status

We presented far-red optical spectroscopy of 298 sources in Paper V; optical and/or near-infrared spectroscopy has since been obtained for the remaining 220 targets. If near-infrared data suggested that a source is an L dwarf within 20 pc, additional optical spectroscopy was obtained since  $M_J$  of M and L dwarfs is better correlated with optical spectral types than infrared types.

---

<sup>2</sup><http://simbad.u-strasbg.fr/>

Figure 1 summarizes the current status of our observations. Optical spectroscopy has been obtained for 495 objects. Based on near-infrared spectroscopy, we eliminate seventeen sources as either extragalactic objects or ultracool dwarfs well beyond our 20-pc distance limit. One source, 2MASSI J0028208+224905, has near-infrared spectroscopy indicative of possible membership in the 20-pc 2MU2 sample and still requires optical observations. For five objects, we list data from the literature—three from Keck (Kirkpatrick et al. 2001b; Kirkpatrick et al., in prep.) and two from the Sloan Digital Sky Survey (SDSS, Fan et al. 2000; Hawley et al. 2002).

Our infrared spectroscopic observations of ultracool dwarfs will be discussed in a future paper (Cruz et al., in prep.). Here, we present far-red optical spectra for 197 sources from the 2MU2 sample that previously lacked sufficient data.

### 3. Far-red Spectroscopic Observations

We have obtained new optical spectra for 198 objects from the 2MU2 sample (including one re-observation of an object originally reported in Paper V) using NOAO facilities and the 3.5-m Apache Point Observatory<sup>3</sup>. The instrumental setups and data reduction techniques used for these data are the same as those described in Paper V. The objects we used as spectral standards are listed in Table 1.

For all observations, Tables 2–6 list the coordinates (as the 2MASS designation) and the near-infrared photometry from the 2MASS Second Incremental Data Release PSC<sup>4</sup>, date of observation, and telescope used. Several objects were observed on multiple observing runs to improve the signal-to-noise of the spectra or to monitor for H $\alpha$  emission line variability; all observations are listed and the active objects are noted.

Observations were obtained with the RC Spectrograph on the Kitt Peak 2.1-m telescope (KP 2.1 m) during four runs: 2001 November 1–6, 2002 July 3–8, 2003 March 13–15, and 2003 Oct 8–12. For all runs, the 400 line mm<sup>-1</sup> grating, blazed at 8000 Å, was used with the OG 550 order blocking filter to give spectra covering 6000–10000 Å. Observations were made using a 1''2–1''5 slitwidths to accommodate various conditions. We obtained an average resolution of 5.8 Å (3.1 pixels). Internal quartz flats and HeNeAr arcs were taken at each position to correct for fringing for all targets except for the one object observed during 2001

---

<sup>3</sup>Spectra will be made available from DwarfArchives.org and upon request from K. L. C, [kelle@amnh.org](mailto:kelle@amnh.org).

<sup>4</sup>There are usually small differences between the astrometry and photometry given in the 2MASS Second Release and the values in the final All-Sky Data Release.

November (2MASS J0959560+200234) where calibration frames were taken nightly.

The Double Imaging Spectrograph (DIS II) on the 3.5-m telescope at Apache Point Observatory (APO) was used on 2002 April 10, 2002 May 14, 2002 May 30, and 2002 July 10–11. A 1''-wide slit and the medium resolution grating with 300 line  $\text{mm}^{-1}$  on the red camera was used to cover 6000–10000 Å at a resolution of 7.3 Å (2.4 pixels). Conditions were mostly clear with 0''.8–1''.2 seeing.

The MARS instrument on the Mayall 4-m telescope (KP 4 m) on Kitt Peak was used for three runs: 2002 September 25–28, 2003 July 9–14, and 2004 February 10–12. The VG0850-450 grism was used for all three runs with 1''.5–2'' slitwidths, to cover 6300–10000 Å at a spectral resolution  $\sim 10$  Å (3.3 pixels). An older CCD detector was used in 2002 September than in the two subsequent runs. The main difference between the two detectors is the cosmic-ray event rate, which does not affect the spectral data presented here. The conditions in 2003 July were significantly hampered by the combination of a nearly full moon and smoke from the nearby Aspen fire. The conditions were clear for the other runs.

Observations were obtained on 2003 April 20–23 and 2006 January 13–14 with the RC spectrograph and Loral 3K CCD on the Blanco 4-m telescope (CT 4 m). We used a 1''-wide slit, an OG 515 filter to block higher orders, and a 315 line  $\text{mm}^{-1}$  grating blazed at 7500 Å to cover the range 5500–10000 Å with a resolution of 7 Å (3.5 pixels). All six nights were clear with seeing ranging from 0''.5 to 1''.5.

Data were obtained with the CTIO 1.5-m (CT 1.5 m) telescope on 2003 November 7–11 with a Loral 1K CCD and the RC Spectrograph. A total lunar eclipse on 9 November enabled the observations of several fainter objects. We employed 1''.5-wide slit, an OG 530 filter to block higher orders, and a 400 line  $\text{mm}^{-1}$  grating blazed at 8000 Å to cover 6300–9000 Å at a resolution of 6.5 Å (3 pixels). Conditions were clear and the seeing ranged from 0''.7 to 0''.9.

The Gemini Multi-Object Spectrometer (GMOS, Hook et al. 2004) was used on both Gemini North (GN) and South (GS) during queue observations taken during 2004 September–2005 March (Program IDs: GN-2004B-Q-10 and GS-2004B-Q-30). The RG610\_G0307 filter and R400\_G5305 disperser was used on GN, while on GS the RG610\_G0331 filter and R400\_G5325 disperser was implemented to cover 6000–10000 Å. On both telescopes, the nod and shuffle mode was used with a 0''.75-wide slit to provide good sky subtraction and a resolution of 5.5 Å (4 pixels). Additionally, two consecutive observations were taken with different central wavelengths to obtain spectral coverage over the chip gaps.

A comparison between the Gemini North data from semester 2004B and other observations of ultracool dwarfs reveals an inconsistency in the flux calibration. For example, 2M 0025+47 (L4) was observed with Gemini North and, as can be seen in Figure 2, has a

significantly steeper spectral slope longward of 8700 Å than the two other L4 dwarfs plotted, both of which were observed with Gemini South. While we are continuing to investigate the source of this problem, with the aim of correcting it, our ability to spectral type is not hindered since we observed spectral standards with the same observational setup and data reduction procedure. (This sound methodology also enabled us to recognize that it was a systematic problem and not a true property of the new objects observed.)

All of the various data were bias-subtracted, flat-fielded, wavelength-calibrated, and flux-calibrated using IRAF<sup>5</sup>. The CCDRED package and the DOSLIT routine were used for the KPNO, CTIO, and APO data while the Gemini GMOS package was used for the Gemini data.

To wavelength calibrate, HeNeAr or CuAr lamps were taken nightly for most of the observations, at each position for the KP 2.1 m data, and only a few times over the semester for the Gemini queue observations. Flux-calibration was done using observations of the flux standards BD +26 2606, BD +17 4708, Feige 56, Feige 110, HD 19445, Hiltner 600, G191-B2B, and LTT 2415 (Oke & Gunn 1983; Massey et al. 1988; Massey & Gronwall 1990; Hamuy et al. 1994). None of the spectra were corrected for telluric absorption.

#### 4. Results: Spectral Types, Magnitudes, and Distances

We have measured spectral types, estimated absolute magnitudes, and derived distances for all the observed dwarfs in the same manner as described in Paper V. For the late-type dwarfs (spectral types M7 and later), we have assigned a unique, five digit “2MUCD” (2MASS Ultracool Dwarf) reference number in addition to the full 2MASS designation. These data are listed in Tables 2–4.

Spectral types are determined via side-by-side comparison with spectra of spectral standards. The spectral standards we used are listed in Table 1. Data for many spectral standards were taken during the course of our observations<sup>6</sup>. However, we supplemented our data with high signal-to-noise Keck I + LRIS data available for L dwarf spectral standards<sup>7</sup>.

---

<sup>5</sup>IRAF is distributed by the National Optical Astronomy Observatories, which are operated by the Association of Universities for Research in Astronomy, Inc., under cooperative agreement with the National Science Foundation.

<sup>6</sup>Data for these and other spectral standards are available from [http://research.amnh.org/~kelle/M\\_standards/](http://research.amnh.org/~kelle/M_standards/)

<sup>7</sup>Available from <http://DwarfArchives.org>.

The resulting uncertainty on spectral type is  $\pm 0.5$  subtypes except where low signal-to-noise data result in uncertainties of 1 or 2 types, noted in the tables by a single or double colon respectively<sup>8</sup>. The spectral types of objects with multiple observations were estimated from the higher signal-to-noise data—typically this is the second observation where the spectrum was obtained with a larger aperture telescope than the first.

For objects with spectral types M6 and later,  $M_J$  is estimated from the spectral type/ $M_J$  calibration derived in Paper V. This  $M_J$  is combined with photometry from the 2MASS Second Incremental Data Release PSC to yield  $M_{K_S}$  and spectrophotometric distances. The uncertainties in both the estimated absolute magnitudes and distance are dominated by the uncertainty in the spectral type. Table 2 lists the data for 12 objects with types M6 and later that appear to be within 20 pc. Data for 94 more distant late-type objects are listed in Table 3.

Absolute  $J$  magnitudes for objects with spectral types earlier than M6 are estimated using the TiO5, CaH2, and CaOH spectral indices as described in Cruz & Reid (2002, Paper III). For four objects (2MASSI J0510239–280053, M4; 2MASSI J0544167–204909, M5; 2MASSI J1242271+445140, M5; 2MASSI J1436418–153048, M5), at least two of the three spectral-index relations yield two estimates for  $M_J$ . Since these objects fall well outside our distance limit and spectral type criteria, we have chosen to adopt  $M_J = 8.5 \pm 0.7$  and list the distance as a range. We list data for 34 distant, early-to-mid M dwarfs in Table 4.

Not surprisingly, spectroscopy revealed a number of the candidates to be distant giants or carbon stars. Rough spectral types ( $\pm 1$ ) for the 33 giants were measured via comparison to giant standards (Kirkpatrick et al. 1997; Garcia 1989) and are listed in Table 5. The 17 carbon stars are listed in Table 6.

In Table 7 we list new spectral data for six dwarfs that were presented in Paper V. For five of these, we previously listed data from the literature but we have since reobserved them with our instrumental setup to maintain consistency in the sample. One object, 2MASSI J0326422–210205, was reobserved to obtain a higher signal-to-noise spectrum than that presented in Paper V; these new data revealed a lithium absorption feature (discussed in § 5.1). There is general agreement between our new spectral types and those previously quoted.

Five objects with spectral features indicative of low gravity are listed in Table 8 and discussed below in § 5.3. Included among the low-gravity spectra is DENIS J043627.8–411446,

---

<sup>8</sup>In previous papers in this series, a question mark was used to indicate uncertainty in the spectral type due to a low signal-to-noise spectrum. Here we adopt the more standard notation of a colon.



which was listed in Paper V with data from the literature and 2MASS J04433761+0002051, which was previously classified as a normal dwarf in Paper V.

## 5. Interesting Individual Objects

### 5.1. Lithium Detections

We have detected the Li I absorption line at 6708 Å in six objects in the entire 2MU2 sample. Two of these detections were included in Paper V and are in the 20-pc sample: 2MASS J0652307+471034 and 2MASS J2057540–025230.

Here we present four new detections, although all lie beyond 20 parsecs. Figure 2 displays the spectra of these objects. All four have strong lithium absorption and are spectral type L4–L5: 2MASS J0025036+475919 with  $EW=10\pm 2$  Å (also candidate wide companion, see § 5.5 below), 2MASS J0421072–630602 with  $EW=6\pm 2$  Å, 2MASS J0310140–275645 with  $EW=10\pm 1$  Å, and 2MASS J0326422–210205 with  $EW=11\pm 5$  Å.

The DUSTY theoretical models by Chabrier et al. (2000) suggest that the continued presence of undepleted lithium indicates that these dwarfs are less than one gigayear old. Given the absolute magnitudes and effective temperatures inferred from the spectral types, we find that undepleted lithium suggest these objects are 500 Myr old with masses of  $50 M_{Jup}$ .

Our original observations of 2M 0326–21<sup>9</sup>, with the CTIO 4-meter, lacked sufficient signal-to-noise to permit detection of the lithium line and, based on those data, we estimated a spectral type of L5:. New observations with Gemini South not only reveal lithium absorption, but also provide an improved spectral type of L4 (Table 7).

It is noteworthy that all of these new detections were obtained with Gemini 8-m telescopes. The majority of our observations of L dwarfs were obtained with 4-m class telescopes which are simply not sensitive enough to reliably detect the relatively weak Li I absorption line.

---

<sup>9</sup>Source designations in this article are abbreviated in the manner 2M hhmm±dd, where 2MASS has been further abbreviated as 2M; the suffix is the sexagesimal right ascension (hours and minutes) and declination (degrees) at J2000.0 equinox.

## 5.2. L/T Transition Objects

The optical spectra of the two latest objects in the new data presented here, 2MASS J1043075+222523 and 2MASS J2325453+425148, are shown in Figure 3. The spectrum of 2M 2325+42 is consistent with a spectral type of L8. On the other hand, the red spectrum of 2M 1043+22 is significantly steeper than that of both 2M 2235+42 and the L8 spectral standard. (All three spectra were obtained with the same instrumental setup and data reduction procedure.)

Infrared spectra show that 2M 1043+22 lacks significant methane absorption in the  $H$  band, thus ruling out a T spectral type (Cruz et al., in prep.). As a result, we adopt a spectral type of L8 for 2M 1043+22. We note, however, that it is the reddest L8 dwarf (where the spectral type is based on optical data).

One possible explanation for the unusual spectrum of 2M 1043+22 is that it is an unresolved binary similar to SDSS J042348.57–041403.5 (Burgasser et al. 2005b) and DENIS-P J225210.7–173013 (Reid et al. 2006c). The binary frequency among late-type L dwarfs/early-type T dwarfs has been found to twice as high as that of all other L and T dwarfs (Burgasser et al. 2006b; Liu et al. 2006) and high resolution imaging observations of 2M 1043+22 are warranted.

Additionally, our optical spectrum of 2M 1043+22 shows a feature near the wavelength of  $H\alpha$  that might be consistent with emission. This would be similar to the unusual T dwarfs 2MASS J10475385+2124234 and SDSS J125453.90–012247.4 found with weak  $H\alpha$  emission by Burgasser et al. (2003b). Further observations are required to verify the reality of the emission in 2M 1043+22.

## 5.3. Low-Gravity Objects

Objects with spectral features indicating low surface gravities ( $\log(g) < 5$  cgs) are of particular interest as low gravity implies low mass. In addition, low-mass brown dwarfs with late-type M and early-type L spectral types must be younger than their equivalently-classified higher-mass counterparts. Thus, low gravity suggests both low mass and youth. A growing number of late-type dwarfs with low-gravity features are now being uncovered in field samples (Gizis 2002; Kirkpatrick et al. 2006a; Kirkpatrick et al., in prep.) and their study is emerging as new way to probe the evolutionary properties of brown dwarfs and to study their age and mass distributions.

Through comparison to both late-type giants and objects found in young clusters, several

gravity-sensitive spectral features have been identified. In particular, we have used enhanced VO bands (7330–7530, 7850–8000 Å), less-broad K I doublet (7665, 7699 Å), and weaker Na I doublet (8183, 8195 Å) as diagnostics (Martín et al. 1996; Gizis et al. 1999; Gorlova et al. 2003; McGovern et al. 2004; Kirkpatrick et al. 2006a).

Five objects with these low-gravity features were presented in Paper V and we present an additional five here. They are listed, along with their proper motions, in Table 8 and their spectra are displayed in Figures 4–7.

The spectrum of 2MASSI J0443376+000205 most resembles an M9 and using this spectral type results in a distance estimate within 20 pc. Even though this object has low-gravity features, we include it in the sample used to measure the luminosity function.

The spectra of the two objects in Figure 6, 2MASSI J0241115–032658 and 2MASSI J2213449–213607, are later than any of the low-gravity objects from Paper V. While noisy, these spectra are comparable to the spectrum of 2MASS J01415823–4633574, recently described by Kirkpatrick et al. (2006a) and estimated to have an age of 1–50 Myr and a mass of 6–25  $M_{Jup}$ . All three objects are most comparable to an L1 dwarf but exhibit strong VO molecular absorption and weak K I and Na I absorption lines. Unlike 2M 0141–46, H $\alpha$  emission is not detected in either of our new objects.

The spectrum of 2MASSI J1615425+495321 most resembles an L4 dwarf (Figure 7) but, despite the poorer signal of the spectrum, departures from the spectral signatures of normal (old) field dwarfs are evident. In particular, the hydride bands of CaH, CrH, and FeH are much weaker as are the core and wings of the normally strong K I doublet. The bluer slope at the shortest wavelengths can likewise be attributed to weaker absorption by the normally broad Na I “D” doublet located off the short-wavelength end of the plot. Weaker alkali lines and hydride bands are hallmarks of lower gravity, leading us to believe that this is a young, field L dwarf.

As with 2M 0141–46, we suspect these candidate young objects to be possible members of the nearby young associations such as the Tucana/Horologium association or the  $\beta$  Pic moving group. We are currently in the process of measuring their UVW space motions to definitively test for membership—proper motions are already in hand and radial velocity measurements of the brighter candidates are underway. In addition, these objects are the focus of high-resolution imaging programs searching for even fainter companions.

#### 5.4. Two Unusually Blue L Dwarfs: Metal Poor?

We have identified two objects in the 20-pc 2MU2 sample (included in Table 9) that have unusually blue colors for their spectral type: 2MASS J1300425+191235 (L1) and 2MASS J1721039+334415 (L3). We first pointed out these objects in Paper V. The  $(J - K_S)$  colors for these two objects are 0.3 and 0.6 magnitudes bluer than the mean for their spectral types (Kirkpatrick et al. 2000), a significant deviation suggesting unusual atmospheric properties.

In L dwarfs, variations in  $(J - K_S)$  color for a given  $T_{eff}$  can be linked to differences in condensate opacity and metallicity. Condensates are largely responsible for the red near-infrared colors of these objects, with the collective dust particles acting as a warm pseudo-blackbody source that radiates predominately at near- and mid-infrared wavelengths (Ackerman & Marley 2001). A reduction in the condensates in the photosphere, due perhaps to more efficient sedimentation to lower layers in the atmosphere, can lead to bluer near-infrared colors (see Marley et al. 2002, Figure 1). Knapp et al. (2004) and Chiu et al. (2006) suggest this scenario for seven blue L dwarfs identified in the Sloan Digital Sky Survey.

As one of the brightest L dwarfs, 2M 1300+19 has been moderately well studied. Gelino et al. (2002) and Maiti et al. (2005) both found nonperiodic variability, with the former study suggesting that such variability is evidence for an atmospheric event such as the creation or dissipation of a large storm. If the condensate cloud layer on this object is optically thinner (less condensates), then variations in cloud coverage may be more readily detectable. McLean et al. (2003) acquired a  $J$ -band spectrum of 2M 1300+19 and noted that this object has “the highest equivalent widths in K I of any L1, or indeed almost any other L type.” As the  $J$  band is highly sensitive to condensate opacity in L dwarfs (Ackerman & Marley 2001), a reduction in overall condensates may explain the greater optical depth of this line.

A second possibility is reduced atmospheric metallicity, a characteristic of low-mass subdwarfs. With fewer metal species, most molecular opacity is diminished with the exception of  $H_2$  absorption at  $K_S$  band. The combination of weaker opacity from metal molecules and enhanced  $H_2$  leads to bluer  $(J - K_S)$  colors (Linsky 1969; Saumon et al. 1994; Borysow et al. 1997).

Two metal-poor L subdwarfs have already been identified in 2MASS data, 2MASS J05325346+8246465 (Burgasser et al. 2003a) and 2MASS J16262034+3925190 (Burgasser 2004a), and both are quite blue,  $(J - K) = 0.26$  and  $-0.03$ , respectively<sup>10</sup>. The redder

---

<sup>10</sup>LSR 1610-0040 was identified as an L subdwarf by Lépine et al. (2003a) but recent work has concluded that it is more likely to be a metal-poor M6 dwarf (Cushing & Vacca 2006; Reiners & Basri 2006) or a peculiar binary (A. Burgasser 2006, private communication).

colors of 2M 1300+19 and 2M 1721+33 suggest that they are not as metal-poor as these L subdwarfs, and their optical spectra do not exhibit the stronger metal-hydride bands (6750 Å CaH, 8611 Å CrH, 8692 Å FeH) and weaker metal oxides bands (7053, 8432 Å TiO) expected for metal-poor ultracool dwarfs (Burgasser et al. 2006a). Nevertheless, the possibility remains that these objects could be “mild” subdwarfs, with sufficient metal-deficiency to enhance H<sub>2</sub> absorption.

In addition to being outliers in color space, 2M 1300+19 and 2M 1721+33 stand out kinematically. By combining our spectrophotometric distance with proper motions, we have been investigating the kinematics of the 20-pc 2MU2 sample (Schmidt et al. 2006, in prep.). These two objects have two of the three highest tangential velocities in the entire sample:  $V_{tan} = 139 \pm 15$  km s<sup>-1</sup> and  $98 \pm 8$  km s<sup>-1</sup> for 2M 1721+33 and 2M 1300+19, respectively. (The second fastest is 2MASSI J0251148–035245 with  $V_{tan} = 125 \pm 13$  km s<sup>-1</sup>.) These kinematics suggest thick disk membership, which would be consistent with slight metal-deficiency ( $[Fe/H] \approx -0.5$ ).

The blue colors of these peculiar L dwarfs may also result from a *combination* of slight metal deficiency and reduced condensate formation. Burgasser et al. (2003a) and Burgasser et al. (2006a) found evidence that condensate formation was inhibited in L subdwarf atmospheres due to the persistence of TiO molecular bands and Ti I and Ca I lines in their optical spectra. These species are generally absent in L dwarf spectra due to their incorporation into condensates. While we find no evidence for these features in the spectra of 2M 1300+19 and 2M 1721+33, the combination of slight metal-deficiency and somewhat reduced condensate formation may tip the near-infrared colors of these objects significantly blueward. Because metallicity significantly impacts the composition and chemistry of low temperature atmospheres, identifying and studying metallicity effects in blue L dwarfs provide critical empirical constraints for the next generation of theoretical atmosphere models.

### 5.5. Candidate Wide Ultracool Companions

Low-mass stars and brown dwarfs found as wide companions to higher-mass main sequence stars provide opportunities to test evolutionary and atmospheric models since the objects are assumed to be coeval and thus have the same age and metallicity. We have uncovered three ultracool dwarfs, included in Table 3, that are likely wide companions to higher-mass stars. These discoveries, and others, will be discussed by Solomon et al. (2006, in prep.).

HD 225118 and 2MASSI J0003422–282241: This G8 and M7.5 constitute a common proper motion pair separated by 1.1 arcminutes (1700–2600 AU). We measured the proper motion of the M7.5 to be  $(\mu_\alpha, \mu_\delta) = 228 \pm 57, -135 \pm 37$  mas yr<sup>-1</sup>. HD 225118 was observed by the Hipparcos satellite (Perryman & ESA 1997) and was found to have  $(\mu_\alpha, \mu_\delta) = 280 \pm 1.2, -143 \pm 0.73$  mas yr<sup>-1</sup>; in good agreement with the motion of the ultracool dwarf. The parallax of HD 225118 measured by Hipparcos yields a distance of  $39.5 \pm 1.7$  pc. Adopting this distance for the ultracool dwarf yields  $M_J = 10.1 \pm 0.1$ , nearly one magnitude brighter than what is expected for an M7.5. Thus, we suspect the wide ultracool companion might be an unresolved binary itself. An M7 or M8-type companion would bring the spectrophotometric distance into agreement with the Hipparcos distance estimate. If resolved, this would further support the higher binary fraction among widely separated companions found by Burgasser et al. (2005a). For HD 225118, Nordström et al. (2004) estimate a mass of  $\sim 0.9 M_\odot$  and the age is not well constrained (upper limit of 15.8 Gyr).

HD 2057 and 2MASSI J0025036+475919: These L4 and F8 dwarfs appear to be common proper motion companions separated by 3.6 arcminutes (7000–9000 AU). The Hipparcos proper motion for the F8,  $(\mu_\alpha, \mu_\delta) = 274 \pm 0.31, 11 \pm 0.87$  mas yr<sup>-1</sup>, is consistent with our measured value for the ultracool dwarf,  $(\mu_\alpha, \mu_\delta) = 312 \pm 39, -9 \pm 44$  mas yr<sup>-1</sup>. While the projected physical separation is double that of the widest currently known multiple system with an ultracool dwarf component, Gl 584C at 3600 AU (Kirkpatrick et al. 2001a; Reid et al. 2001), it is not unreasonable based on the log-normal relation between maximum separation and the total mass of the system found by Reid et al. (2001).

Again, our spectrophotometric distance and the Hipparcos distance are discrepant. This time, however, we have already resolved the ultracool wide companion into an equal luminosity binary (Reid et al. 2006b). Taking this binarity into account yields a spectrophotometric distance of  $32 \pm 7$  pc, within  $1.5\sigma$  of the Hipparcos distance of  $42 \pm 2$  pc. Additionally, as mentioned above in § 5.1, lithium absorption present in the spectrum of the ultracool dwarf implies an age less than 1 Gyr and probably closer to 500 Myr. For HD 2057, Nordström et al. (2004) find an age of  $\sim 1.1$  Gyr. However, with an upper limit of 3.6 Gyr and no lower limit given, this age is uncertain.

BD+13 1727 and 2MASSI J0739438+130507: These M8 and K5 dwarfs are a common proper motion pair with a separation of 10.5 arcseconds (380 AU). Their common proper motions were recognized while cross-referencing our sample with the LSPM catalog (Lépine & Shara 2005). The Tycho-2 (Høg et al. 2000) proper motion for BD+13 1727,  $(\mu_\alpha, \mu_\delta) = -76.1 \pm 1.3, -156.5 \pm 1.2$  mas yr<sup>-1</sup>, agrees well with the LSPM proper motion of the ultracool dwarf,  $(\mu_\alpha, \mu_\delta) = -69 \pm 8, -145 \pm 8$  mas yr<sup>-1</sup>.

Our spectrophotometric distance for the M8 is  $36.3 \pm 3.1$  pc. No parallax or additional information on the primary could be found in the literature.

### 5.6. Suspected Unresolved Ultracool Binaries

Ultracool binaries with small separations, like wide systems, place constraints on star formation models (Burgasser et al. 2006c). We have noticed two objects, originally presented in Paper V, that, based on trigonometric parallax measurements, appear to be significantly overluminous, suggesting that they are unresolved binaries. Both of these objects are being targeted for ground-based, high-resolution imaging.

These two objects were also misclassified by Reid et al. (1995, hereafter PMSU) as having earlier spectral types than revealed by our new spectra. The PMSU spectral types are based on the TiO5 index/spectral type relation which turns around at M7 (Cruz & Reid 2002, Figure 3). Using the early-type branch of the calibration resulted in the assignment of a too-early spectral type. The spectral types estimated from our new spectra agree well with those predicted by the late-type TiO5/spectral type relation derived by Cruz & Reid.

LHS 1604 (2M 0351–00): While PMSU assigned a spectral type of M6 ( $TiO5 = 0.18$ ), our observations reveal a spectral type of M7.5 (Paper V). Using our spectral type/ $M_J$  relation, we estimate  $M_J = 10.96 \pm 0.21$ . However, the parallax of  $68.1 \pm 1.8$  mas (van Altena et al. 1995) combined with the the 2MASS  $J$  magnitude of  $11.262 \pm 0.023$ , implies  $M_J = 10.43 \pm 0.06$ . This  $\sim 0.6$  magnitude overluminosity suggests that the object might be an unresolved binary. We find that an M7.5/M9 pair would be consistent with the astrometric results. While this object is included in our total space density estimates, it is not included in our analysis of space density per magnitude because the parallax indicates a magnitude brighter than our brightest  $M_J$  bin ( $M_J = 10.5$ ).

LHS 3406 (2M 1843+40): For this object, PMSU estimated a spectral type of M5.5 ( $TiO5 = 0.24$ ) while we find a spectral type of M8, indicating  $M_J = 11.16 \pm 0.18$  (Paper V). However, the parallax of  $70.7 \pm 0.8$  (Monet et al. 1992) and the 2MASS  $J$  magnitude of  $11.299 \pm 0.028$  yield  $M_J = 10.55 \pm 0.04$ . This overluminosity by  $\sim 0.6$  magnitudes could be explained if the object is an M8/M9 unresolved binary pair. Additionally, this object was misclassified as a dwarf nova (U Gem variable, Downes et al. 1997) but has since been recognized as an M dwarf by the cataclysmic variable community (Liu et al. 1999). Unfortunately, we were unable to locate the original data that the dwarf nova classification was based on to investigate the possibility of a flare event.

## 6. The 20-pc 2MU2 Sample and the Luminosity Function

As described below, the 2MU2 sample covers 36% of the celestial sphere. Within that area, we identify 99 objects in 91 systems with spectral types between M7 and L8 and estimated distances within 20 pc of the Sun—we dub these the 20-pc 2MU2 sample. Over half of these systems were added to this sample through the observations described in this series of papers. Table 9 lists relevant data for all objects in the 20-pc 2MU2 sample. Additionally, we list systems with distance estimates within  $1\sigma$  of 20 parsecs in Table 10.

In Figure 10, we show the spectral type distribution of the 20-pc sample with both the distance source and multiplicity properties distinguished. Trigonometric parallaxes are available for 30 systems; distances for the remaining sources are spectrophotometric. Among the 91 systems, ten are multiple and contribute eight additional objects. The color-magnitude and color-color diagrams of the sample are shown in Figure 11. In Figure 12, we show the  $(J - K_S)$  color distribution for different spectral types.

We use these data to build on the space density analysis given in Paper V, and derive an improved estimate of the  $J$ - and  $K$ -band luminosity functions for ultracool dwarfs. We describe how we estimate our sky coverage in § 6.1. Sample completeness is clearly an important factor in this analysis, and we address that issue in § 6.2. The Malmquist bias corrections appropriate to the sample are described in § 6.3, binarity is discussed in § 6.4, and the derived luminosity function is presented in § 6.5.

### 6.1. Areal Sky Coverage

The total areal sky coverage of the 2MASS Second Release PSC is 19,641.6 deg<sup>2</sup> imaged in 27,493  $6^\circ \times 8.5'$  tiles. From this, we excluded 3807 tiles with central galactic latitudes within 10 degrees of the Galactic plane, reducing the coverage by 2878.1 deg<sup>2</sup>. Parts of the remaining 16,763.5 deg<sup>2</sup> were excluded to eliminate star formation regions, the Magellanic clouds, and other highly reddened or crowded regions (listed in Paper V, Tables 2 and 3). However, these regions were selected by galactic coordinates, whereas the 2MASS imaging tiles are mapped in equatorial coordinates. Additionally, many of these regions had only partial tile coverage in the 2MASS Second Release PSC.

In order to quantify the areal coverage excluded in these regions, we made use of the HIST\_ND algorithm written by J.D. Smith to histogram the coordinates of the point sources eliminated by the positional cuts onto a two-dimensional grid in a rectangular region aligned with the coordinate axes and of easily calculable area. The fraction of the non-zero elements in the resultant array was used as the estimate of the fraction of the area filled by the



eliminated point sources and thus provided a measure of the area of the excluded region, taking into account the discontinuous sky coverage of the 2MASS Second Release PSC.

While the resulting measurement of the area is very sensitive to the histogram bin size chosen, the results are accurate to a few degrees—sufficient for our purposes. As many of the regions are aligned with the coordinate axes in one system, but not in the other, the areas were measured in both galactic and celestial systems to give an estimate of the uncertainties. The resulting measurement of the area removed due to positional cuts is  $1940 \pm 10 \text{ deg}^2$ .

Bright stars ( $K < 4$ ) represent a further minor source of confusion, since their extended halo on the 2MASS scans rules out the possibility of detecting faint sources within as much as a few arcminutes. However, the total area obscured in this manner is less than  $15 \text{ deg}^2$ , producing negligible impact on our statistics.

The final areal coverage of the 2MU2 sample is  $14,823.5 \text{ deg}^2$ , or 36% of the celestial sphere (9% smaller than the  $16,350 \text{ deg}^2$  previously stated in Paper V).

## 6.2. Completeness

The 2MU2 sample has been carefully constructed and extensive spectroscopic follow-up observations have been completed to yield a complete sample of M7–L8 type dwarfs to 20 parsecs over 36% of the sky. Below we discuss our observational, spectral type and the resulting volume completeness.

### 6.2.1. Observational Completeness

As discussed in § 2, we lack sufficient data for one object, 2MASSI J0028208+224905, that infrared spectroscopy identifies as a late-type L dwarf at 20–25 pc. It is possible that optical spectroscopy might result in a spectral type of L7 or later, moving it within the 20-pc limit. If this is the case, it would contribute to the 14.25 or 14.75  $M_J$  bin of  $\Phi(M_J)$ . For this reason, and other more significant ones discussed in § 6.5, our measurement of  $\Phi(14 < M_J < 15)$  and  $\Phi(12.5 < M_{K_S} < 13)$  are lower limits.

### 6.2.2. Spectral Type Incompleteness

The 2MU2 sample is a color- and magnitude-defined sample. These selection criteria result in incompleteness at the extremes of the range of spectral type covered by our survey.

For example, we are incomplete for M7 dwarfs due to the  $(J - K_S) > 1.0$  selection criterion; several M7 dwarfs are known with  $(J - K_S)$  colors bluer than this limit, including VB 8, the M7 archetype.

We have quantified this incompleteness through analysis of a sample of ultracool dwarfs with  $J < 16.5$  and trigonometric parallax measurements from Dahn et al. (2002) or Vrba et al. (2004). We obtained photometry for these objects from the 2MASS Second Incremental Data Release PSC where available and otherwise used the data from the 2MASS All-Sky PSC. We refer to this sample as the “ultracool dwarf trigonometric” (UCDt) sample. Adjusting the measured  $M_J$  to a distance of 20 pc shows the systems as they would appear at the far edge of our volume limit. Figure 13 displays those data against our selection criteria, marking objects that are excluded. Blue M7 and M8 dwarfs, some L7 and L8 dwarfs, and unusual objects are likely to be excluded from the 2MU2 sample.

**Late-M Dwarfs** Considering earlier types, two M7 dwarfs in the UCDt sample, GRH 2208–2007 (M7.5) and VB 8 (M7), are excluded by both the  $J/(J - K_S)$  and  $(J - H)/(H - K_S)$  selection criteria. While all of the M8 dwarfs in the UCDt sample fall within our criteria, they also appear to be cut-off by the  $(J - K_S) = 1.0$  limit (Figure 11). To see this more clearly, in Figure 12 we show the  $(J - K_S)$  distribution for M7, M8, and M9 dwarfs in the 20-pc 2MU2 sample—while the M7 and M8 distributions appear truncated, the M9 distribution does not.

We cannot use the UCDt sample to estimate the resultant incompleteness, since it includes only three M7 and six M8 dwarfs. Instead, we have compiled data for M7 and M8 dwarfs listed in the literature that were not selected using  $(J - K_S)$  color as a criterion. In Figure 14 we examine the  $(J - K_S)$  distribution of these objects. Three of the fourteen M7 dwarfs have  $(J - K_S) < 1$  and we use a binomial distribution to estimate  $78.6_{-14.3}^{+7.9}\%$  of M7 dwarfs are redder than  $(J - K) = 1$ . Applying this correction to the observed number of 21 M7 dwarfs in the 20-pc 2MU2 sample yields a corrected number of 26.7 dwarfs, and the luminosity functions are changed accordingly. None of the twelve M8 dwarfs found in the literature have  $(J - K_S) < 1$ . While the 20-pc 2MU2 sample is likely incomplete for M8 dwarfs, the effect is small ( $\sim 10\%$ ) and we do not correct the luminosity function for missing M8 dwarfs.

**Late-L Dwarfs** At later types, the 2MU2 sample is incomplete since pressure-induced  $H_2$  absorption and perhaps dust settling (Knapp et al. 2004) leads to some L7 and L8 dwarfs having colors bluer than our selection criteria. The UCDt sample includes four L7 and six L8 dwarfs—one L7.5 and four L8 dwarfs are excluded in the  $J/(J - K_S)$  plane. While this incompleteness affects  $14 < M_J < 15$  and  $12.5 < M_{K_S} < 13$ , we have not computed explicit

completeness corrections for those spectral types for two reasons. First, the incompleteness is by magnitude, and therefore distance dependent; there is no incompleteness for late-type sources within 11 pc, for example. Second, and more significantly, early T dwarfs, which are not included in our survey, contribute to the space density of ultracool dwarfs in the same  $M_J$  range as L7 and L8 dwarfs ( $14 < M_J < 15$ ). In the  $K_S$  band, on the other hand, T dwarfs are fainter than L dwarfs and do not contribute to the space density in our  $M_{K_S}$  range of interest (Vrba et al. 2004). Thus, we take our measured  $\Phi(14 < M_J < 15)$  as a lower-limit due to both missing L and T dwarfs while  $\Phi(12.5 < M_{K_S} < 13)$  is incomplete only due to missing late-L dwarfs.

**Unusual M9 and L0 Dwarfs** One M9 dwarf and two L0 dwarfs in the UCDt sample have unusual ( $H - K_S$ ) colors ( $\sim 0.35$ ): PC 0025+0447 (M9.5), SDSS J143517.20–004612.9 (L0), and SDSS J225529.09–003433.4 (L0:). PC 0025+0447 is recognized as a highly unusual object that is young, has low-gravity features, and has persistent, extremely strong  $H\alpha$  emission ( $EW \sim 100 \text{ \AA}$ ). The two SDSS objects are faint ( $J > 15.6$ ) and the photometric errors on SDSS 1435–00 are substantial ( $\sim 0.1$ ). We propose that either these three objects are unusual in a similar, as-yet-unrecognized way, or more likely, that the uncertainties in the 2MASS photometry, either due to systematic errors or coincidence, have resulted in a similar blue ( $H - K_S$ ) color. No correction is applied to the luminosity functions based on these three objects.

**Other Excluded Objects** Two additional objects in the UCDt sample are excluded by the  $(J-H)/(H-K_S)$  selection criteria: GJ 1048B (L1) with  $(J-H) = 0.69$ ,  $(H-K_S) = 0.67$  and SDSS J144600.60+002452.0 (L6) with  $(J-H) = 1.38$ ,  $(H-K_S) = 0.58$ . The  $(H-K_S)$  color of GJ 1048B is unusually red for its spectral type and is probably due to its proximity to GJ 1048A resulting in  $\sim 0.1$  photometric uncertainties. For an L6, SDSS 1446+00 appears unusually red in  $(J-H)$  and the 2MASS photometry is fairly robust with uncertainties ranging from 0.035 in  $H$  band to 0.082 magnitudes in  $J$  band. However, the 2MASS flag ‘ndet’ equals 264566 indicating that there were only 2 detections at  $J$  band out of 6 possible, 4 detections out of 5 possible at  $H$  band, and 6 out of 6 at  $K_S$  band. Thus, with only 2 detections, the quoted  $J$  magnitude is highly suspect. Using the transformation given in the 2MASS Explanatory Supplement<sup>11</sup> we convert the UKIRT MKO photometry listed in Geballe et al. (2002) to the 2MASS system and find  $JHK_S$  colors that are not anomalous when compared to other late-L dwarfs. A more accurate 2MASS  $J$  magnitude is probably

---

<sup>11</sup>[http://www.ipac.caltech.edu/2mass/releases/allsky/doc/sec6\\_4b.html](http://www.ipac.caltech.edu/2mass/releases/allsky/doc/sec6_4b.html)

15.6 rather than the 15.9 listed in both the 2MASS Second Release PSC and the All-Sky PSC. No correction is applied to the luminosity functions based on these two objects.

### 6.2.3. Volume Completeness

We show the space densities for two sets of 4-pc thick spherical shells for five absolute magnitude bins in Figure 15. (Note that these bins are coarser than those used in  $\Phi(M_J)$  and  $\Phi(M_{K_S})$  and the last two bins overlap.) The distance at which the sample begins to be incomplete is indicated by a downturn in the measured space densities. The 2MU2 sample appears to be complete to 20 parsecs at all magnitudes except for the two faintest ( $14 < M_J < 15$ ). This is likely due to our incompleteness at the latest-L types and, as discussed above, we take our measurement of the luminosity functions to be a lower limit at the relevant magnitudes.

## 6.3. Malmquist Bias

We have adopted a unique value of  $M_J$  for each spectral type,  $M_{obs}$ , where the true situation is a dispersion of absolute magnitudes about some average for each spectral type. As a result, the sample is biased towards more luminous objects at a given spectral type. The intrinsically less luminous objects (where the true intrinsic absolute magnitude,  $M_0 > M_{obs}$ ) are systematically excluded because using  $M_{obs}$  overestimates their distance and thus they are more likely to fall outside of the distance limit. Similarly, a greater number of overluminous objects are included in the sample because their distances are underestimated. This is classical Malmquist Bias and we must correct the estimated absolute magnitude for those 69 objects in the sample without trigonometric parallax data (Malmquist 1920).

Since we expect nearby M and L dwarfs to be uniformly distributed throughout the Solar Neighborhood we can use Malmquist’s formula to correct the absolute magnitudes,

$$M_0 = M_{obs} - 1.38\sigma^2 \tag{1}$$

where  $\sigma$  is the uncertainty in  $M_{obs}$ . The uncertainty in  $M_{obs}$  depends partly on the scatter in the  $M_J$ /spectral-type relation, but mostly on the uncertainties in the spectral type estimates. Combining these, we derive uncertainties of  $0.13 < \sigma < 0.42$  mags resulting in corrections of 0.02 to 0.24 mags. These corrections are applied to our measured  $\Phi(M_J)$  and  $\Phi(M_{K_S})$ .

#### 6.4. Unresolved Binary Systems

Unrecognized binarity is likely to affect the statistical properties of the 20-pc 2MU2 sample. The sample includes members of 10 known multiple systems. Eight of those systems have trigonometric parallax data. Four are systems where one component falls beyond the spectral type limits of the present sample. Those systems are: LHS 1070 (2M 0024–27), where the primary is an M5.5 dwarf; G 216-7 (2M 2237+29), where G 216-7A is an M0 dwarf; SDSS J042348.57–041403.5, where the secondary is an early-type T dwarf (Burgasser et al. 2005b); and DENIS-P J020529.0–115925, where a possible T-type component has been reported (Bouy et al. 2005).

More than half of the sources in the 20-pc 2MU2 sample have either high spatial-resolution ground-based observations (Koerner et al. 1999; Close et al. 2003; Siegler et al. 2005) or imaging by the Hubble Space Telescope (Reid et al. 2001; Gizis et al. 2003; Reid et al. 2006b). Of the 55 systems that have been targeted, nine are resolved as close binaries, yielding an observed binary fraction of  $17_{-4}^{+6}\%$ , consistent with prior analysis (Gizis et al. 2003; Bouy et al. 2003; Burgasser et al. 2006b). (See Reid et al. (2006b) for a thorough discussion of the binary frequency of our 20-pc sample.) Applying this binary fraction to the 36 unobserved objects suggests that there are approximately five currently unresolved binaries included in our measurement of  $\Phi(M_J)$  and  $\Phi(M_{K_S})$ . Indeed, as discussed in § 5.6, we already suspect two objects to be unresolved binaries based on their overluminosity.

Burgasser (2004b) has modeled multiplicity corrections for a wide range of scenarios for a magnitude-limited observational sample. The vast majority (34/36) of sources that lack high-resolution imaging also lack trigonometric parallax data. As a result, these sources are effectively a magnitude-limited sample, and Burgasser’s analysis is appropriate. In the most extreme case of a binary fraction of 50%, the correction is only 20% to the late-L dwarfs. Under more likely circumstances (binary fraction  $\sim 20\%$ ), the space density of late-M dwarfs is overestimated by 5% while the density of late-L dwarfs is underestimated by about 8%. We also note that  $\sim 5\%$  of the sources in our sample may prove to be unrecognized spectroscopic ( $\Delta < 2$  AU) binaries (Reid et al. 2002c; Basri & Reiners 2006). Nonetheless, we expect the effects on  $\Phi(M_J)$  and  $\Phi(M_{K_S})$  due to unrecognized binarity to be small ( $< 10\%$ ) and we do not apply any corrections for them.

#### 6.5. The Luminosity Function

We show the Malmquist-corrected  $J$ - and  $K_S$ -band luminosity functions derived from the 20-pc 2MU2 sample in Figure 16 and list the measured space densities in Table 11. As

outlined earlier in this section (§ 6.2.2), the color-magnitude criteria used to define the sample lead to incomplete sampling at spectral types M7/M8 and L7/L8. We have made explicit allowance for the incompleteness at M7, increasing the space density at  $M_J = 10.75 \pm 0.25$  by 41%.

The correction factors are more difficult to assess at the latest spectral types, however. Due to the incompleteness at late-L types, we take our measured  $\Phi(M_{K_S})$  as a lower limit in the faintest magnitude bin ( $12.5 < M_{K_S} < 13$ ). In addition to late-L dwarfs, T dwarfs contribute to the faintest two bins ( $14 < M_J < 15$ ) of  $\Phi(M_J)$ . Trigonometric parallax results show that brown dwarfs *brighten* from  $M_J \sim 15$  at spectral type T0 to  $M_J \sim 14.5$  at type T3/4 (Dahn et al. 2002; Tinney et al. 2003; Vrba et al. 2004). This behavior is probably related to the clearing of dust clouds within the atmosphere, allowing the  $\tau = 1$  photospheric level to descend to greater physical depths (and higher temperatures) at wavelengths near  $1.2 \mu\text{m}$  (Burgasser et al. 2002; Knapp et al. 2004). In any case, our survey was not designed to identify field T dwarfs, and our measured space densities must represent a lower limit to  $\Phi(M_J)$  at  $M_J > 14$ .

## 7. Discussion

Integrating our results for the luminosity function, we derive a space density of  $8.7 \pm 0.8 \times 10^{-3} \text{ pc}^{-3}$  for M7–L8 dwarfs. Ultracool M dwarfs, spectral types M7 to M9.5, contribute a density of  $4.9 \pm 0.6 \times 10^{-3} \text{ pc}^{-3}$ . We find the space density of L dwarfs to be  $\geq 3.8 \pm 0.6 \times 10^{-3} \text{ pc}^{-3}$ , with L0–L3 dwarfs contributing  $1.7 \pm 0.4 \times 10^{-3} \text{ pc}^{-3}$  and late-type L dwarfs responsible for at least  $2.2 \pm 0.4 \times 10^{-3} \text{ pc}^{-3}$ . Our results are in good agreement with the space density of  $4.5 \times 10^{-3} \text{ pc}^{-3}$  derived for ultracool M dwarfs by Gizis et al. (2000), but exceed by almost a factor of two their initial estimate of the local L dwarf density. Since we are using a significantly larger sample than Gizis et al., our measured densities are likely more accurate.

Putting these results in a wider context, Figure 17 superimposes  $\Phi(M_J)$  as derived from our ultracool sample against results for the 8-pc sample (Reid et al. 2003b). As discussed in Reid et al. (2004), 95% of the 8-parsec stars have reliable trigonometric parallaxes; the  $J$ -band photometry is taken either from 2MASS or, for bright stars, drawn from the literature and transformed, if necessary, to the CIT system. The derived space densities are listed in Table 12. While the 8-pc sample includes only a handful of ultracool dwarfs, it is clear that the two datasets are in excellent agreement, with the new data confirming the sharp decline in number densities at  $M_J > 10$ . In order to get an idea of the space densities in the  $I$  band,  $M_I \sim 13$  for M7 and  $(I - J)$  ranges from 2.4–4 for M7–L8 (Dahn et al. 2002).

The overall morphology of the  $J$ -band luminosity function reflects the convolution of the underlying mass function,  $\Psi(M)$ , and the  $M_J$ -mass relation. Qualitatively,  $\Phi(M_J)$  increases for  $0 < M_J < 7$  since the mass function increases with decreasing mass. At fainter magnitudes,  $\Phi(M_J)$  turns over not because  $\Psi(M)$  changes drastically, but because the slope of the  $M_J$ -mass relation changes—while  $\frac{\delta Mass}{\delta M_J} \sim 0.4 M_\odot \text{ mag}^{-1}$  for  $M_J < 7$ ,  $\frac{\delta Mass}{\delta M_J} \sim 0.07 M_\odot \text{ mag}^{-1}$  for  $7 < M_J < 10$  (Delfosse et al. 2000).

Our analysis shows that  $\Phi(M_J)$  declines sharply with decreasing luminosity beyond  $M_J = 10$ , reaching a minimum at  $M_J \sim 13$ , roughly corresponding to spectral type L4. Formally, our data indicate that the space densities remain approximately constant at fainter magnitudes; however, since our measurements are lower limits,  $\Phi(M_J)$  likely increases at  $M_J > 14$ .

Our field survey has uncovered both very low-mass stars and sub-stellar mass brown dwarfs from the local population. Assuming a typical age of 2–5 Gyrs for a field dwarf, even the most massive brown dwarfs have cooled to L-dwarf temperatures. Moreover, theoretical models (e.g., Burrows et al. 2001) indicate that the hydrogen-burning limit (for solar abundances) corresponds to a temperature of  $\sim 1700$  K, or spectral type  $\sim$ L4 (Golimowski et al. 2004). Thus, early-type L dwarfs include a mix of stars and brown dwarfs, with brown dwarfs acquiring increasing dominance from L0 to L4 until they are the sole contributors at  $M_J \gtrsim 13.5$ .

As discussed elsewhere (Chabrier 2003; Burgasser 2004b; Allen et al. 2005), the morphology of the luminosity function is due to this mix of stars and brown dwarfs in the ultracool regime and is qualitatively in accord with theoretical expectations. The drop in number density from M7 to L4 reflects a further contraction in  $\frac{\delta Mass}{\delta M_J}$ . The population of the very lowest-mass stars that appear as L dwarfs span an extremely small range in mass ( $0.075 < M_\odot < 0.085$ ) and, as a result, are rare. The brown dwarfs in this effective temperature regime are relatively young and are at the high-mass extreme, near the hydrogen-burning limit.

Brown dwarfs dominate the counts beyond the plateau in  $\Phi(M_J)$  at  $M_J \sim 13.5$  ( $\sim$ L4), and the upturn in number densities reflects the slow down in cooling rates at lower temperatures. For example, a  $0.07 M_\odot$  brown dwarf takes 2.7 Gyrs to evolve down the L dwarf sequence, but remains a (cooling) T dwarf ( $T_{eff} \approx 1400\text{--}600$  K) for  $\sim 30$  Gyrs, or more than 2 Hubble times; a low-mass,  $0.025 M_\odot$  brown dwarf spends only 120 Myrs as an L dwarf, but 1.5 Gyrs as a T dwarf (Burrows et al. 2001).

As noted in § 6.5, early-type T dwarfs also contribute to the  $\Phi(M_J)$  at magnitudes fainter than  $M_J = 14$ . Evolutionary models suggest that there may be as many as 80 T0–T5

dwarfs within 20 parsecs (Burgasser 2004b), as compared with the 12 late-type L dwarfs contributing to our luminosity function at  $M_J > 14$ . Incorporating those cooler dwarfs in the analysis is likely to lead to a steeply increasing  $\Phi(M_J)$ .

Clearly, one of the aims in deriving the luminosity function for ultracool dwarfs is setting constraints on the mass function, usually parameterized as a power-law,  $\frac{dN}{dM} \propto M^{-\alpha}$ , where the Salpeter value is  $\alpha = 2.5$ . Schultheis et al. (2006) have recently proposed that  $\alpha > 2$  at low masses (implying that brown dwarfs and low-mass stars essentially account for dark matter). This is in contrast to values of  $\alpha \sim 1$  derived in most other analysis, such as Reid et al. (2002a)<sup>12</sup>. A full discussion of this issue is beyond the scope of the present paper. However, we note that the Schultheis et al. analysis rests on matching models against the *V*-band luminosity function for nearby stars, and is therefore very weakly constrained for  $0.1M_\odot < M < 0.15M_\odot$  and essentially unconstrained at lower masses. Burgasser (2004b) and Allen et al. (2005) have shown that our initial results presented in Paper V (which are in general agreement with the luminosity function derived here) are consistent with a range of values of  $\alpha < 1.5$ . While this upper limit is not fully satisfying, it is in disagreement with the steeply re-rising mass function as proposed by Schultheis et al..

## 8. Summary

We have mined the 2MASS Second Incremental Data Release PSC for ultracool dwarfs within 20 parsecs of the Sun. Extensive spectroscopic follow-up has led to the discovery of  $\sim 100$  L dwarfs and  $\sim 200$  late-M dwarfs—over 50 of these are within 20 pc (Paper V, and this paper), doubling the local census of ultracool dwarfs. In these data we have also uncovered several wide binaries, a handful of young objects, and two slightly metal-poor L dwarfs. Combining our data with previously known nearby late-type dwarfs, we have used 99 objects in 91 systems to estimate the *J* and *K<sub>S</sub>*-band luminosity functions of ultracool dwarfs in the Solar Neighborhood. This work has provided the first robust estimate of the luminosity function of late-type stars and brown dwarfs. We have measured the density of late-M dwarfs (M7–M9.5) to be  $4.9 \pm 0.6 \times 10^{-3} \text{ pc}^{-3}$  and the density of L dwarfs to be at least  $3.8 \pm 0.6 \times 10^{-3} \text{ pc}^{-3}$ . Reliable discrimination between different models for the underlying mass function must await observational surveys that probe brown dwarfs at temperatures below  $\sim 600$  K, likely near the boundary between T and Y dwarfs.

---

<sup>12</sup>Note that Schultheis et al. are incorrect in suggesting that the nearby star sample employed in this analysis has significant incompleteness.



We would like to acknowledge the numerous NOAO telescope operators and support staff at Kitt Peak, Cerro Tololo, Cerro Panchon, and Mauna Kea that made this work possible and endured our busy observing program: S. Adams, A. Alvarez, T. Beck, M. Bergmann, R. Carrasco, G. Doppmann, E. Eastburn, A. Fhima, B. Gillespie, P. Gomez, A. Guerra, M. Hainaut-Rouelle, H. Halbedel, D. Harmer, K. Labrie, L. Macri, H. Mathis, A. Matulonis, D. Maturana, S. Pizarro, P. Prado, K. Roth, K. Volk, and D. Willmarth. We also thank the NOAO Telescope Allocation committees for their enduring support of this project. We acknowledge Finlay Mungall for observing assistance. K. L. C is supported by a NSF Astronomy and Astrophysics Postdoctoral Fellowship under AST-0401418. This research was partially supported by a grant from the NASA/NSF NStars initiative, administered by JPL, Pasadena, CA. This publication makes use of data products from the Two Micron All Sky Survey, which is a joint project of the University of Massachusetts and Infrared Processing and Analysis Center/California Institute of Technology, funded by the National Aeronautics and Space Administration and the National Science Foundation; the NASA/IPAC Infrared Science Archive, which is operated by the Jet Propulsion Laboratory/California Institute of Technology, under contract with the National Aeronautics and Space Administration. Based on observations obtained with the Apache Point Observatory 3.5-meter telescope, which is owned and operated by the Astrophysical Research Consortium. Based on observations obtained at the Gemini Observatory, which is operated by the Association of Universities for Research in Astronomy, Inc., under a cooperative agreement with the NSF on behalf of the Gemini partnership: the National Science Foundation (United States), the Particle Physics and Astronomy Research Council (United Kingdom), the National Research Council (Canada), CONICYT (Chile), the Australian Research Council (Australia), CNPq (Brazil) and CONICET (Argentina) This research has made use of the SIMBAD database, operated at CDS, Strasbourg, France.

*Facilities:* FLWO:2MASS, CTIO:2MASS, Mayall (MARS), Blanco (RC Spec), Gemini:South (GMOS), Gemini:Gillett (GMOS), KPNO:2.1m (GoldCam), CTIO:1.5m (RC Spec), ARC (DIS II)

## REFERENCES

- Ackerman, A. S. & Marley, M. S. 2001, ApJ, 556, 872
- Allen, P. R., Koerner, D. W., Reid, I. N., & Trilling, D. E. 2005, ApJ, 625, 385
- Basri, G. & Reiners, A. 2006, AJ, 132, 663
- Bessell, M. S. 1991, AJ, 101, 662

- Borysow, A., Jorgensen, U. G., & Zheng, C. 1997, *A&A*, 324, 185
- Bouy, H., Brandner, W., Martín, E. L., Delfosse, X., Allard, F., & Basri, G. 2003, *AJ*, 126, 1526
- Bouy, H., Martín, E. L., Brandner, W., & Bouvier, J. 2005, *AJ*, 129, 511
- Burgasser, A. J. 2002, Ph.D. Thesis
- . 2004a, *ApJ*, 614, L73
- . 2004b, *ApJS*, 155, 191
- Burgasser, A. J., Cruz, K. L., & Kirkpatrick, J. D. 2006a, *ApJ*, submitted
- Burgasser, A. J., Kirkpatrick, J. D., Burrows, A., Liebert, J., Reid, I. N., Gizis, J. E., McGovern, M. R., Prato, L., & McLean, I. S. 2003a, *ApJ*, 592, 1186
- Burgasser, A. J., Kirkpatrick, J. D., Cruz, K. L., Reid, I. N., Leggett, S. K., Liebert, J., Burrows, A., & Brown, M. E. 2006b, *ApJ*, in press (astro-ph/0605577)
- Burgasser, A. J., Kirkpatrick, J. D., Liebert, J., & Burrows, A. 2003b, *ApJ*, 594, 510
- Burgasser, A. J., Kirkpatrick, J. D., & Lowrance, P. J. 2005a, *AJ*, 129, 2849
- Burgasser, A. J., Marley, M. S., Ackerman, A. S., Saumon, D., Lodders, K., Dahn, C. C., Harris, H. C., & Kirkpatrick, J. D. 2002, *ApJ*, 571, L151
- Burgasser, A. J., Reid, I. N., Leggett, S. K., Kirkpatrick, J. D., Liebert, J., & Burrows, A. 2005b, *ApJ*, 634, L177
- Burgasser, A. J., Reid, I. N., Siegler, N., Close, L., Allen, P., Lowrance, P., & Gizis, J. 2006c, in *Planets and Protostars V*, ed. B. Reipurth, D. Jewitt, & K. Keil (Tucson: University of Arizona Press) (astro-ph/0602122)
- Burrows, A., Hubbard, W. B., Lunine, J. I., & Liebert, J. 2001, *Reviews of Modern Physics*, 73, 719
- Chabrier, G. 2003, *PASP*, 115, 763
- Chabrier, G. & Baraffe, I. 2000, *ARA&A*, 38, 337
- Chabrier, G., Baraffe, I., Allard, F., & Hauschildt, P. 2000, *ApJ*, 542, 464

- Chiu, K., Fan, X., Leggett, S. K., Golimowski, D. A., Zheng, W., Geballe, T. R., Schneider, D. P., & Brinkmann, J. 2006, *AJ*, 131, 2722
- Close, L. M., Siegler, N., Freed, M., & Biller, B. 2003, *ApJ*, 587, 407
- Close, L. M., Siegler, N., Potter, D., Brandner, W., & Liebert, J. 2002, *ApJ*, 567, L53
- Costa, E., Méndez, R. A., Jao, W.-C., Henry, T. J., Subasavage, J. P., Brown, M. A., Ianna, P. A., & Bartlett, J. 2005, *AJ*, 130, 337
- Crifo, F., Phan-Bao, N., Delfosse, X., Forveille, T., Guibert, J., Martín, E. L., & Reylé, C. 2005, *A&A*, 441, 653
- Cruz, K. L., Burgasser, A. J., Reid, I. N., & Liebert, J. 2004, *ApJ*, 604, L61
- Cruz, K. L. & Reid, I. N. 2002, *AJ*, 123, 2828
- Cruz, K. L., Reid, I. N., Liebert, J., Allen, P. R., Kirkpatrick, J. D., Burgasser, A. J., & Solomon, A. R. 2006, in prep.
- Cruz, K. L., Reid, I. N., Liebert, J., Kirkpatrick, J. D., & Lowrance, P. J. 2003, *AJ*, 126, 2421
- Cushing, M. C. & Vacca, W. D. 2006, *AJ*, 131, 1797
- Dahn, C. C., Harris, H. C., Vrba, F. J., Guetter, H. H., Canzian, B., Henden, A. A., Levine, S. E., Luginbuhl, C. B., Monet, A. K. B., Monet, D. G., Pier, J. R., Stone, R. C., Walker, R. L., Burgasser, A. J., Gizis, J. E., Kirkpatrick, J. D., Liebert, J., & Reid, I. N. 2002, *AJ*, 124, 1170
- Deacon, N. R., Hambly, N. C., & Cooke, J. A. 2005, *A&A*, 435, 363
- Delfosse, X., Forveille, T., Ségransan, D., Beuzit, J.-L., Udry, S., Perrier, C., & Mayor, M. 2000, *A&A*, 364, 217
- Delfosse, X., Tinney, C. G., Forveille, T., Epchtein, N., Bertin, E., Borsenberger, J., Copet, E., de Batz, B., Fouque, P., Kimeswenger, S., Le Bertre, T., Lacombe, F., Rouan, D., & Tiphene, D. 1997, *A&A*, 327, L25
- Downes, R., Webbink, R. F., & Shara, M. M. 1997, *PASP*, 109, 345
- Fan, X., Knapp, G. R., Strauss, M. A., Gunn, J. E., Lupton, R. H., Ivezić, Ž., Rockosi, C. M., Yanny, B., Kent, S., Schneider, D. P., Kirkpatrick, J. D., Annis, J., Bastian, S., Berman, E., Brinkmann, J., Csabai, I., Federwitz, G. R., Fukugita, M., Gurbani,

- V. K., Hennessy, G. S., Hindsley, R. B., Ichikawa, T., Lamb, D. Q., Lindenmeyer, C., Mantsch, P. M., McKay, T. A., Munn, J. A., Nash, T., Okamura, S., Pauls, A. G., Pier, J. R., Rechenmacher, R., Rivetta, C. H., Sergey, G., Stoughton, C., Szalay, A. S., Szokoly, G. P., Tucker, D. L., York, D. G., & The SDSS Collaboration. 2000, *AJ*, 119, 928
- Forveille, T., Beuzit, J.-L., Delorme, P., Ségransan, D., Delfosse, X., Chauvin, G., Fusco, T., Lagrange, A.-M., Mayor, M., Montagnier, G., Mouillet, D., Perrier, C., Udry, S., Charton, J., Gigan, P., Conan, J.-M., Kern, P., & Michet, G. 2005, *A&A*, 435, L5
- Freed, M., Close, L. M., & Siegler, N. 2003, *ApJ*, 584, 453
- Garcia, B. 1989, *Bull. Inf. Centre Donnees Stellaires*, 36, 27
- Geballe, T. R., Knapp, G. R., Leggett, S. K., Fan, X., Golimowski, D. A., Anderson, S., Brinkmann, J., Csabai, I., Gunn, J. E., Hawley, S. L., Hennessy, G., Henry, T. J., Hill, G. J., Hindsley, R. B., Ivezić, Ž., Lupton, R. H., McDaniel, A., Munn, J. A., Narayanan, V. K., Peng, E., Pier, J. R., Rockosi, C. M., Schneider, D. P., Smith, J. A., Strauss, M. A., Tsvetanov, Z. I., Uomoto, A., York, D. G., & Zheng, W. 2002, *ApJ*, 564, 466
- Gelino, C. R., Kulkarni, S. R., & Stephens, D. C. 2006, *PASP*, 118, 611
- Gelino, C. R., Marley, M. S., Holtzman, J. A., Ackerman, A. S., & Lodders, K. 2002, *ApJ*, 577, 433
- Gizis, J. E. 2002, *ApJ*, 575, 484
- Gizis, J. E., Monet, D. G., Reid, I. N., Kirkpatrick, J. D., Liebert, J., & Williams, R. J. 2000, *AJ*, 120, 1085
- Gizis, J. E. & Reid, I. N. 1997, *PASP*, 109, 849
- Gizis, J. E., Reid, I. N., Knapp, G. R., Liebert, J., Kirkpatrick, J. D., Koerner, D. W., & Burgasser, A. J. 2003, *AJ*, 125, 3302
- Gizis, J. E., Reid, I. N., & Monet, D. G. 1999, *AJ*, 118, 997
- Golimowski, D. A., Leggett, S. K., Marley, M. S., Fan, X., Geballe, T. R., Knapp, G. R., Vrba, F. J., Henden, A. A., Luginbuhl, C. B., Guetter, H. H., Munn, J. A., Canzian, B., Zheng, W., Tsvetanov, Z. I., Chiu, K., Glazebrook, K., Hoversten, E. A., Schneider, D. P., & Brinkmann, J. 2004, *AJ*, 127, 3516

- Gorlova, N. I., Meyer, M. R., Rieke, G. H., & Liebert, J. 2003, *ApJ*, 593, 1074
- Hamuy, M., Suntzeff, N. B., Heathcote, S. R., Walker, A. R., Gigoux, P., & Phillips, M. M. 1994, *PASP*, 106, 566
- Hartwick, F. D. A., Cowley, A. P., & Mould, J. R. 1984, *ApJ*, 286, 269
- Hawkins, M. R. S. & Bessell, M. S. 1988, *MNRAS*, 234, 177
- Hawley, S. L., Covey, K. R., Knapp, G. R., Golimowski, D. A., Fan, X., Anderson, S. F., Gunn, J. E., Harris, H. C., Ivezić, Ž., Long, G. M., Lupton, R. H., McGehee, P. M., Narayanan, V., Peng, E., Schlegel, D., Schneider, D. P., Spahn, E. Y., Strauss, M. A., Szkody, P., Tsvetanov, Z., Walkowicz, L. M., Brinkmann, J., Harvanek, M., Hennessy, G. S., Kleinman, S. J., Krzesinski, J., Long, D., Neilsen, E. H., Newman, P. R., Nitta, A., Snedden, S. A., & York, D. G. 2002, *AJ*, 123, 3409
- Henry, T. J., Franz, O. G., Wasserman, L. H., Benedict, G. F., Shelus, P. J., Ianna, P. A., Kirkpatrick, J. D., & McCarthy, D. W. 1999, *ApJ*, 512, 864
- Høg, E., Fabricius, C., Makarov, V. V., Urban, S., Corbin, T., Wycoff, G., Bastian, U., Schwkendiek, P., & Wicenec, A. 2000, *A&A*, 355, L27
- Hook, I. M., Jørgensen, I., Allington-Smith, J. R., Davies, R. L., Metcalfe, N., Murowinski, R. G., & Crampton, D. 2004, *PASP*, 116, 425
- Irwin, M., McMahon, R. G., & Reid, N. 1991, *MNRAS*, 252, 61P
- Kendall, T. R., Maun, N., Azzopardi, M., & Gigoyan, K. 2003, *A&A*, 403, 929
- Kirkpatrick, J. D. 1992, Ph.D. Thesis
- Kirkpatrick, J. D., Barman, T. S., Burgasser, A. J., McGovern, M. R., McLean, I. S., Tinney, C. G., & Lowrance, P. J. 2006a, *ApJ*, 639, 1120
- Kirkpatrick, J. D., Dahn, C. C., Monet, D. G., Reid, I. N., Gizis, J. E., Liebert, J., & Burgasser, A. J. 2001a, *AJ*, 121, 3235
- Kirkpatrick, J. D., Henry, T. J., & Irwin, M. J. 1997, *AJ*, 113, 1421
- Kirkpatrick, J. D., Henry, T. J., & McCarthy, D. W. 1991, *ApJS*, 77, 417
- Kirkpatrick, J. D., Henry, T. J., & Simons, D. A. 1995, *AJ*, 109, 797
- Kirkpatrick, J. D., Kirkpatrick, J. D., Kirkpatrick, J. D., & Kirkpatrick, J. D. 2006b, in prep.

—. 2006c, in prep.

—. 2006d, in prep.

Kirkpatrick, J. D., Liebert, J., Cruz, K. L., Gizis, J. E., & Reid, I. N. 2001b, *PASP*, 113, 814

Kirkpatrick, J. D., Reid, I. N., Liebert, J., Cutri, R. M., Nelson, B., Beichman, C. A., Dahn, C. C., Monet, D. G., Gizis, J. E., & Skrutskie, M. F. 1999, *ApJ*, 519, 802

Kirkpatrick, J. D., Reid, I. N., Liebert, J., Gizis, J. E., Burgasser, A. J., Monet, D. G., Dahn, C. C., Nelson, B., & Williams, R. J. 2000, *AJ*, 120, 447

Knapp, G. R., Leggett, S. K., Fan, X., Marley, M. S., Geballe, T. R., Golimowski, D. A., Finkbeiner, D., Gunn, J. E., Hennawi, J., Ivezić, Z., Lupton, R. H., Schlegel, D. J., Strauss, M. A., Tsvetanov, Z. I., Chiu, K., Hoversten, E. A., Glazebrook, K., Zheng, W., Hendrickson, M., Williams, C. C., Uomoto, A., Vrba, F. J., Henden, A. A., Luginbuhl, C. B., Guetter, H. H., Munn, J. A., Canzian, B., Schneider, D. P., & Brinkmann, J. 2004, *AJ*, 127, 3553

Koerner, D. W., Kirkpatrick, J. D., McElwain, M. W., & Bonaventura, N. R. 1999, *ApJ*, 526, L25

Lépine, S., Rich, R. M., & Shara, M. M. 2003a, *ApJ*, 591, L49

—. 2003b, *AJ*, 125, 1598

Lépine, S. & Shara, M. M. 2005, *AJ*, 129, 1483

Leggett, S. K., Geballe, T. R., Fan, X., Schneider, D. P., Gunn, J. E., Lupton, R. H., Knapp, G. R., Strauss, M. A., McDaniel, A., Golimowski, D. A., Henry, T. J., Peng, E., Tsvetanov, Z. I., Uomoto, A., Zheng, W., Hill, G. J., Ramsey, L. W., Anderson, S. F., Annis, J. A., Bahcall, N. A., Brinkmann, J., Chen, B., Csabai, I., Fukugita, M., Hennessy, G. S., Hindsley, R. B., Ivezić, Ž., Lamb, D. Q., Munn, J. A., Pier, J. R., Schlegel, D. J., Smith, J. A., Stoughton, C., Thakar, A. R., & York, D. G. 2000, *ApJ*, 536, L35

Leinert, C., Allard, F., Richichi, A., & Hauschildt, P. H. 2000, *A&A*, 353, 691

Leinert, C., Weitzel, N., Richichi, A., Eckart, A., & Tacconi-Garman, L. E. 1994, *A&A*, 291, L47

Lépine, S. 2005, *AJ*, 130, 1680

- Liebert, J., Boroson, T. A., & Giampapa, M. S. 1984, *ApJ*, 282, 758
- Liebert, J., Kirkpatrick, J. D., Cruz, K. L., Reid, I. N., Burgasser, A., Tinney, C. G., & Gizis, J. E. 2003, *AJ*, 125, 343
- Linsky, J. L. 1969, *ApJ*, 156, 989
- Liu, M. C. and Leggett, S. K. and Golimowski, D. A. and Chiu, K. and Fan, X. and Geballe, T. R. and Schneider, D. P. and Brinkmann, J. 2006, *ApJ*, 647, 1393
- Liu, M. C. & Leggett, S. K. 2005, *ApJ*, 634, 616
- Liu, W., Hu, J. Y., Li, Z. Y., & Cao, L. 1999, *ApJS*, 122, 257
- Lodieu, N., Scholz, R.-D., & McCaughrean, M. J. 2002, *A&A*, 389, L20
- Luyten, W. J. 1979a, LHS catalogue. A catalogue of stars with proper motions exceeding  $0''5$  annually (Minneapolis: University of Minnesota, 1979, 2nd ed.)
- . 1979b, New Luyten Catalog of stars with proper motions larger than two tenths of an arcsecond (Minneapolis: University of Minnesota, 1979, 2nd ed.)
- Maiti, M., Sengupta, S., Parihar, P. S., & Anupama, G. C. 2005, *ApJ*, 619, L183
- Malmquist, K. G. 1920, *Lund Medd. Astron. Obs. Ser. II*, 22
- Marley, M. S., Seager, S., Saumon, D., Lodders, K., Ackerman, A. S., Freedman, R. S., & Fan, X. 2002, *ApJ*, 568, 335
- Martin, E. L., Brandner, W., & Basri, G. 1999, *Science*, 283, 1718
- Martín, E. L., Delfosse, X., Basri, G., Goldman, B., Forveille, T., & Zapatero Osorio, M. R. 1999, *AJ*, 118, 2466
- Martín, E. L., Rebolo, R., & Zapatero-Osorio, M. R. 1996, *ApJ*, 469, 706
- Massey, P. & Gronwall, C. 1990, *ApJ*, 358, 344
- Massey, P., Strobel, K., Barnes, J. V., & Anderson, E. 1988, *ApJ*, 328, 315
- McGovern, M. R., Kirkpatrick, J. D., McLean, I. S., Burgasser, A. J., Prato, L., & Lowrance, P. J. 2004, *ApJ*, 600, 1020
- McLean, I. S., McGovern, M. R., Burgasser, A. J., Kirkpatrick, J. D., Prato, L., & Kim, S. S. 2003, *ApJ*, 596, 561

- Monet, D. G., Dahn, C. C., Vrba, F. J., Harris, H. C., Pier, J. R., Luginbuhl, C. B., & Ables, H. D. 1992, *AJ*, 103, 638
- Morrison, J. E., Röser, S., McLean, B., Bucciarelli, B., & Lasker, B. 2001, *AJ*, 121, 1752
- Nordström, B., Mayor, M., Andersen, J., Holmberg, J., Pont, F., Jørgensen, B. R., Olsen, E. H., Udry, S., & Mowlavi, N. 2004, *A&A*, 418, 989
- Oke, J. B. & Gunn, J. E. 1983, *ApJ*, 266, 713
- Perryman, M. A. C. & ESA. 1997, The HIPPARCOS and TYCHO catalogues. Astrometric and photometric star catalogues derived from the ESA HIPPARCOS Space Astrometry Mission (The Hipparcos and Tycho catalogues. Astrometric and photometric star catalogues derived from the ESA Hipparcos Space Astrometry Mission, Publisher: Noordwijk, Netherlands: ESA Publications Division, 1997, Series: ESA SP Series vol no: 1200, ISBN: 9290923997 (set))
- Phan-Bao, N., Crifo, F., Delfosse, X., Forveille, T., Guibert, J., Borsenberger, J., Epchtein, N., Fouqué, P., Simon, G., & Vetois, J. 2003, *A&A*, 401, 959
- Phan-Bao, N., Guibert, J., Crifo, F., Delfosse, X., Forveille, T., Borsenberger, J., Epchtein, N., Fouqué, P., & Simon, G. 2001, *A&A*, 380, 590
- Pokorny, R. S., Jones, H. R. A., Hambly, N. C., & Pinfield, D. J. 2004, *A&A*, 421, 763
- Ratzka, T. and Leinert, C. and Allard, F., in prep.
- Reid, I. N. 2003, *AJ*, 126, 2449
- Reid, I. N. & Cruz, K. L. 2002, *AJ*, 123, 2806
- Reid, I. N., Cruz, K. L., Allen, P., Mungall, F., Kilkenny, D., Liebert, J., Hawley, S. L., Fraser, O. J., Covey, K. R., & Lowrance, P. 2003a, *AJ*, 126, 3007
- Reid, I. N., Cruz, K. L., Allen, P., Mungall, F., Kilkenny, D., Liebert, J., Hawley, S. L., Fraser, O. J., Covey, K. R., Lowrance, P., Kirkpatrick, J. D., & Burgasser, A. J. 2004, *AJ*, 128, 463
- Reid, I. N., Cruz, K. L., Laurie, S. P., Liebert, J., Dahn, C. C., Harris, H. C., Guetter, H. H., Stone, R. C., Canzian, B., Luginbuhl, C. B., Levine, S. E., Monet, A. K. B., & Monet, D. G. 2003b, *AJ*, 125, 354
- . 2006a, in prep.



- Reid, I. N. & Gizis, J. E. 2005, *PASP*, 117, 676
- Reid, I. N., Gizis, J. E., & Hawley, S. L. 2002a, *AJ*, 124, 2721
- Reid, I. N., Gizis, J. E., Kirkpatrick, J. D., & Koerner, D. W. 2001, *AJ*, 121, 489
- Reid, I. N., Hawley, S. L., & Gizis, J. E. 1995, *AJ*, 110, 1838
- Reid, I. N., Kilkenny, D., & Cruz, K. L. 2002b, *AJ*, 123, 2822
- Reid, I. N., Kirkpatrick, J. D., Liebert, J., Burrows, A., Gizis, J. E., Burgasser, A., Dahn, C. C., Monet, D., Cutri, R., Beichman, C. A., & Skrutskie, M. 1999, *ApJ*, 521, 613
- Reid, I. N., Kirkpatrick, J. D., Liebert, J., Gizis, J. E., Dahn, C. C., & Monet, D. G. 2002c, *AJ*, 124, 519
- Reid, I. N., Lewitus, E., Allen, P. R., Cruz, K. L., & Burgasser, A. J. 2006b, *AJ*, 132, 891
- Reid, I. N., Lewitus, E., Burgasser, A. J., & Cruz, K. L. 2006c, *ApJ*, 639, 1114
- Reiners, A. & Basri, G. 2006, *AJ*, 131, 1806
- Reylé, C. & Robin, A. C. 2004, *A&A*, 421, 643
- Ruiz, M. T., Anguita, C., Maza, J., & Roth, M. 1990, *AJ*, 100, 1270
- Ruiz, M. T., Leggett, S. K., & Allard, F. 1997, *ApJ*, 491, L107+
- Ruiz, M. T., Wischnjewsky, M., Rojo, P. M., & Gonzalez, L. E. 2001, *ApJS*, 133, 119
- Saumon, D., Bergeron, P., Lunine, J. I., Hubbard, W. B., & Burrows, A. 1994, *ApJ*, 424, 333
- Schmidt, S. J., Cruz, K. L., Bongiorno, B., Reid, I. N., & Liebert, J. 2006, *AJ*, submitted.
- Schneider, D. P., Knapp, G. R., Hawley, S. L., Covey, K. R., Fan, X., Ramsey, L. W., Richards, G. T., Strauss, M. A., Gunn, J. E., Hill, G. J., MacQueen, P. J., Adams, M. T., Hill, G. M., Ivezić, Ž., Lupton, R. H., Pier, J. R., Saxe, D. H., Shetrone, M., Tufts, J. R., Wolf, M. J., Brinkmann, J., Csabai, I., Hennessy, G. S., & York, D. G. 2002, *AJ*, 123, 458
- Schultheis, M. and Robin, A. C. and Reylé, C. and McCracken, H. J. and Bertin, E. and Mellier, Y., & Le Fèvre, O. 2006, *A&A*, 447, 185
- Siegler, N., Close, L. M., Cruz, K. L., Martín, E. L., & Reid, I. N. 2005, *ApJ*, 621, 1023

- Skrutskie, M. F., Cutri, R. M., Stiening, R., Weinberg, M. D., Schneider, S., Carpenter, J. M., Beichman, C., Capps, R., Chester, T., Elias, J., Huchra, J., Liebert, J., Lonsdale, C., Monet, D. G., Price, S., Seitzer, P., Jarrett, T., Kirkpatrick, J. D., Gizis, J. E., Howard, E., Evans, T., Fowler, J., Fullmer, L., Hurt, R., Light, R., Kopan, E. L., Marsh, K. A., McCallon, H. L., Tam, R., Van Dyk, S., & Wheelock, S. 2006, *AJ*, 131, 1163
- Solomon, A. R., Cruz, K. L., Schmidt, S. J., Reid, I. N., & Kirkpatrick, J. D. 2006, in prep.
- Thorstensen, J. R. & Kirkpatrick, J. D. 2003, *PASP*, 115, 1207
- Tinney, C. G. 1996, *MNRAS*, 281, 644
- Tinney, C. G., Burgasser, A. J., & Kirkpatrick, J. D. 2003, *AJ*, 126, 975
- Tinney, C. G., Mould, J. R., & Reid, I. N. 1993, *AJ*, 105, 1045
- Tinney, C. G., Reid, I. N., Gizis, J., & Mould, J. R. 1995, *AJ*, 110, 3014
- van Altena, W. F., Lee, J. T., & Hoffleit, E. D. 1995, *The general catalogue of trigonometric [stellar] parallaxes* (New Haven, CT: Yale University Observatory, —c1995, 4th ed., completely revised and enlarged)
- Vrba, F. J., Henden, A. A., Luginbuhl, C. B., Guetter, H. H., Munn, J. A., Canzian, B., Burgasser, A. J., Kirkpatrick, J. D., Fan, X., Geballe, T. R., Golimowski, D. A., Knapp, G. R., Leggett, S. K., Schneider, D. P., & Brinkmann, J. 2004, *AJ*, 127, 2948
- Wilson, J. C. 2002, Ph.D. Thesis, Cornell Univ.

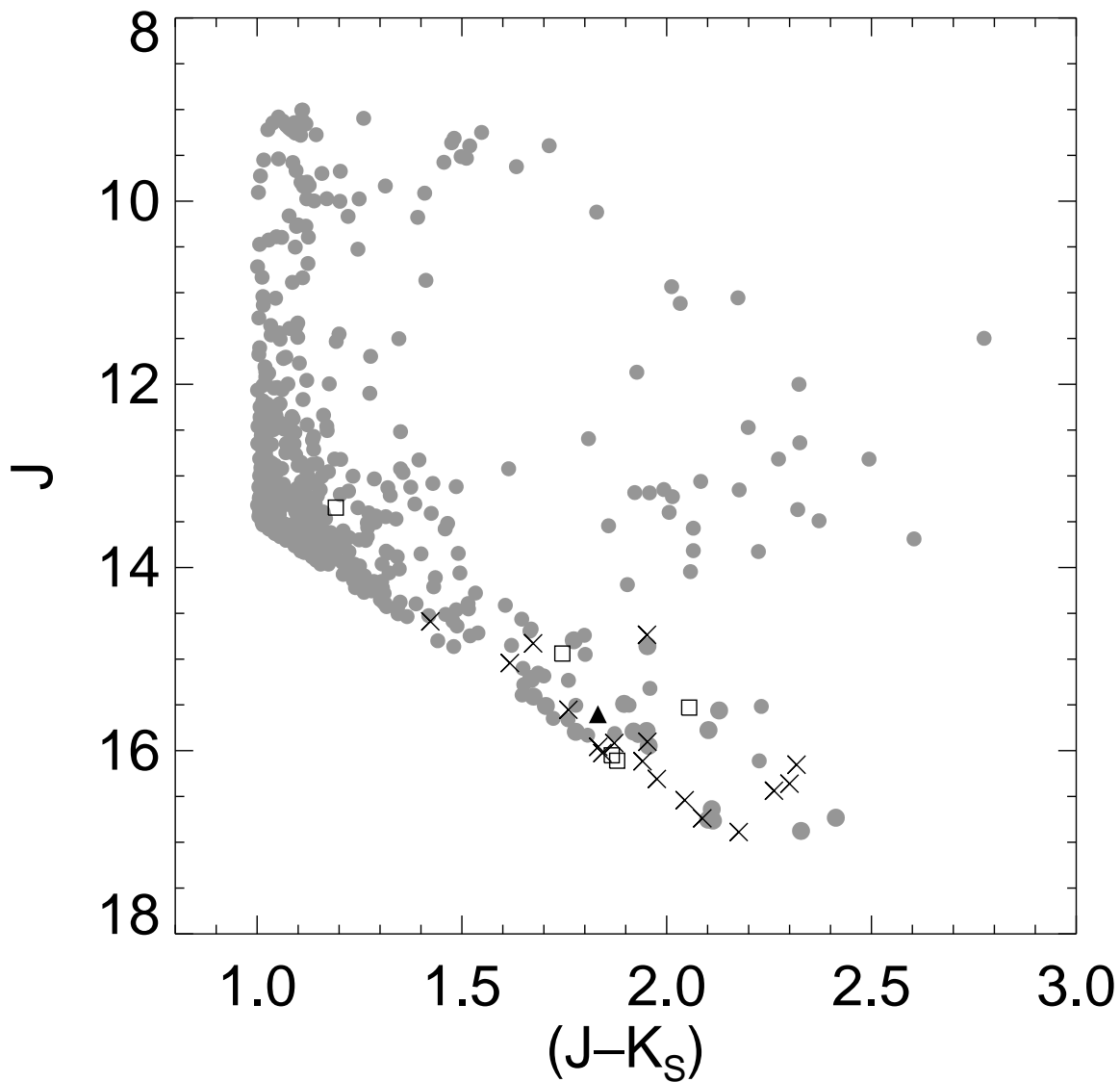


Fig. 1.— Status of the follow-up observations of the 518 candidate ultracool dwarfs in the 2MU2 sample. Far-red optical spectra (*circles*) have been obtained for 495 objects in the sample. Near-infrared spectra have been used to eliminate 17 fainter targets from the 20-pc 2MU2 sample (*crosses*) and to identify one object near the 20-pc distance limit that requires supplemental far-red data to determine its membership (*triangle*). Five objects have been classified using data from the literature (*squares*).

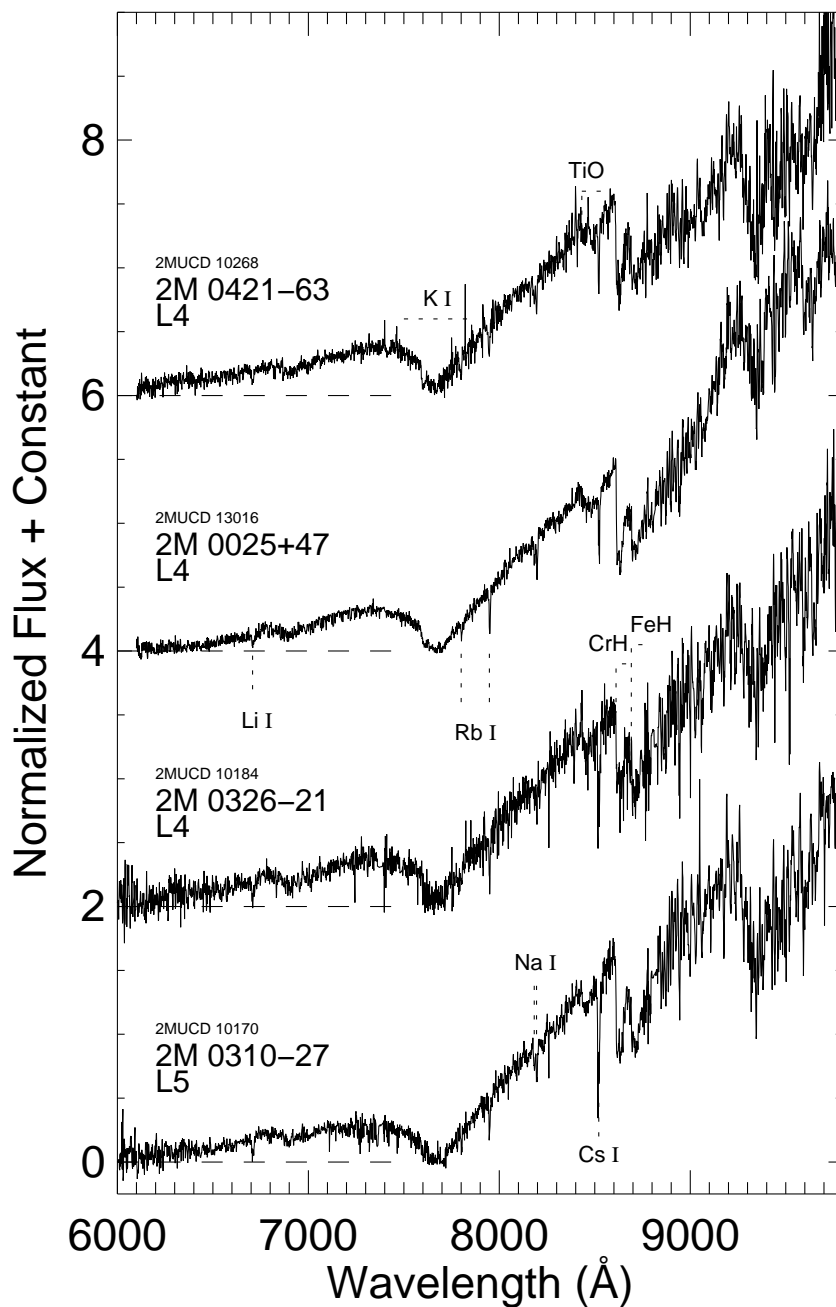


Fig. 2.— Gemini spectra of mid-L dwarfs where lithium absorption is detected. From top to bottom, the objects shown are: 2M 0421-63, 2M 0025+47, 2M 0326-21, and 2M 0310-27. The steep red slope of 2M 0025+47 is due to a problem with our Gemini North flux calibration. The bottom spectrum is not offset and the zero points of the offset spectra are shown by dashed lines.

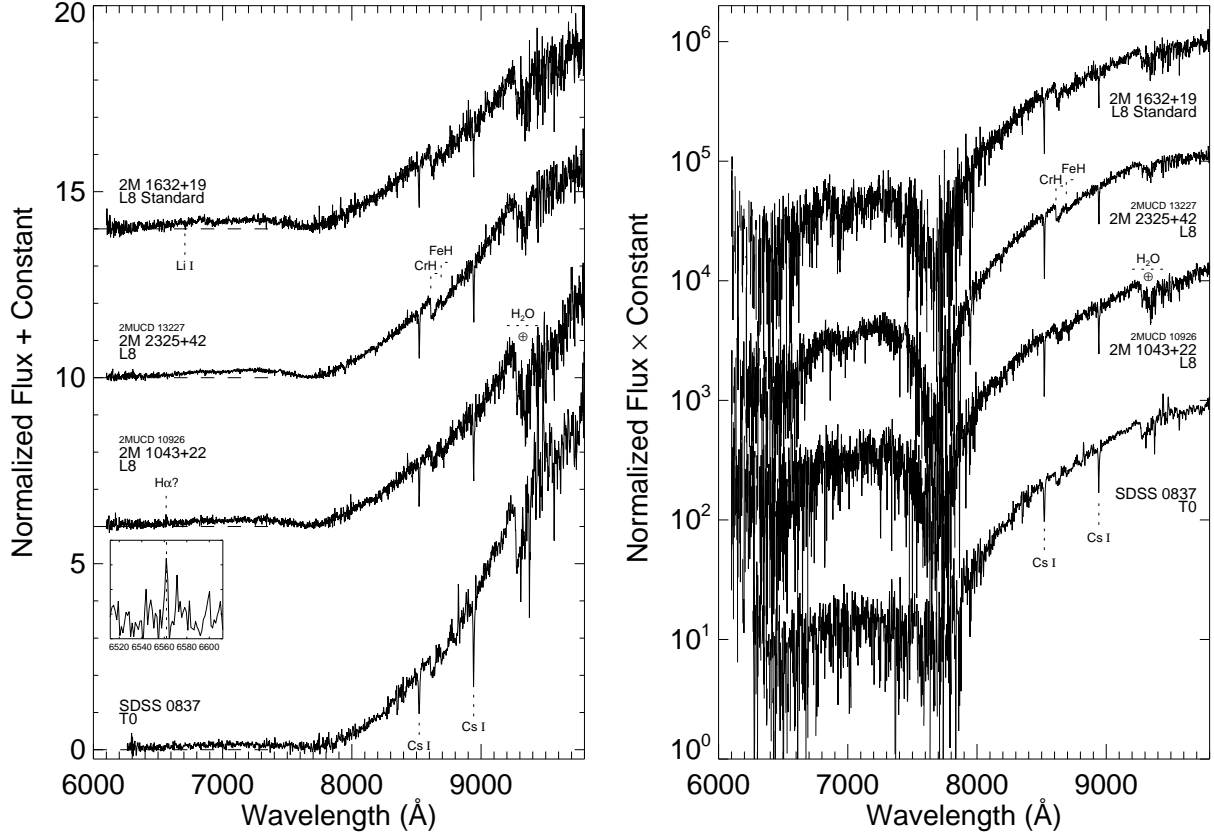


Fig. 3.— Spectra of the two latest-type objects in the present sample, 2M 2325+42 (*second-to-top*) and 2M 1043+22 (*second-to-bottom*), with the L8 spectral standard 2M 1632+19 (*top*, Kirkpatrick et al. 1999) and early-T dwarf SDSS 0837–00 (Leggett et al. 2000; Burgasser et al. 2003b; Kirkpatrick et al., in prep.). The bottom spectrum is not offset and the zero points of the offset spectra are shown by dashed lines.

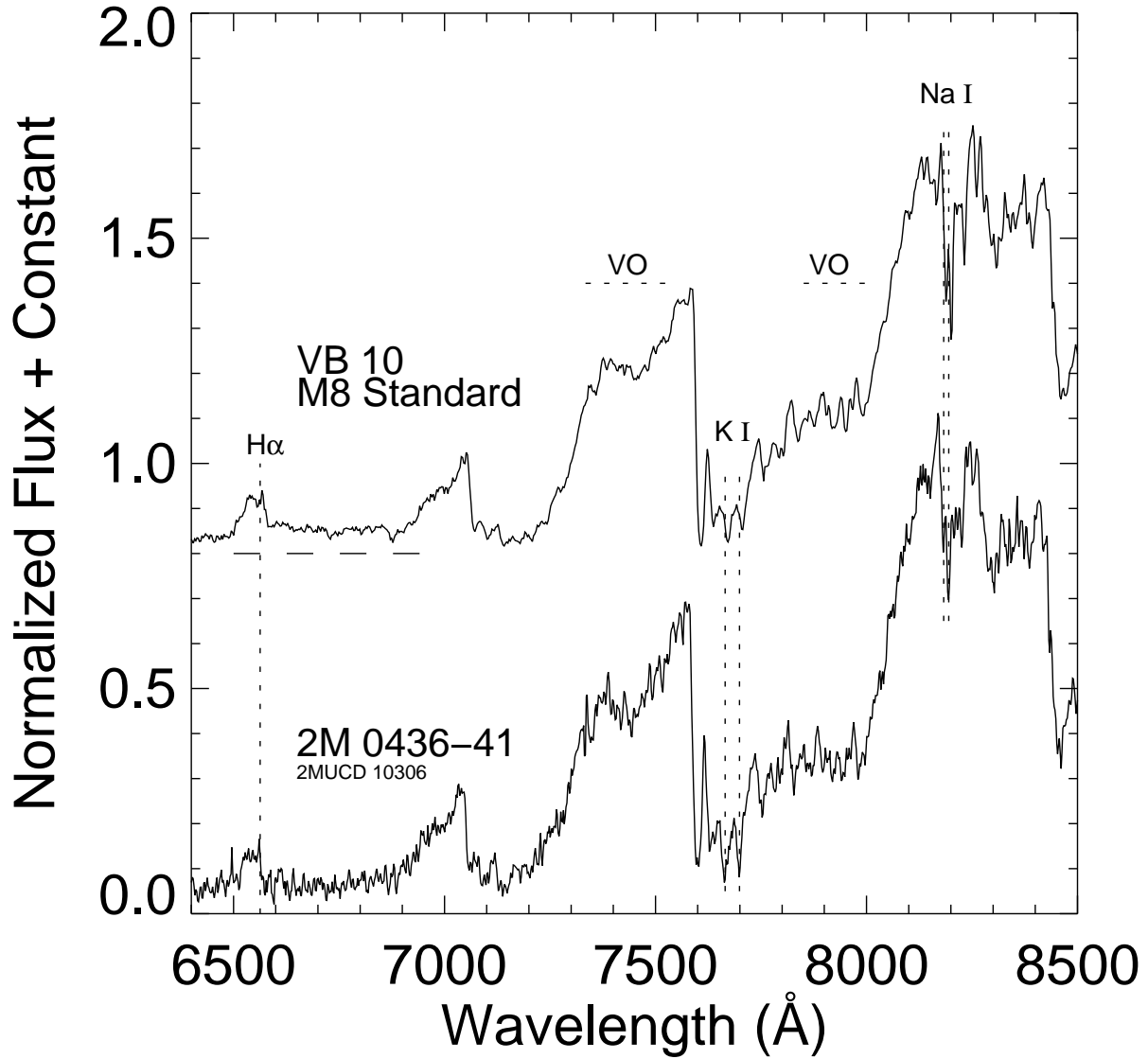


Fig. 4.— Spectrum of the low-gravity dwarf 2M 0436–41 with the M8 standard VB 10. Pressure/gravity sensitive features are marked. The bottom spectrum is not offset and the zero point of VB 10 is shown by a dashed line.

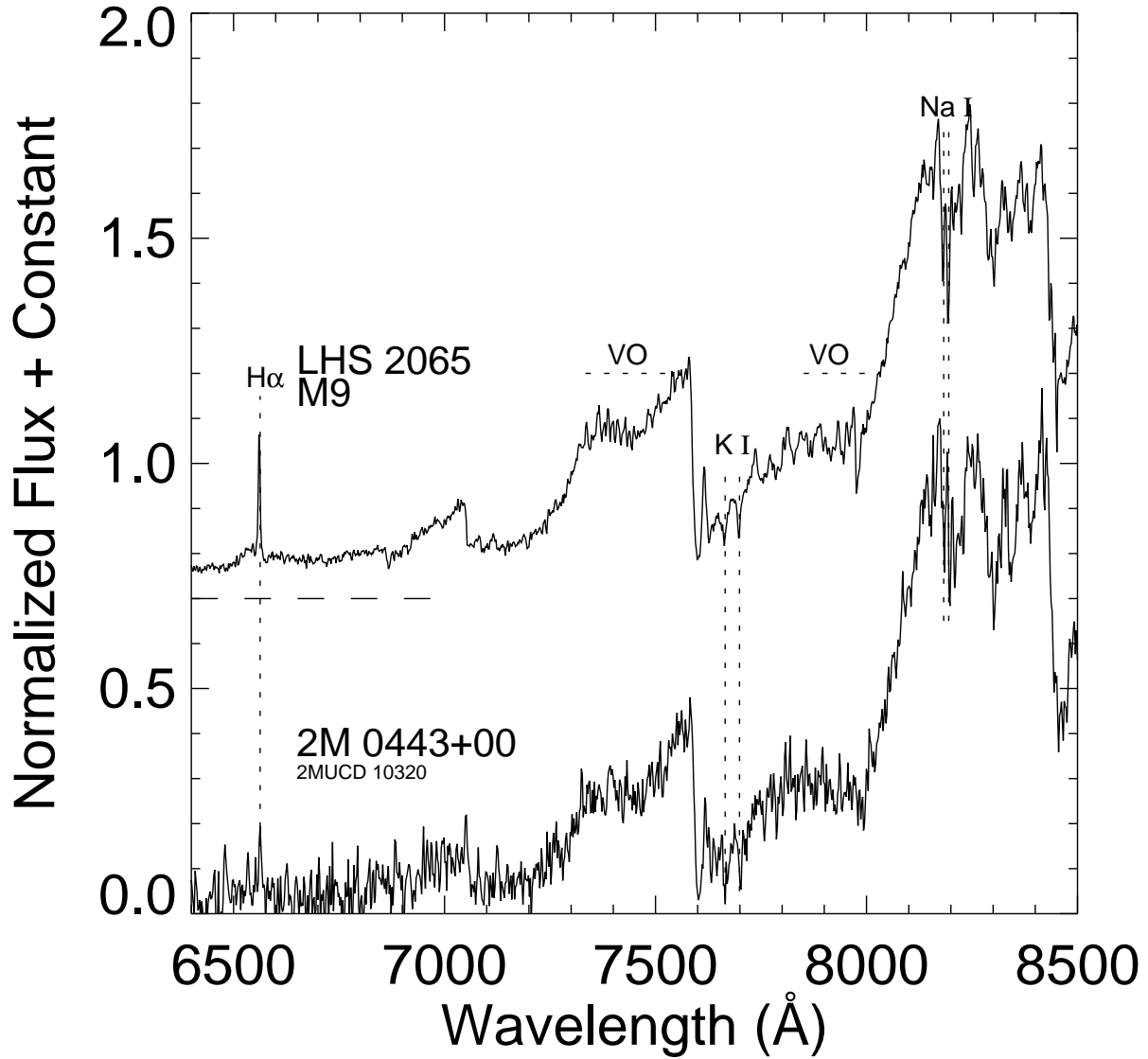


Fig. 5.— Spectrum of the low gravity dwarf 2M 0443+00 with the M9 standard LHS 2065. Pressure/gravity sensitive features are marked. The bottom spectrum is not offset and the zero point of LHS 2065 is shown by a dashed line.

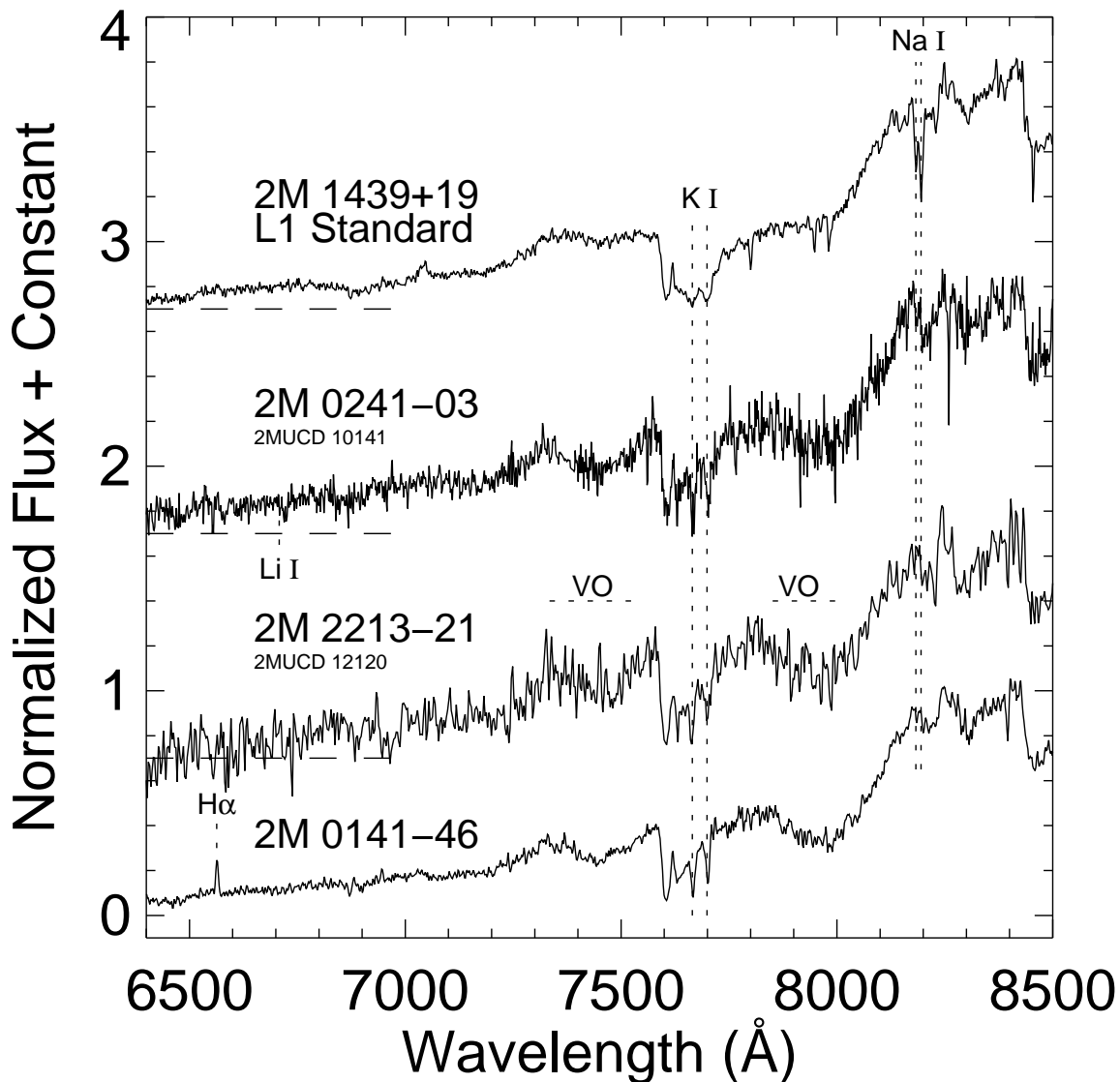


Fig. 6.— Spectrum of the low-gravity dwarfs, 2M 0241–03 (*second-to-top*) and 2M 2213–21 (*second-to-bottom*), with the L1 standard 2M 1439+19 (*top*, Kirkpatrick et al. 1999) and the young field dwarf 2M 0141-46 (*bottom*, Kirkpatrick et al. 2006a). Pressure/gravity sensitive features are marked. The locations of the  $H\alpha$  emission line and Li I absorption line are labeled but these features are not present in all spectra. The bottom spectrum is not offset and the zero points of the offset spectra are shown by dashed lines.



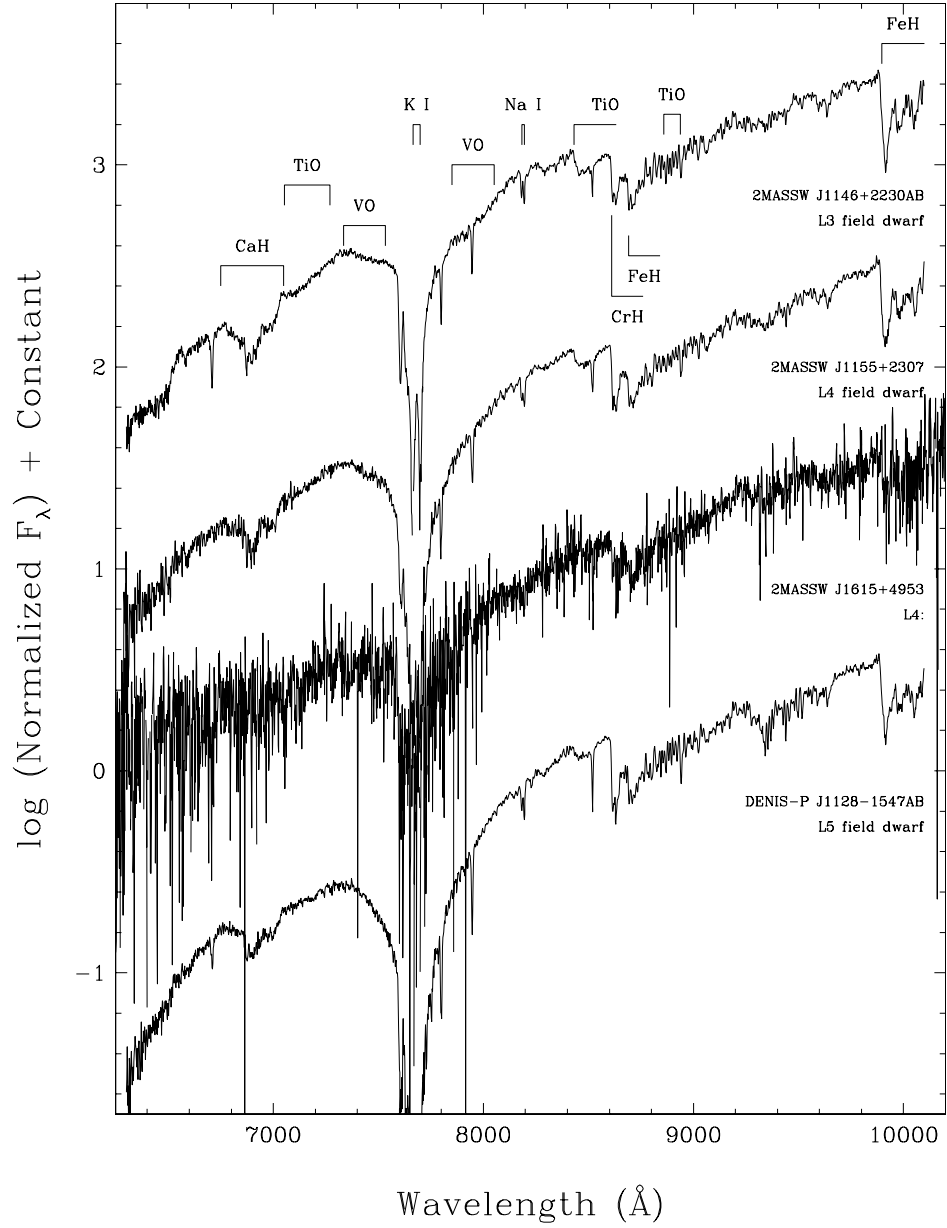


Fig. 7.— Spectrum of the low-gravity dwarf 2M 1615+49 compared to spectral standards of type L3, L4, and L5 from Kirkpatrick et al. (1999). The flux of each spectrum has been normalized to unity at 8250  $\text{\AA}$ , and constant offsets have been added.

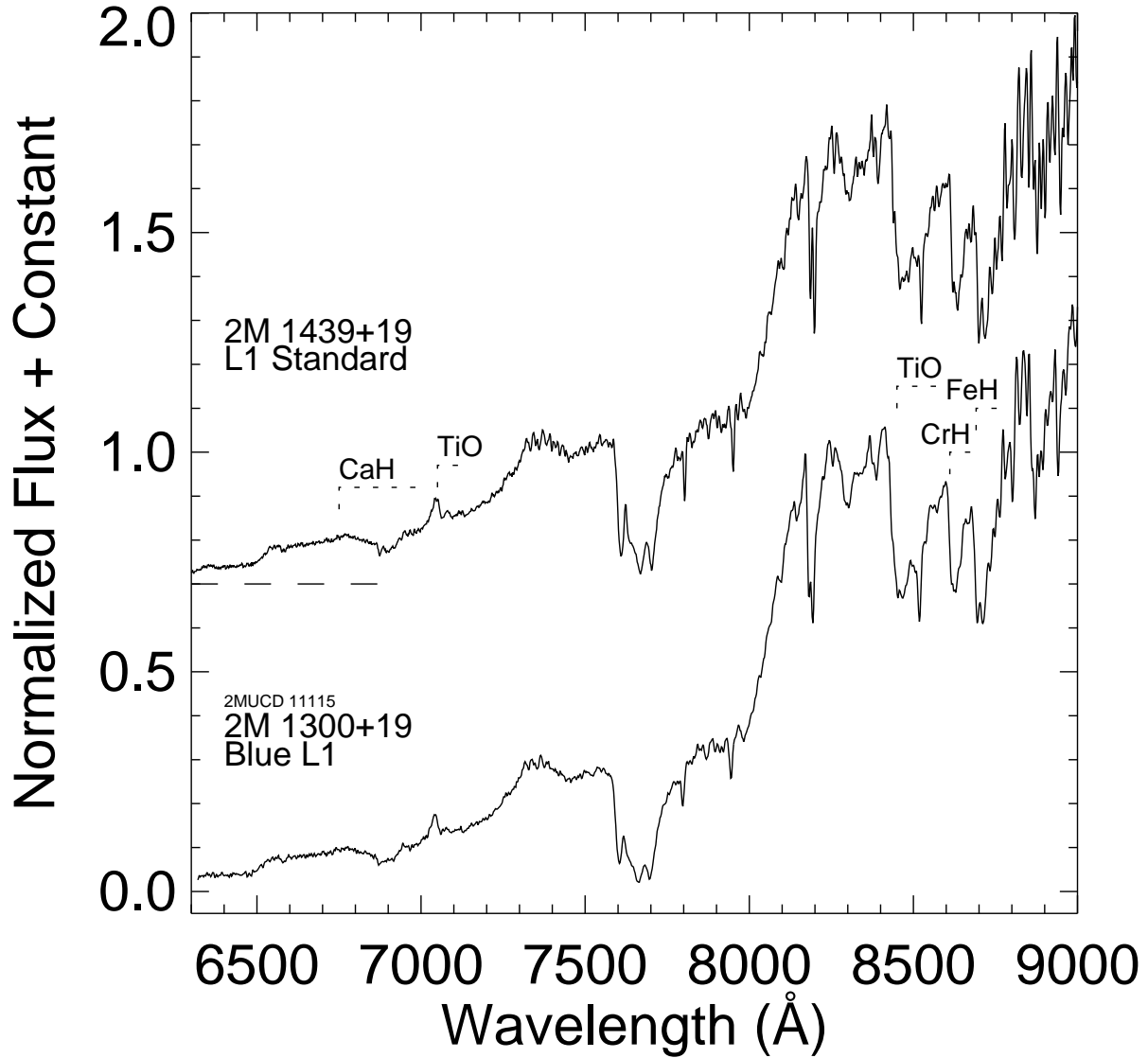


Fig. 8.— Spectrum of blue L1 dwarf, 2M 1300+19 with the L1 standard 2M 1439+19 (Kirkpatrick et al. 1999). Metallicity-sensitive spectral features are marked. Despite blue near-infrared colors and fast kinematics, the spectrum of 2M 1300+19 does not exhibit any unusual features. The bottom spectrum is not offset and the zero point of the spectral standard is shown by a dashed line.

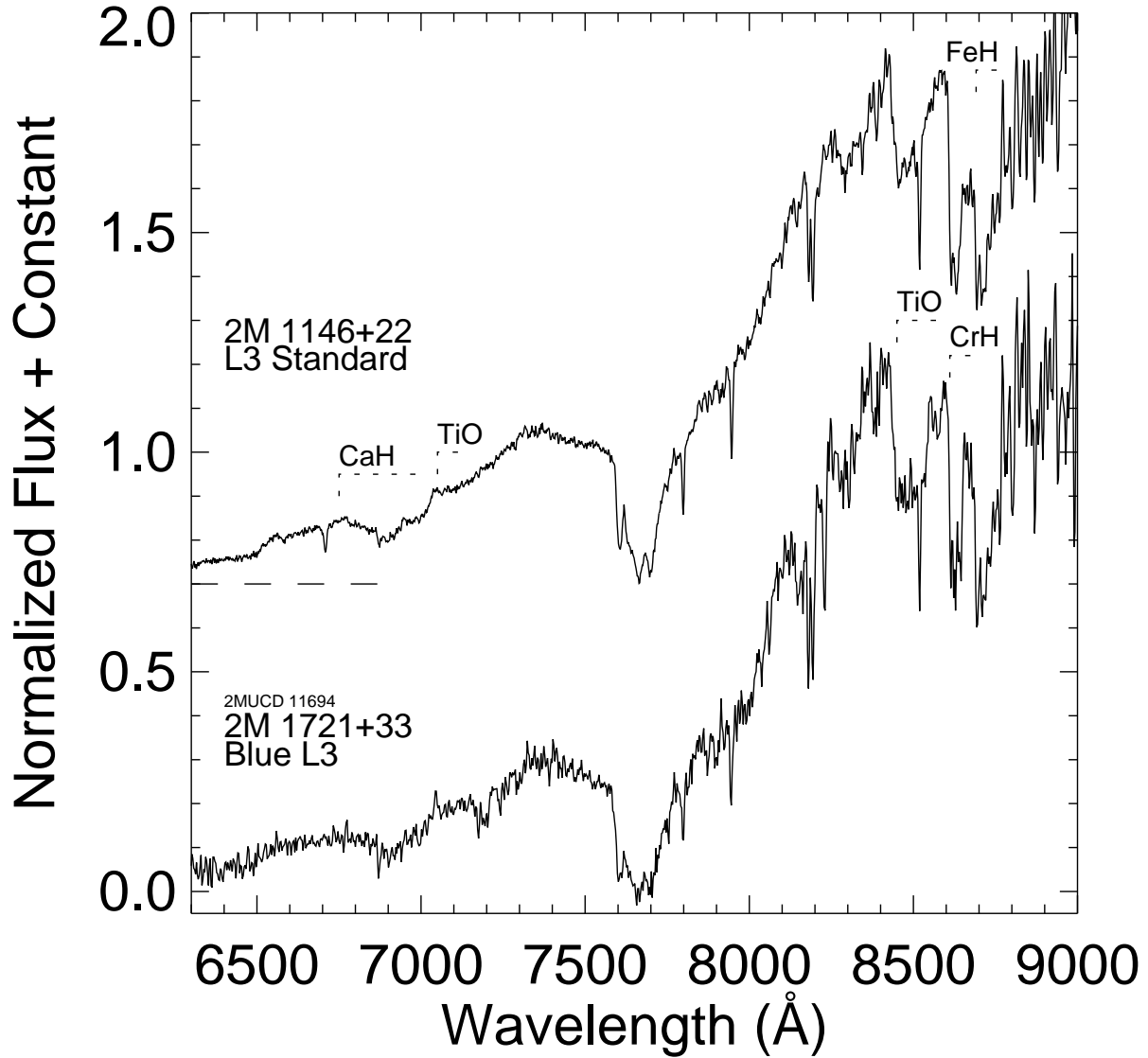


Fig. 9.— Spectrum of blue L3 dwarf, 2M 1721+33 with the L3 standard 2M 1146+22 (Kirkpatrick et al. 1999). Metallicity-sensitive spectral features are marked. Despite blue near-infrared colors and fast kinematics, the spectrum of 2M 1721+33 does not exhibit any unusual features. The bottom spectrum is not offset and the zero point of the spectral standard is shown by a dashed line.

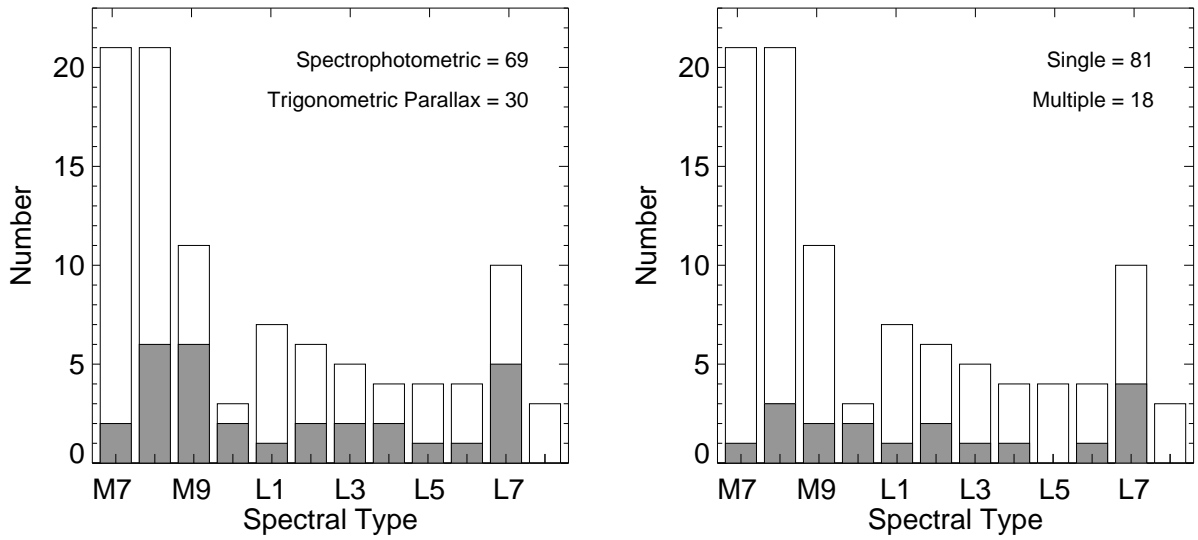


Fig. 10.— Spectral type distribution of the 20-pc 2MU2 sample. In the left panel, objects with distances based on trigonometric parallax measurements (*shaded*) are distinguished from those with spectrophotometric distance estimates (*not shaded*). In the right panel, objects in multiple systems (*shaded*) are distinguished from single objects (*not shaded*).

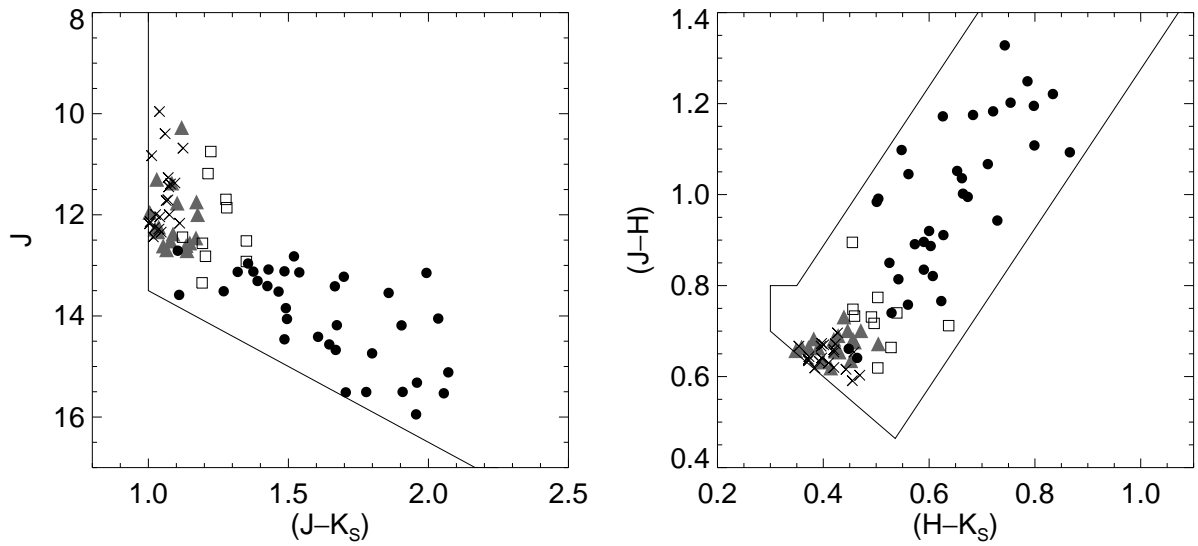


Fig. 11.— Color-magnitude and color-color selection criteria (*solid line*) and distribution of the 20-pc 2MU2 sample grouped by spectral type: M7 and M7.5 (*crosses*), M8 and M8.5 (*triangles*), M9 and M9.5 (*squares*), and L dwarfs (*circles*). The two blue L dwarfs near  $(J - K_S) = 1.1$  in the left panel and  $(H - K_S) = 0.45$  in the right panel are discussed in § 5.4.

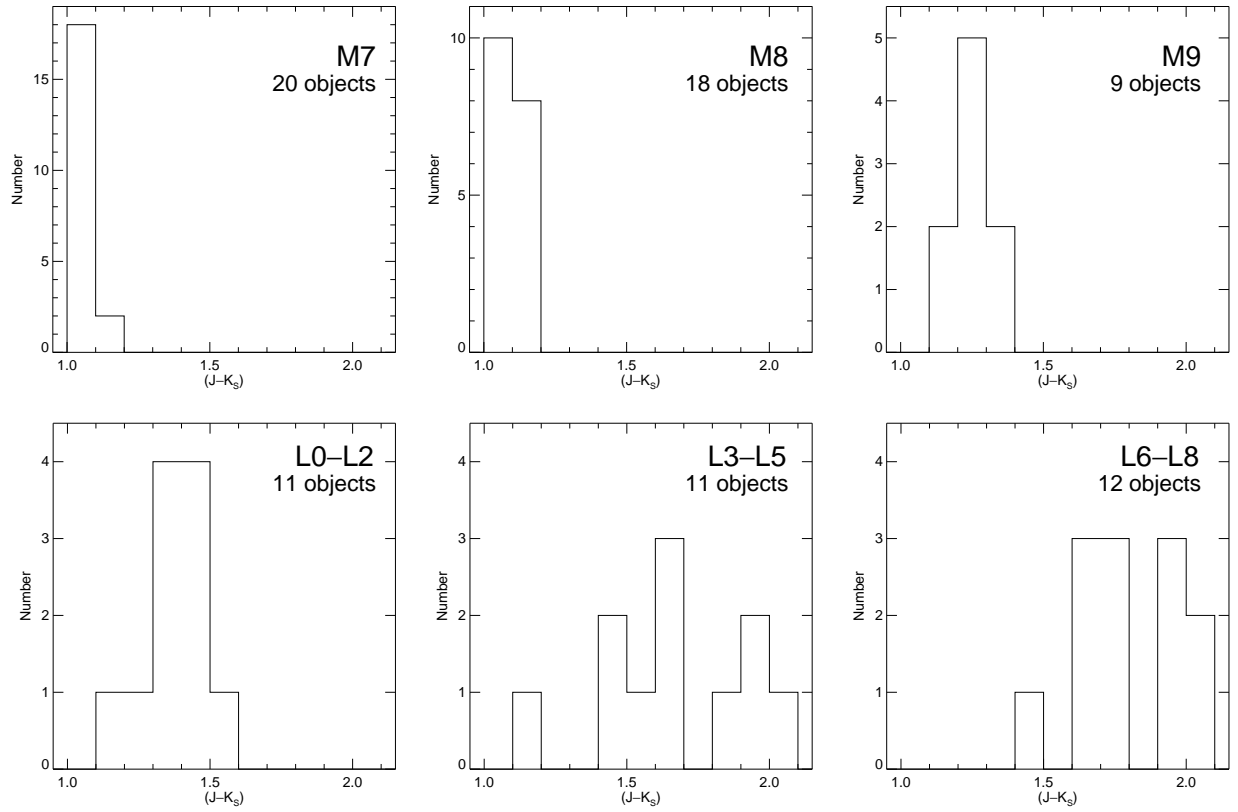


Fig. 12.—  $(J - K_S)$  distribution for single dwarfs in the 20-pc 2MU2 sample.

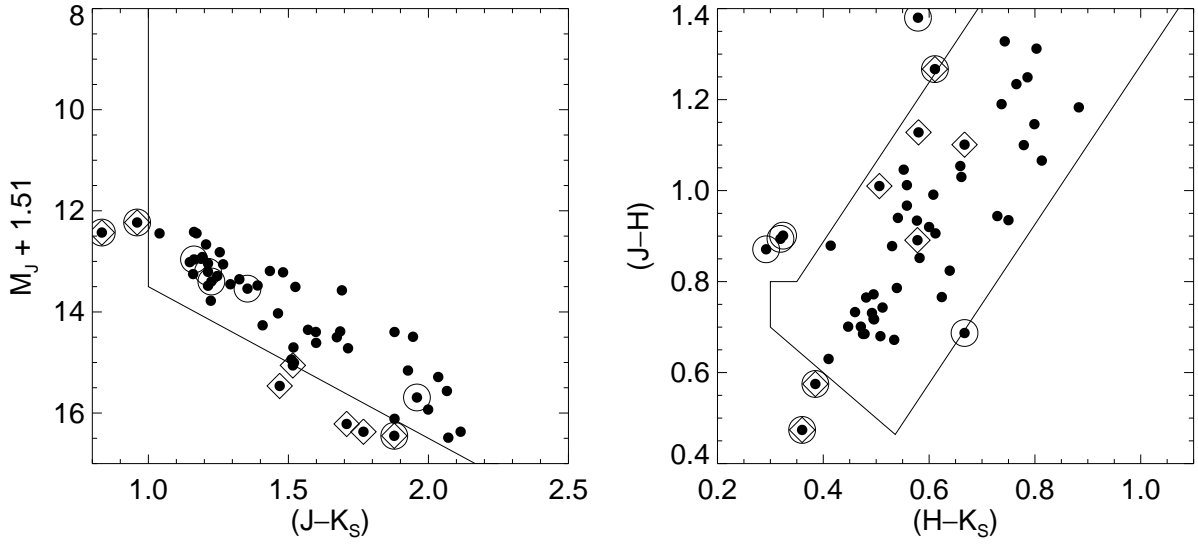


Fig. 13.— Color-magnitude and color-color diagram of M7–L8 dwarfs with parallax measurements and  $J < 16.5$  (UCDt sample, *filled circles*), and our selection criteria (*solid lines*).  $M_J$  has been shifted by 1.51 to reflect our distance limit of 20 pc. Objects that are excluded by our selection criteria in  $J/(J - K_S)$  (*diamonds*) and  $(J - H)/(H - K_S)$  (*open circles*) are marked in both panels and discussed in § 6.2.2.

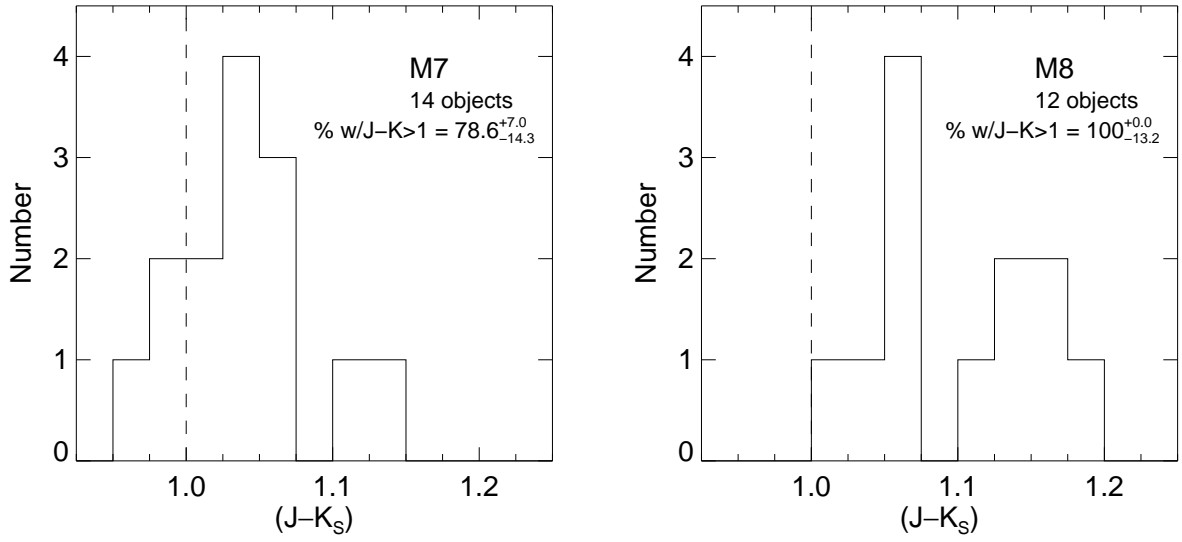


Fig. 14.—  $(J - K_S)$  distribution for M7 and M8 dwarfs not discovered using  $(J - K_S)$  color as a search criterion. The resulting fraction of M7 dwarfs with  $(J - K_S) > 1$  is applied as a correction to our derived  $\Phi(M_J)$  and  $\Phi(M_{K_S})$ .



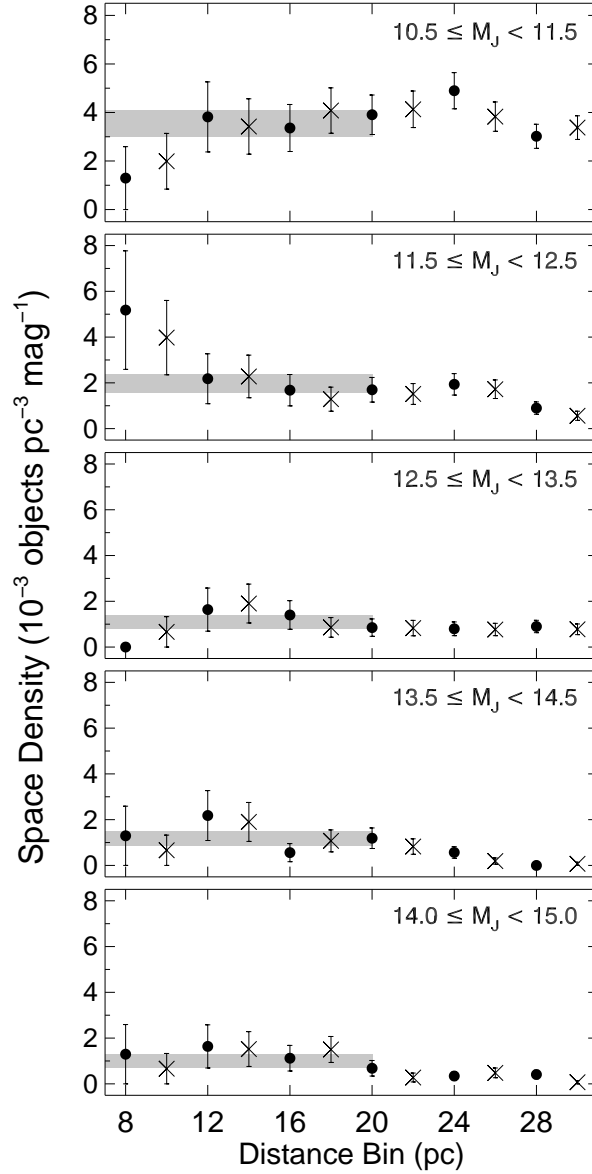


Fig. 15.— Malmquist corrected space densities for two sets of spherical shells for the 2MU2 sample as a function of  $M_J$ . The densities are shown for spherical shells with inner and outer radii from 0–8, 8–12, 12–16, 16–20, 20–24, 24–28 pc (*circles*) and 0–10, 10–14, 14–18, 18–22, 22–26, 26–30 pc (*crosses*). The density for each shell is plotted at the distance of the outer radius (e.g., the density for the 8–12 pc shell is plotted at 12 pc). The shaded bar indicates the overall density for each  $M_J$  bin and the associated Poisson uncertainty. These  $M_J$  bins are coarser than those used in  $\Phi(M_J)$  and  $\Phi(M_{K_S})$ , one magnitude wide instead of 0.5 magnitudes, and the two faintest overlap due to the odd number of bins.

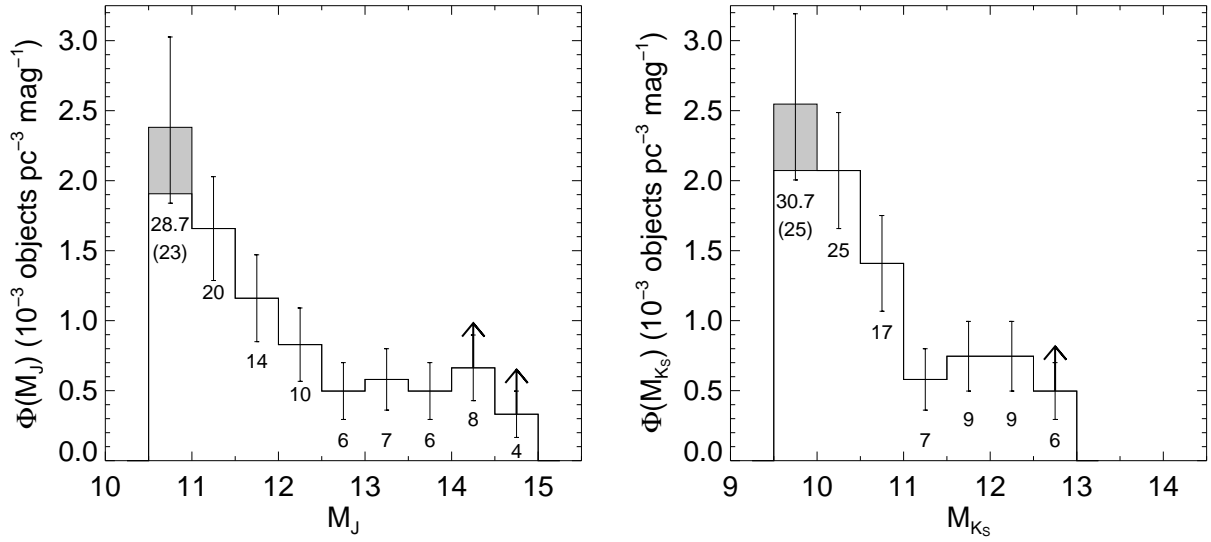


Fig. 16.— Malmquist corrected near-infrared luminosity function with Poisson uncertainties (*unshaded*) and the correction for missing M7 dwarfs (*shaded*, § 6.2.2). Each bin is labeled with the number of objects used to calculate the space density. The space densities are listed in Table 11. Our measurement is a lower limit for  $14 < M_J < 15$  and  $12.5 < M_{K_s} < 13$  because the 2MU2 sample is incomplete for L7 and L8 dwarfs and does not include early and mid-T dwarfs.

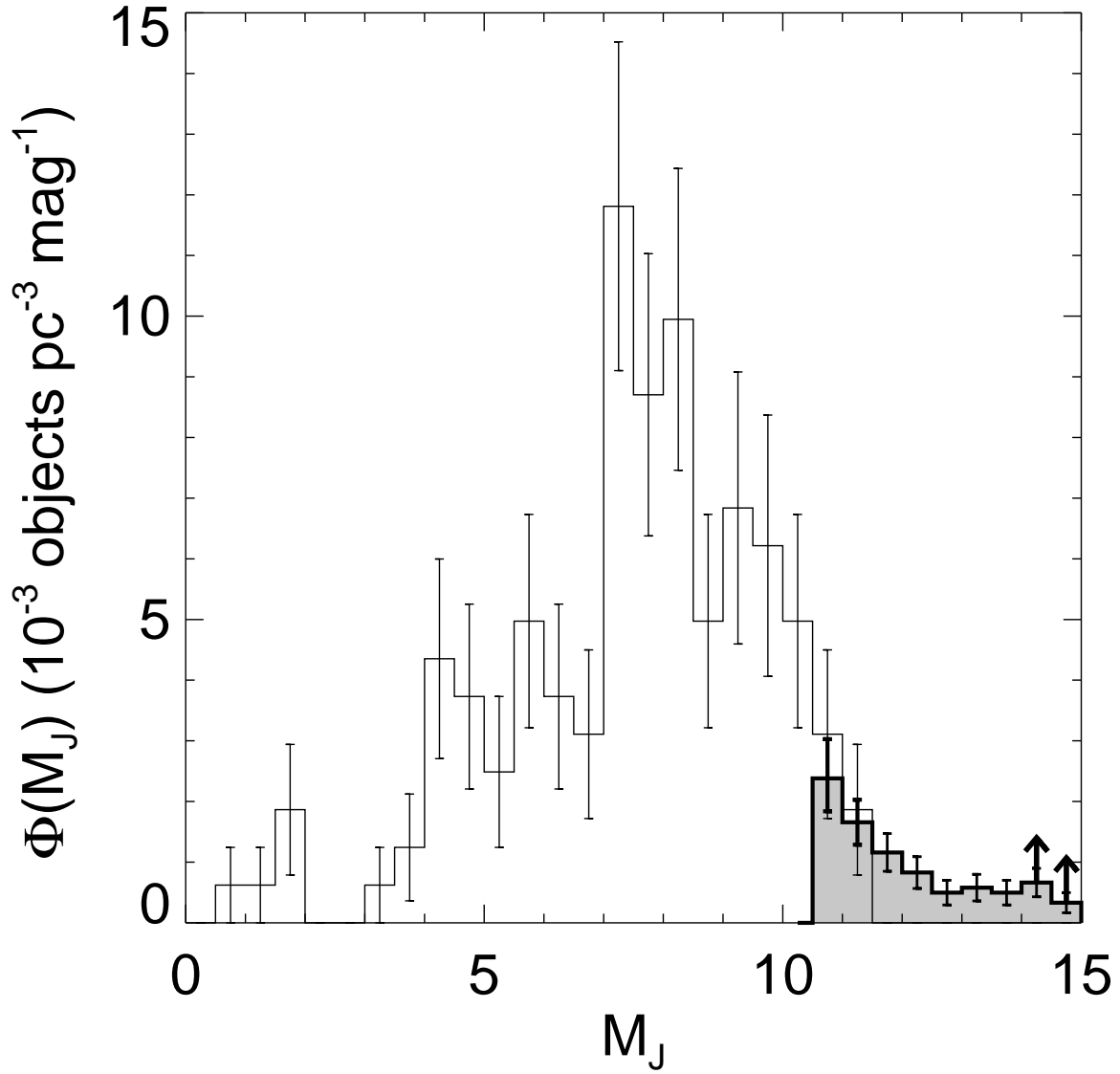


Fig. 17.—  $J$ -band luminosity function of the 8-pc (Reid et al. 2003b, *unshaded*) and 20-pc 2MU2 (*shaded*) samples. The plotted densities are listed in Tables 11 and 12.

Table 1. Spectral Standards Used

Optical Sp. Type	Object	Telescope	Ref.
M1.5	G1 205	KP 2.1 m	1
M2.5	G1 250B	CT 1.5 m	1
M4.5	G1 83.1	CT 4 m	1
M5.5	G1 65	CT 4 m	1
M6	LHS 1326 <sup>a</sup>	KP 2.1 m	2
M7	VB 8	KP 4 m	1
M8	VB 10	KP 4 m	1
M9	LHS 2065	CT 4 m	1
L0	2MASS J03454316+2540233	Keck I	3
L1	2MASS J14392837+1929150	Keck I	3
L2	Kelu 1	Keck I	3
L3	DENIS-P J1058.7–1548	Keck I	3
L4	2MASS J11550087+2307058	Keck I	3
L4.5	2MASS J06523073+4710348	GN	4
L5	DENIS-P J1228.2–1547	Keck I	3
		GS	
L6	2MASS J08503593+1057156	Keck I	3
L7	DENIS-P J0205.4–1159	Keck I	3
		GS	
L8	2MASS J16322911+1904407	Keck I	3
		GN	

Note. — While M and L dwarf spectral standards were taken during the course of our observations, we supplemented our data with the publicly available high signal-to-noise Keck I + LRIS spectra (DwarfArchives.org).

<sup>a</sup>Not actually a spectral standard.

References. — (1) Kirkpatrick et al. (1991); (2) Reid et al. (1995); (3) Kirkpatrick et al. (1999); (4) Reid et al. (2006a)

Table 2. M6–L8 Dwarfs Discovered Within 20 pc

2MASS Designation <sup>a</sup>	2MUCD #	Other Name	2MASS <i>J</i>	2MASS <i>J – H</i>	2MASS <i>J – K<sub>S</sub></i>	Obs. Date (UT)	Telescope	Optical Sp. Type	<i>M<sub>J</sub></i>	<i>d</i> (pc)	Other Refs.
0123112–692138	13056		12.335	0.619	1.034	2003 Nov 8	CT 1.5 m	M8	11.16±0.18	17.2±1.4	
						2006 Jan 15	CT 4 m				
0138215–732058	13063		11.508	0.720	1.056	2003 Nov 9	CT 1.5 m	M6	10.12±0.37	19.0±3.3	
						2006 Jan 15	CT 4 m				
0318540–342129	10176		15.530	1.221	2.055		Keck I	L7	14.45±0.30	16.5±2.3	1
0340094–672405	10202		14.740	1.172	1.799	2006 Jan 14	CT 4 m	L7::	14.45±0.90	11.4±4.7	
0544115–243301	10444		12.518	0.656	1.079	2002 Sep 25	KP 4 m	M8	11.16±0.18	18.7±1.6	
0700366+315726	10617		12.922	0.967	1.614	2003 Oct 12	KP 2.1 m	L3.5comb <sup>b</sup>	12.49±0.06 <sup>b</sup>	12.2±0.3 <sup>b</sup>	2, 3
						2004 Feb 10	KP 4 m				
1043075+222523	10926		15.947	1.202	1.956	2004 Nov 7	GN	L8	14.77±0.50	17.2±4.0	
1440229+133923	11230	LSPM J1440+1339	12.379	0.635	1.088	2002 Jul 5	KP 2.1 m	M8	11.16±0.18	17.6±1.5	4, 5
1534570–141848	11346		11.390	0.659	1.079	2002 Jul 4	KP 2.1 m	M7	10.73±0.25	13.5±1.6	6
						2006 Jan 14	CT 4 m				
2002507–052152	11946		15.320	1.093	1.959	2002 Sep 27	KP 4 m	L6	14.02±0.30	18.2±2.6	
						2003 Apr 23	CT 4 m				
2325453+425148	13227		15.512	1.052	1.705	2004 Sep 20	GN	L8	14.77±0.30	14.1±2.0	
2351504–253736	12220		12.458	0.731	1.170	2002 Jul 5	KP 2.1 m	M8	11.16±0.18	18.2±1.5	

<sup>a</sup>The 2MASS designation is 2MASS Jhhmmss[.]s±ddmmss.

<sup>b</sup>This object has been resolved into two components (Reid et al. 2006b) and the spectral type listed here is for the unresolved system. The distance and *M<sub>J</sub>* for the system is based on a trigonometric parallax (Thorstensen & Kirkpatrick 2003).

References. — (1) Kirkpatrick et al., in prep. (2) Thorstensen & Kirkpatrick (2003); (3) Reid et al. (2006b); (4) Lépine & Shara (2005); (5) Lépine (2005); (6) Gizis (2002).

Table 3. M7–L8 Dwarfs Discovered Outside 20 pc

2MASS Designation <sup>a</sup>	2MUCD #	Other Names	2MASS <i>J</i>	2MASS <i>J – H</i>	2MASS <i>J – K<sub>S</sub></i>	Obs. Date (UT)	Telescope	Optical Sp. Type	<i>M<sub>J</sub></i>	<i>d</i> (pc)	Other Refs.
0000286–124515	10001		13.166	0.746	1.223	2002 Jul 07	KP 2.1 m	M8.5	11.32±0.15	23.4±1.7	
0003422–282241	10002	HD 225118B? <sup>b</sup>	13.063	0.699	1.108	2002 Sep 25	KP 4 m	M7.5	10.96±0.21	26.3±2.6	
0007078–245804	10003	LEHPM 193	13.147	0.684	1.095	2002 Sep 26	KP 4 m	M7	10.73±0.25	30.4±3.5	1, 2
0010001–203112	10006		14.153	0.761	1.285	2002 Sep 25	KP 4 m	L0	11.73±0.13	30.5±1.9	
0021162–664405	13013		13.663	0.715	1.269	2004 Aug 09	CT 4 m	M7::	10.73±1.01	38.5±17.9	
0023475–323925	10017		12.646	0.641	1.002	2002 Sep 28	KP 4 m	M7	10.73±0.25	24.1±2.8	
0025036+475919	13016	HD 2057B? <sup>b</sup>	14.859	1.210	1.953	2004 Sep 22	GN	L4: <sup>c</sup>	13.09±0.22	22.5±2.4	
0050244–153818	10045	SIPS 0050–1538	13.765	0.673	1.126	2002 Sep 26	KP 4 m	L1:	12.00±0.29	22.5±3.0	3
0053540+500149	10049		13.702	0.686	1.071	2002 Sep 25	KP 4 m	M7.5	10.96±0.21	35.3±3.4	
0055046–305200	10050		13.062	0.772	1.137	2002 Sep 26	KP 4 m	M8:	11.16±0.35	24.1±3.9	
0103079+450929	10058		13.704	0.745	1.265	2002 Sep 25	KP 4 m	M9	11.47±0.14	28.0±1.9	
0107160–151757	10066		13.341	0.625	1.059	2002 Sep 26	KP 4 m	M7	10.73±0.25	33.2±3.9	
0112216–703123	13050		13.498	0.681	1.128	2003 Nov 09	CT 1.5m	M7:	10.73±0.50	35.7±8.3	
0121525–685518	13054		12.885	0.676	1.044	2003 Nov 08	CT 1.5m	M7	10.73±0.25	26.9±3.1	
0131183+380155	13061		14.694	1.022	1.666	2004 Feb 12	KP 4 m	L4:	13.09±0.44	20.9±4.3	
0230155+270406	10119		14.255	0.770	1.279	2002 Jan 25	KP 4 m	L0:	11.73±0.26	32.0±3.9	
						2002 Sep 26	KP 4 m				
0310140–275645	10170		15.813	1.151	1.873	2002 Sep 28	KP 4 m	L5: <sup>c</sup>	13.55±0.24	28.3±3.2	
						2005 Oct 11	GS				
0320171–102612	10177		13.865	0.747	1.149	2002 Sep 26	KP 4 m	M8	11.16±0.18	34.8±2.9	
0325013+225303	13119		15.410	1.095	1.675	2004 Oct 19	GN	L3	12.67±0.20	35.3±3.3	
0342162–681732	10204		16.876	1.507	2.328	2004 Dec 11	GS	L2:	12.31±0.34	81.9±13.8	
0355201+143929	10223		13.814	0.706	1.106	2002 Sep 28	KP 4 m	M8	11.16±0.18	34.0±2.9	
0407089–234829	10240		13.767	0.698	1.148	2002 Sep 26	KP 4 m	M8:	11.16±0.35	33.3±5.4	
0417474–212919	10264		13.854	0.728	1.177	2002 Sep 26	KP 4 m	M8	11.16±0.18	34.7±2.9	
0421072–630602	10268		15.561	1.281	2.128	2004 Dec 12	GS	L4: <sup>c</sup>	13.09±0.22	31.1±3.3	
0436501–180326	10307		13.667	0.677	1.110	2002 Sep 25	KP 4 m	M7	10.73±0.25	38.6±4.5	
0518461–275645	10381		15.279	0.957	1.651	2002 Sep 28	KP 4 m	L0:	11.73±0.26	51.3±6.3	
0518599–282837A	10383		16.050	1.224	1.866		Keck I	L6.5pec <sup>d</sup>	13.9±0.3	36±5	4, 5
0518599–282837B									14.0±0.3	36±5	4, 6
0534584–151143	10396		13.151	0.636	1.154	2002 Sep 25	KP 4 m	M9	11.47±0.14	21.7±1.4	
0536199–192039	10397		15.791	1.107	1.919	2005 Jan 10	GS	L1:	12.00±0.29	57.3±7.8	
0605019–234226	10499		14.505	0.778	1.344	2002 Sep 27	KP 4 m	L0:	11.73±0.26	35.9±4.4	
0639559–741844	13147		15.794	1.105	1.778	2004 Dec 11	GS	L5	13.55±0.24	28.0±3.3	

Table 3—Continued

2MASS Designation <sup>a</sup>	2MUCD #	Other Names	2MASS <i>J</i>	2MASS <i>J - H</i>	2MASS <i>J - K<sub>S</sub></i>	Obs. Date (UT)	Telescope	Optical Sp. Type	<i>M<sub>J</sub></i>	<i>d</i> (pc)	Other Refs.
0739438+130507	10662	BD+13 1727B?/LSPM J0739+1305 <sup>b</sup>	13.957	0.613	1.214	2004 Dec 30	GS				
0821501+453201	10715		13.469	0.720	1.142	2002 Sep 26	KP 4 m	M8	11.16±0.18	36.3±3.1	7
0953212-101420	10857		13.445	0.814	1.314	2004 Feb 10	KP 4 m	M7.5	10.96±0.21	31.7±3.1	
1011395+201903	10886		13.860	0.783	1.186	2003 Apr 22	CT 4 m	L0	11.73±0.13	22.0±1.4	
1028404-143843	10910		13.091	0.643	1.064	2003 Apr 21	CT 4 m	M7 <sup>e</sup>	10.73±0.25	29.6±3.5	8
1128255+783101	10992	LSPM J1128+7831	13.397	0.619	1.007	2002 Jul 08	KP 2.1 m	M7:	10.73±0.50	34.1±7.9	7, 9
1147048+142009	11012	LSPM J1147+1420	13.296	0.637	1.041	2002 Jul 07	KP 2.1 m	M7	10.73±0.25	32.5±3.8	7
1216216+445634	11053		16.763	1.293	2.113	2004 Nov 11	GN	L5	13.55±0.24	43.8±6.4	
1221506-084319	11062		13.534	0.613	1.014	2002 Jul 07	KP 2.1 m	M8	11.16±0.18	29.9±2.5	
1231214+495923	11076		14.639	0.949	1.488	2004 Feb 11	KP 4 m	L2	12.31±0.17	29.2±2.3	
1303239+360249	11117		13.646	0.779	1.136	2002 Apr 10	APO	M8	11.16±0.18	31.5±2.6	
1312070+393744	11130		14.146	0.741	1.250	2002 Apr 10	APO	L0:	11.73±0.26	30.4±3.7	
1323521+301433	11139		13.681	0.608	1.103	2002 Apr 10	APO	M8.5	11.32±0.15	29.7±2.2	
1332234+154219	11152		13.509	0.671	1.054	2002 Jul 07	KP 2.1 m	M7	10.73±0.25	35.9±4.2	
1336406+374323	11156		14.397	0.778	1.313	2002 Jul 10	APO	L1 <sup>e</sup>	12.00±0.14	30.2±2.0	
						2002 Jul 11	APO				
1337311+493836	11157		13.739	0.668	1.165	2002 May 14	APO	L0	11.73±0.13	25.2±1.6	
						2003 Jul 10	KP 4 m				
1357096+554449	11179		14.152	0.823	1.304	2002 Apr 10	APO	M9	11.47±0.14	34.5±2.3	
1357149-143852	11180	DENIS-P J1357-1438	12.852	0.654	1.107	2002 Apr 10	APO	M9	11.47±0.14	34.5±2.3	
1404449+463429	11190		14.352	0.814	1.301	2003 Mar 13	KP 2.1 m	M7	10.73±0.25	26.5±3.1	10
1405040+291831	11191		14.352	0.814	1.301	2002 Jul 11	APO	L0:	11.73±0.26	33.4±4.1	
1412227+235410	11196		13.451	0.684	1.009	2002 Jul 07	KP 2.1 m	M7	10.73±0.25	34.9±4.1	
1412227+235410	11196		13.771	0.706	1.099	2002 Jul 07	KP 2.1 m	M9	11.47±0.14	28.9±1.9	
1415202+463659	11199		14.185	0.776	1.241	2002 May 30	APO	M9	11.47±0.14	35.0±2.3	
1434582-233557	11219	CE 455	12.900	0.614	1.025	2002 Jul 06	KP 2.1 m	M7	10.73±0.25	27.1±3.2	11
1440303+123334	11231		14.427	0.848	1.316	2002 Jul 11	APO	M9	11.47±0.14	39.1±2.6	
1441045+271932	11233		13.022	0.609	1.033	2002 Jul 05	KP 2.1 m	M7	10.73±0.25	28.7±3.4	
1453230+154308	11259		13.222	0.636	1.019	2002 Jul 05	KP 2.1 m	M7.5	10.96±0.21	28.3±2.8	
1453484+373316	11260		13.170	0.638	1.034	2002 Jul 05	KP 2.1 m	M7	10.73±0.25	30.7±3.6	
1510295+361948	11300		13.963	0.736	1.174	2002 Jul 10	APO	M9	11.47±0.14	31.6±2.1	
1536191+330514	11351		13.663	0.676	1.056	2002 Jul 05	KP 2.1 m	M7	10.73±0.25	38.5±4.5	
1550084+145517	11452		14.746	0.934	1.520	2002 Jul 11	APO	L2:	12.31±0.34	30.7±4.8	



Table 3—Continued

2MASS Designation <sup>a</sup>	2MUCD #	Other Names	2MASS <i>J</i>	2MASS <i>J - H</i>	2MASS <i>J - K<sub>S</sub></i>	Obs. Date (UT)	Telescope	Optical Sp. Type	<i>M<sub>J</sub></i>	<i>d</i> (pc)	Other Refs.
			14.746	0.934	1.520	2003 Apr 21	CT 4 m	L2:	12.31±0.34	30.7±4.8	
1556502+520656	11474		13.883	0.707	1.134	2002 Jul 10	APO	M7	10.73±0.25	42.6±5.0	
1557327+175238	11478		13.536	0.718	1.087	2002 Jul 04	KP 2.1 m	M7.5	10.96±0.21	32.7±3.2	
1607152+312525	11511		12.745	0.696	1.018	2002 Jul 04	KP 2.1 m	M6	10.12±0.37	33.5±5.8	
1608246+195747	11515		13.521	0.712	1.142	2002 May 30	APO	M9	11.47±0.14	25.8±1.7	
1612413+173028	11528		13.678	0.591	1.096	2002 Jul 07	KP 2.1 m	M7	10.73±0.25	38.8±4.5	
1613455+170827	11531		13.438	0.757	1.290	2002 May 30	APO	M9.5	11.60±0.13	23.3±1.5	
1617003+131349	11549		13.328	0.569	1.010	2002 Jul 04	KP 2.1 m	M7	10.73±0.25	33.0±3.8	
1645220+300407	11658		15.217	1.019	1.669	2004 Sep 19	GN	L3	12.67±0.20	32.3±3.0	
1711135+232633	11684		14.512	0.865	1.460	2002 Sep 27	KP 4 m	L0:	11.73±0.26	36.0±4.4	
1717045+150953	11690		13.612	0.659	1.112	2002 Sep 25	KP 4 m	M7	10.73±0.25	37.6±4.4	
1923381-330841	11842		13.278	0.609	1.039	2002 Jul 04	KP 2.1 m	M7	10.73±0.25	32.3±3.8	
2025196-255048	12003		14.075	0.693	1.210	2002 Jul 11	APO	M8	11.16±0.18	38.4±3.2	
2026158-294312	12009		14.800	0.867	1.441	2002 Sep 27	KP 4 m	L1:	12.00±0.29	36.3±4.8	
						2003 Apr 21	CT 4 m				
2035203-311008	12026		13.195	0.608	1.060	2002 Jul 04	KP 2.1 m	M7	10.73±0.25	31.1±3.6	
2041428-350644	12037		14.863	0.895	1.480	2002 Sep 26	KP 4 m	L2:	12.31±0.34	32.4±5.0	
2047247+142152	12044		13.006	0.713	1.158	2002 Jul 04	KP 2.1 m	M7.5	10.96±0.21	25.6±2.5	
2123311-234518	12077		13.584	0.707	1.044	2002 Jul 04	KP 2.1 m	M7.5	10.96±0.21	33.4±3.3	
2132114+134158	13177		15.785	1.201	1.951	2004 Sep 20	GN	L6	14.02±0.30	22.5±3.2	
2151254-244100	12091		15.775	1.197	2.102	2004 Nov 11	GS	L3	12.67±0.20	41.7±4.1	
2158045-155009	12101		14.949	1.033	1.801	2002 Sep 26	KP 4 m	L4:	13.09±0.44	23.5±4.8	12
2242531+254257	13206		14.795	1.041	1.773	2004 Nov 06	GN	L3	12.67±0.20	26.6±2.5	
2249091+320549	13209		15.489	1.133	1.896	2004 Sep 21	GN	L5	13.55±0.24	24.4±2.8	
2308099-313122	12172		13.666	0.709	1.073	2002 Jul 11	APO	M7	10.73±0.25	38.6±4.5	
2310185-175909	12177	SSSPM 2310-1759	14.397	0.819	1.388	2002 Sep 25	KP 4 m	L0:	11.73±0.26	34.1±4.1	13
2323134-024435	12183		13.582	0.680	1.122	2002 Jul 05	KP 2.1 m	M8.5	11.32±0.15	28.3±2.1	
2329479-160755	12189		13.334	0.609	1.088	2002 Jul 05	KP 2.1 m	M9	11.47±0.14	23.6±1.5	
2330225-034718	12190		14.526	0.797	1.419	2002 Sep 26	KP 4 m	L1:	12.00±0.29	32.0±4.2	
2337166-093324	12201		13.411	0.698	1.129	2002 Jul 05	KP 2.1 m	M7.5	10.96±0.21	30.9±3.0	
2341286-113335	12208		13.609	0.677	1.068	2002 Jul 06	KP 2.1 m	M8	11.16±0.18	31.0±2.6	
2344062-073328	12212		14.850	0.986	1.621	2002 Sep 26	KP 4 m	L4.5	13.32±0.23	20.2±2.2	
2346547-315353	12215	SIPS 2346-3153	13.296	0.640	1.091	2002 Jul 05	KP 2.1 m	M8	11.16±0.18	26.8±2.2	3
2352050-110043	12221		12.868	0.693	1.146	2002 Jul 06	KP 2.1 m	M7	10.73±0.25	26.7±3.1	

Table 3—Continued

2MASS Designation <sup>a</sup>	2MUCD #	Other Names	2MASS <i>J</i>	2MASS <i>J - H</i>	2MASS <i>J - K<sub>S</sub></i>	Obs. Date (UT)	Telescope	Optical Sp. Type	<i>M<sub>J</sub></i>	<i>d</i> (pc)	Other Refs.
2353594–083331	12223	DENIS-P J2353–0833	13.062	0.705	1.117	2002 Sep 25	KP 4 m	M8.5	11.32±0.15	22.3±1.6	10

<sup>a</sup>The 2MASS designation is 2MASS Jhhmmss[.]s±ddmmss.

<sup>b</sup>Ultracool common proper motion companion to a star as discussed in § 5.5.

<sup>c</sup>Spectrum shows lithium absorption line as shown in Figure 2 and discussed in § 5.1.

<sup>d</sup>Probable L/T binary (Cruz et al. 2004; Burgasser et al. 2006b). Combined-light optical spectral type from Kirkpatrick et al., in prep..

<sup>e</sup>Variable and/or flaring object that will be discussed in detail in Schmidt et al. (2006, in prep.).

References. — (1) Reylé & Robin (2004); (2) Pokorný et al. (2004); (3) Deacon et al. (2005); (4) Cruz et al. (2004); (5) Kirkpatrick et al., in prep.; (6) Burgasser et al. (2006b); (7) Lépine & Shara (2005); (8) Schmidt et al. (2006); (9) Lépine (2005); (10) Phan-Bao et al. (2001); (11) Ruiz et al. (2001); (12) Kirkpatrick et al., in prep.; (13) Lodieu et al. (2002).

Table 4. Early-to-Mid Type M Dwarfs Discovered Outside 20 pc

2MASS Designation <sup>a</sup>	Other Names	2MASS <i>J</i>	2MASS <i>J - H</i>	2MASS <i>J - K<sub>S</sub></i>	Obs. Date (UT)	Telescope	Optical Sp. Type	<i>M<sub>J</sub></i>	<i>d</i> (pc)	Other Refs.
0017185-040606		12.485	0.642	1.025	2002 Jul 07	KP 2.1 m	M6.5	10.5±0.3	25±4	
0107590-200423		12.817	0.614	1.024	2002 Sep 27	KP 4 m	M6	10.1±0.4	35±6	
0355403-112310		12.947	0.645	1.010	2002 Sep 27	KP 4 m	M6	10.1±0.4	37±6	
0411063+124748		12.777	0.652	1.015	2002 Sep 28	KP 4 m	M6	10.1±0.4	34±6	
0510239-280053		12.964	0.646	1.010	2002 Sep 28	KP 4 m	M4	8.5±0.7	60-100	
0544167-204909		14.394	1.002	1.515	2002 Sep 25	KP 4 m	M5	8.5±0.7	110-180	
0818332-003628		16.639	1.302	2.110	2004 Dec 12	GS	M6	10.1±0.4	202±38	
0941115+425403		16.753	1.288	2.101	2004 Nov 07	GN	M5	9.3±0.4	312±59	
0959560+200234	LHS 2215	12.244	0.629	1.048	2001 Nov 3	KP 2.1 m	M6.5 <sup>b</sup>	10.46±0.31	22.8±3.2	1, 2, 3, 4, 5
1144050+604348		12.290	0.598	1.015	2002 Jul 08	KP 2.1 m	M6	10.1±0.4	27±5	
1222143+565559	LSPM J1222+5655	13.662	0.697	1.099	2002 Jul 08	KP 2.1 m	M6	10.1±0.4	51±9	6
1239285+134142	LSPM J1239+1341	13.595	0.705	1.042	2002 Jul 07	KP 2.1 m	M6	10.1±0.4	50±9	6
1242271+445140	LSPM J1242+4451	13.592	0.615	1.088	2002 Jul 08	KP 2.1 m	M5	8.5±0.7	75-130	6
1312393+183559	LSPM J1312+1835	13.238	0.654	1.115	2002 Apr 10	APO	M5	9.6±0.3	54±7	6
1411392+602447		13.461	0.684	1.016	2002 Jul 07	KP 2.1 m	M6	10.1±0.4	47±8	
1414153-141822		13.499	0.559	1.014	2002 Jul 06	KP 2.1 m	M6	10.1±0.4	47±8	
1436418-153048		13.128	0.626	1.010	2002 Jul 06	KP 2.1 m	M5	8.5±0.7	65-115	
1450366+472357	LSPM J1450+4723	13.374	0.663	1.012	2002 Jul 05	KP 2.1 m	M6	10.1±0.4	45±8	6
1529456+821532		13.437	0.610	1.032	2002 Jul 05	KP 2.1 m	M5	6.6±0.5	244±53	
1628170+133420	LSPM J1628+1334	11.674	0.662	1.004	2002 Jul 04	KP 2.1 m	M5	7.4±0.5	72±15	6, 7
1631136+192200		13.457	0.724	1.052	2002 Jul 04	KP 2.1 m	M5	9.7±0.4	56±11	
1734419+123105	LHS 2980	13.095	0.715	1.031	2002 Jul 04	KP 2.1 m	M1	6.4±0.1	222±15	1
2002066-023314		10.502	0.779	1.093	2002 Jul 05	KP 2.1 m	M3	7.1±0.2	48±4	
2003438-144917		13.580	0.718	1.029	2002 Jul 04	KP 2.1 m	M5	9.5±0.2	65±5	
2040269-152316		13.656	0.761	1.089	2002 Jul 04	KP 2.1 m	M2	7.2±0.2	200±22	
2107247-335733	DENIS-P J2107-3357	12.213	0.613	1.056	2002 Jul 07	KP 2.1 m	M6	10.1±0.4	26±5	8, 9
2208546-244911		12.897	0.707	1.016	2002 Jul 04	KP 2.1 m	M6	10.1±0.4	36±6	

Table 4—Continued

2MASSI Designation <sup>a</sup>	Other Names	2MASS <i>J</i>	2MASS <i>J – H</i>	2MASS <i>J – K<sub>S</sub></i>	Obs. Date (UT)	Telescope	Optical Sp. Type	<i>M<sub>J</sub></i>	<i>d</i> (pc)	Other Refs.
2215171–045919	LP 699- 64	13.441	0.688	1.004	2002 Jul 04	KP 2.1 m	M6	10.1±0.4	46±8	10
2229444–192324		13.512	0.696	1.025	2002 Jul 04	KP 2.1 m	M3	7.0±0.1	197±13	
2309142–353159	LP 985- 98	12.035	0.684	1.049	2002 Jul 03	KP 2.1 m	M5	9.5±0.2	33±2	10
2336142–093606		13.393	0.635	1.094	2002 Jul 05	KP 2.1 m	M6.5	10.5±0.3	39±5	
2338541–124618		12.181	0.557	1.014	2002 Jul 05	KP 2.1 m	M6.5	10.5±0.3	22±3	
2340477+462318		13.320	0.680	1.001	2002 Jul 06	KP 2.1 m	M6	10.1±0.4	44±8	
2353081–082916	LP 763- 14	13.274	0.651	1.017	2002 Jul 06	KP 2.1 m	M5	9.3±0.4	62±11	10

<sup>a</sup>The 2MASS designation is 2MASSI Jhhmmss[.]s±ddmmss.

<sup>b</sup>A spectrum of this object is shown by Bessell (1991) but not mentioned in the text nor assigned a spectral type. It appears to have been overlooked in the subsequent literature on late-type M dwarfs. To our knowledge, it was first formally assigned a spectral type by Reid et al. (2003a, Paper VII) using the same data presented here.

References. — (1) Luyten (1979a, LHS); (2) Bessell (1991); (3) Reid & Cruz (2002, Paper I); (4) Reid et al. (2003a, Paper VII); (5) Reid & Gizis (2005); (6) Lépine & Shara (2005); (7) Lépine (2005); (8) Phan-Bao et al. (2001); (9) Crifo et al. (2005); (10) Luyten (1979b, NLTT).

Table 5. Spectroscopically Confirmed Giants

2MASSI Designation <sup>a</sup>	2MASS $J$	2MASS $J - H$	2MASS $J - K_S$	Obs. Date (UT)	Telescope	Optical Sp. Type
0057017+450949	10.002	0.776	1.202	2002 Jul 08	KP 2.1 m	M8 III
0426258+154502	11.860	0.695	1.021	2002 Sep 26	KP 4 m	M5 III
0557509–135950	12.873	0.741	1.135	2002 Sep 27	KP 4 m	M6 pec III <sup>b</sup>
0712435+395831	9.156	0.743	1.119	2002 Sep 25	KP 4 m	K5 III
1119051+700609	10.276	0.741	1.096	2002 Jul 08	KP 2.1 m	M4 III
1340371–011604	13.492	0.619	1.106	2002 Jul 07	KP 2.1 m	<K5 III
1550248+821009	9.667	0.778	1.095	2002 Jul 10	APO	M7 III
1741494+152317	9.173	0.758	1.071	2002 Sep 25	KP 4 m	M3 III
1750217+132703	9.128	0.759	1.063	2002 Jul 06	KP 2.1 m	M7 III
1804046+220610	9.260	0.788	1.098	2002 Jul 03	KP 2.1 m	M3 III
1807133+150212	9.108	0.799	1.109	2002 Sep 25	KP 4 m	M3 III
1817475+201534	9.825	0.798	1.118	2002 Sep 25	KP 4 m	K5 III
1843260+405033	9.275	0.780	1.144	2002 Jul 03	KP 2.1 m	M3 III
1923327–305502	9.222	0.756	1.083	2002 Jul 03	KP 2.1 m	M5 III
1927415–323251	9.008	0.769	1.109	2002 Jul 05	KP 2.1 m	M5 III
1936154–343109	10.837	0.780	1.111	2002 Sep 25	KP 4 m	M0 III
1941178–262716	10.525	0.835	1.246	2002 Jul 05	KP 2.1 m	M5 III
1959007–223323	9.147	0.720	1.038	2002 Jul 05	KP 2.1 m	M1 III
2000171–270537	9.096	0.771	1.260	2002 Jul 05	KP 2.1 m	M7 III
2002404–294746	9.157	0.720	1.070	2003 Jul 09	KP 4 m	M3 III
2005582–012730	9.314	0.915	1.481	2002 Jul 03	KP 2.1 m	M6 III
2007596–043924	9.576	0.914	1.456	2002 Jul 03	KP 2.1 m	M5 III
2041113+000747	9.220	0.726	1.026	2002 Sep 26	KP 4 m	M0 III
2102375+184551	9.674	0.796	1.203	2003 Apr 20	CT 4 m	M7 III
2124586–012325	9.975	0.782	1.121	2002 Jul 03	KP 2.1 m	M3 III
2133408+292531	9.257	0.789	1.093	2003 Jul 09	KP 4 m	M0 III
2157407–001650	13.662	0.773	1.136	2002 Sep 25	KP 4 m	M4 III
2222068+220849	9.698	0.717	1.158	2003 Jul 09	KP 4 m	M8 III
2233559+403935	9.792	0.785	1.122	2003 Jul 09	KP 4 m	M0 III
2235440+194245	13.501	0.703	1.030	2002 Jul 04	KP 2.1 m	K5 III
2237158+372132	9.006	0.788	1.111	2003 Jul 10	KP 4 m	M3 III
2238182+411355	10.260	0.800	1.100	2002 Sep 25	KP 4 m	M0 III

Table 5—Continued

2MASS I Designation <sup>a</sup>	2MASS <i>J</i>	2MASS <i>J – H</i>	2MASS <i>J – K<sub>S</sub></i>	Obs. Date (UT)	Telescope	Optical Sp. Type
2350294+451749	10.167	0.833	1.222	2002 Jul 06	KP 2.1 m	M4 III

<sup>a</sup>The 2MASS designation is 2MASSI Jhhmmss[.]s±ddmmss.

<sup>b</sup>Spectrum displays H $\alpha$  in emission.

Table 6. Spectroscopically Confirmed Carbon Stars

2MASSI Designation <sup>a</sup>	2MASS $J$	2MASS $J - H$	2MASS $J - K_S$	Obs. Date (UT)	Telescope
0008170–753727	13.826	1.259	2.224	2006 Jan 15	CT 4 m
0027523–705231	13.368	1.382	2.320	2003 Nov 09	CT 1.5 m
0044155–711540	13.398	1.189	2.006	2003 Nov 09	CT 1.5 m
0046008–752112	13.182	1.071	1.922	2003 Nov 09	CT 1.5 m
0107522–692136	13.153	1.288	2.177	2003 Nov 09	CT 1.5 m
0121433–740346	13.688	1.488	2.604	2006 Jan 15	CT 4 m
0126348–703947	12.817	1.478	2.494	2003 Nov 09	CT 1.5 m
0148078–715521	12.471	1.271	2.199	2003 Nov 10	CT 1.5 m
0156260+512521	9.395	1.143	1.713	2003 Jul 09	KP 4 m
0224319+372933	11.498	1.619	2.775	2003 Jul 09	KP 4 m
0554397–144658	12.731	0.767	1.083	2002 Sep 27	KP 4 m
0606344+731027	9.397	0.986	1.519	2002 Sep 25	KP 4 m
1015259–020431	14.045	1.184	2.058	2003 Apr 22	CT 4 m
1504553+354757	12.000	1.322	2.323	2003 Mar 14	KP 2.1 m
1941285–323338	10.865	0.959	1.412	2002 Sep 25	KP 4 m
2002292–245258	9.199	0.774	1.077	2002 Jul 03	KP 2.1 m
2252361+474125	9.624	1.073	1.633	2003 Jul 09	KP 4 m

<sup>a</sup>The 2MASS designation is 2MASSI Jhhmmss[.]s±ddmmss.

Table 7. Objects with New Spectra

2MASS Designation <sup>a</sup>	2MUCD #	Other Names	2MASS <i>J</i>	2MASS <i>J - H</i>	2MASS <i>J - K<sub>S</sub></i>	Obs. Date (UT)	Telescope	Optical Sp. Type	<i>M<sub>J</sub></i>	<i>d</i> (pc)	Other Refs.
0141032+180450	10085		13.822	0.772	1.315	2004 Feb 11	KP 4 m	L1	12.00±0.14	23.1±1.6	1
0326422-210205	10184		16.111	1.337	2.226	2005 Oct 10	GS	L4 <sup>b</sup>	13.09±0.22	40.1±4.5	2
0428509-225322	10286		13.579	0.882	1.459	2004 Feb 11	KP 4 m	L1	12.00±0.14	20.7±1.4	3
1003191-010507	10873	LHS 5165/DENIS-P J1003-0105	12.352	0.667	1.085	2003 Mar 15	KP 2.1 m	M7	10.73±0.25	21.1±2.5	4, 5
1011002+424503	10885	TVLM 263-71765	13.357	0.657	1.056	2004 Feb 10	KP 4 m	M7.5	10.96±0.21	30.1±2.9	6
1515009+484739	11314		14.060	0.991	1.495	2002 Jul 10 2004 Feb 10	APO KP 4 m	L6	14.02±0.30	10.2±1.4	1

<sup>a</sup>The 2MASS designation is 2MASS Jhhmmss[.]s±ddmmss.

<sup>b</sup>Spectrum shows lithium absorption line as shown in Figure 2 and discussed in § 5.1.

References. — (1) Wilson (2002); (2) Paper V; (3) Kendall et al. (2003); (4) Gizis (2002); (5) Phan-Bao et al. (2001); (6) Tinney et al. (1995)



Table 8. Low-Gravity Objects

2MASSI Designation <sup>a</sup>	2MUCD #	Other Name	2MASS <i>J</i>	2MASS <i>J - H</i>	2MASS <i>J - K<sub>S</sub></i>	Obs. Date (UT)	Telescope	Optical Sp. Type <sup>b</sup>	$\mu$ (mas yr <sup>-1</sup> )	PA (°)	$\mu$ Ref.	Other Refs.
0241115-032658	10141		15.831	1.019	1.807	2002 Sep 27 2005 Oct 10	KP 4 m GS	(L1)	57±18	88	1	
0436278-411446	10306	DENIS-P J0436-4114	13.105	0.689	1.043	2003 Nov 08 2006 Jan 15	CT 1.5 m CT 4 m	(M8) <sup>c</sup>	22±18	80	2	1, 2
0443376+000205	10320	SDSS 0443+0002	12.517	0.713	1.350	2002 Jan 28	CT 1.5 m	(M9) <sup>d</sup>	159±78	146	1	3, 4
1615425+495321	11538		16.732	1.441	2.413	2004 Sep 12	GN	(L4)	115±83	287	1	
2213449-213607	12120		15.392	0.975	1.647	2002 Sep 27 2005 Sep 08	KP 4 m GS	(L1)	...	...		

Note. — Spectra are plotted in Figures 4–7.

<sup>a</sup>The 2MASS designation is 2MASSI Jhhmmss[.]s±ddmmss.

<sup>b</sup>The spectral types should be regarded as preliminary since all of these objects have low-gravity spectral features and do not fit into the dwarf spectral sequence as it is currently defined.

<sup>c</sup>These new spectral data supplements the photometric data of Phan-Bao et al. (2003) listed in Paper V.

<sup>d</sup>This is a reclassification based on a reanalysis of the spectrum presented in Paper V.

References. — Proper Motion: (1) This Paper; (2) Phan-Bao et al. (2003).

References. — Other: (1) Phan-Bao et al. (2003); (2) Crifo et al. (2005); (3) Wilson (2002); (4) Hawley et al. (2002).

Table 9. The 20 pc 2MU2 Sample Used to Estimate the Luminosity Function

2MASSI Designation <sup>a</sup>	2MUCD #	Other Names	2MASS <i>J</i>	2MASS <i>J - H</i>	2MASS <i>J - K<sub>S</sub></i>	Optical Sp. Type <sup>b</sup>	<i>M<sub>J</sub></i>	<i>M<sub>K<sub>S</sub></sub></i>	<i>d</i> (pc) <sup>c</sup>	<i>d</i> source <sup>c</sup>	Discovery Refs.	Parallax Refs.
0019262+461407	10013		12.609	0.676	1.135	M8	11.16±0.18	10.02±0.18	19.5 ±1.6	ST	1	
0019457+521317	10014		12.820	0.748	1.204	M9	11.47±0.14	10.26±0.15	18.7 ±1.2	ST	1	
0024246-015819	10018	BRI 0021-0214	11.860	0.740	1.280	M9.5	11.55±0.10	10.27±0.10	11.55±0.53	Parallax	2	1
0024442-270825B	10019	LHS 1070B <sup>d</sup>	9.262	0.730	1.030	M8.5	11.64±0.06	10.49±0.05	7.71±0.14	Parallax	3, 4, 5	2, 3
0024442-270825C		LHS 1070C				L0	11.97±0.08	10.81±0.07	7.71±0.14	Parallax	3, 4, 5	2, 3
0027559+221932A	10022	LP 349-25A	10.608	0.638	1.047	M8:	11.16±0.35	10.13±0.24	10.3 ±1.7	ST	6, 7	
0027559+221932B		LP 349-25B				M9:	11.47±0.28	10.39±0.25	10.3 ±1.7	ST	8	
0109511-034326	10068	LP 647-13	11.695	0.774	1.277	M9	11.47±0.14	10.51±0.06	11.1 ±0.7	ST	1, 6, 9	
0123112-692138	13056		12.335	0.619	1.034	M8	11.16±0.18	10.12±0.18	17.2 ±1.4	ST	10	
0144353-071614	10088		14.187	1.183	1.904	L5	13.55±0.24	11.65±0.24	13.4 ±1.5	ST	1, 11, 12	
0148386-302439	10091		12.282	0.641	1.038	M7.5	10.96±0.21	9.93±0.21	18.4 ±1.8	ST	1	
0205293-115930A <sup>e</sup>	10096	DENIS-P J0205.4-1159A <sup>e</sup>	14.581	0.991	1.599	L7: <sup>e</sup>	13.85±0.07	12.26±0.13	19.8 ±0.6	Parallax	13	4
0205293-115930B		DENIS-P J0205.4-1159B				L7: <sup>e</sup>	13.85±0.07	12.26±0.16	19.8 ±0.6	Parallax	14	4
0213288+444445	10102		13.512	0.740	1.269	L1.5	12.15±0.15	10.88±0.16	18.7 ±1.4	ST	1	
0248410-165121	10149	LP 771-21/BR 0246-1703	12.557	0.701	1.148	M8	11.50±0.19	10.36±0.19	16.23±1.42	Parallax	6, 15	3, 4
0251148-035245	10151		13.082	0.821	1.429	L3	12.67±0.20	11.24±0.20	12.1 ±1.1	ST	1, 16	
0255035-470050	10158	DENIS-P J0255-4700	13.225	1.036	1.698	L8	14.77±0.30	13.07±0.30	4.9 ±0.3	ST	17, 18	
0318540-342129	10176		15.530	1.221	2.055	L7	14.45±0.30	12.39±0.31	16.5 ±2.3	ST	18	
0320596+185423	10179	LP 412- 31	11.744	0.701	1.172	M8 <sup>f</sup>	10.93±0.04	9.76 ±0.04	14.51±0.13	Parallax	6, 19	3, 4
0331302-304238	10186	LP 888- 18	11.371	0.672	1.095	M7.5	10.96±0.21	9.87 ±0.21	12.1 ±1.2	ST	1, 6, 9	
0339352-352544	10201	LP 944- 20/ BRI 0337-3535	10.748	0.731	1.223	M9	12.27±0.05	11.05±0.05	4.97±0.10	Parallax	6	5
0340094-672405	10202		14.740	1.172	1.799	L7::	14.45±0.90	12.65±0.90	11.4 ±4.7	ST	10	
0351000-005244 <sup>g</sup>	10213	LHS 1604	11.262	0.670	1.071	M7.5	10.43±0.06 <sup>g</sup>	9.36±0.06	14.66±0.39	Parallax	1, 3, 20	2
0417374-080000	10261		12.166	0.654	1.112	M7.5	10.96±0.21	9.85±0.21	17.4 ±1.7	ST	1	
0423485-041403 <sup>h</sup>	10276	SDSS J0423-0414 <sup>h</sup>	14.452	1.010	1.516	L7: <sup>h</sup>	14.04±0.07	12.45±0.12	15.17±0.39	Parallax	21	6
0429184-312356A	10287		10.887	0.680	1.086	M7.5:	10.96±0.42	9.89±0.32	11.4 ±1.1	ST	1	
0429184-312356B						L1:	12.00±0.29	10.87±0.33	11.4 ±1.1	ST	22, 23	
0435161-160657	10302	LP 775- 31	10.396	0.616	1.060	M7	10.73±0.25	9.67±0.26	8.6 ±1.0	ST	1, 6, 9	
0439010-235308	10312		14.413	1.045	1.606	L6.5	14.24±0.30	12.64±0.30	10.8 ±1.5	ST	1	
0440232-053008	10316	LP 655- 48	10.681	0.696	1.124	M7	10.73±0.25	9.61±0.26	9.8 ±1.1	ST	1, 6, 9	
0443376+000205	10320	SDSS 0443+0002	12.517	0.713	1.350	(M9) <sup>i</sup>	11.47±0.28	10.12±0.28	16.2 ±2.1	ST	16, 24	
0445538-304820	10329		13.409	0.835	1.425	L2	12.31±0.17	10.88±0.17	16.6 ±1.3	ST	1	
0517376-334902	10380	DENIS-P J0517-3349	11.995	0.672	1.176	M8	11.16±0.18	9.98±0.18	14.7 ±1.2	ST	1, 25	
0523382-140302	10390		13.117	0.896	1.486	L2.5	12.48±0.18	11.00±0.19	13.4 ±1.1	ST	1, 16	

Table 9—Continued

2MASS Designation <sup>a</sup>	2MUCD #	Other Names	2MASS <i>J</i>	2MASS <i>J - H</i>	2MASS <i>J - K<sub>S</sub></i>	Optical Sp. Type <sup>b</sup>	<i>M<sub>J</sub></i>	<i>M<sub>K<sub>S</sub></sub></i>	<i>d</i> (pc) <sup>c</sup>	<i>d</i> source <sup>c</sup>	Discovery Refs.	Parallax Refs.
0544115-243301	10444		12.518	0.656	1.079	M8	11.16±0.18	10.08±0.18	18.7 ±1.6	ST	10	
0652307+471034	10601		13.545	1.175	1.858	L4.5	13.32±0.23	11.46±0.24	11.1 ±1.2	ST	1	
0700366+315726A	10617		12.922	0.967	1.614	L3:	12.80±0.06	11.28±0.22	12.20±0.30	Parallax	26	7
0700366+315726B						L6:	14.00±0.06	12.16±0.53	12.20±0.30	Parallax	23	7
0741068+173845	10666	LHS 1937	11.995	0.633	1.026	M7	10.73±0.25	9.71±0.26	17.9 ±2.1	ST	3, 27	
0746425+200032A	10668		11.742	0.743	1.255	L0.5:	11.82±0.03	10.61±0.11	12.21±0.04	Parallax	28	4
0746425+200032B						L2:	12.36±0.04	11.05±0.18	12.21±0.04	Parallax	29	4
0752239+161215	10673	LP 423- 31	10.831	0.639	1.012	M7	10.73±0.25	9.72±0.26	10.5 ±1.2	ST	1, 6	
0818580+233352	10710		12.137	0.635	1.007	M7	10.73±0.25	9.73±0.26	19.1 ±2.2	ST	7	
0825196+211552	10721		15.116	1.328	2.071	L7.5	14.98±0.05	12.91±0.04	10.66±0.11	Parallax	28	4
0835425-081923	10742		13.149	1.195	1.993	L5	13.55±0.24	11.56±0.24	8.3 ±0.9	ST	1	
0847287-153237	10764		13.519	0.892	1.465	L2	12.31±0.17	10.84±0.17	17.5 ±1.4	ST	1	
0853362-032932	10776	LHS 2065	11.185	0.717	1.213	M9	11.51±0.04	10.29±0.04	8.53±0.11	Parallax	3, 30	3, 8
0859254-194926	10789		15.505	1.067	1.778	L7: <sup>j</sup>	14.45±0.50	12.67±0.51	16.3 ±3.8	ST	1	
0908380+503208	10802		14.564	1.098	1.646	L7: <sup>j</sup>	14.45±0.30	12.80±0.30	10.5 ±1.5	ST	1, 31	
1006319-165326	10877	LP 789- 23	12.041	0.620	1.041	M7.5	10.96±0.21	9.92±0.21	16.4 ±1.6	ST	1, 6, 25	
1010148-040649	10880		15.503	1.108	1.908	L7: <sup>j</sup>	14.45±0.30	12.54±0.31	16.2 ±2.3	ST	1	
1016347+275149	10892	LHS 2243	11.951	0.657	1.005	M8	11.16±0.18	10.15±0.18	14.4 ±1.2	ST	3, 19	
1024099+181553	10906		12.242	0.664	1.037	M8	11.16±0.18	10.12±0.18	16.5 ±1.4	ST	7	
1043075+222523	10926		15.947	1.202	1.956	L8	14.77±0.50	12.81±0.51	17.2 ±4.0	ST	10	
1045240-014957	10929	SDSS J1045-0149	13.129	0.759	1.319	L1	12.00±0.14	10.68±0.15	16.8 ±1.1	ST	1, 24, 32	
1058478-154817	10949	DENIS-P J1058-1548	14.184	0.944	1.673	L3	12.99±0.05	11.32±0.05	17.33±0.30	Parallax	13	4
1104012+195921	10954		14.462	0.984	1.486	L4	13.09±0.22	11.61±0.23	18.8 ±2.0	ST	1	
1108307+683017	10960		13.139	0.912	1.539	L0.5	11.86±0.14	10.32±0.14	18.0 ±1.1	ST	7	
1121492-131308A	10980	LHS 2397aA	11.929	0.672	1.206	M8:	11.17±0.06	10.01±0.05	14.45±0.29	Parallax	3, 33	2, 5, 8
1121492-131308B		LHS 2397aB				L7.5:	15.00±0.06	12.78±0.11	14.45±0.29	Parallax	34	2, 5, 8
1124048+380805	10984		12.710	0.682	1.138	M8.5	11.32±0.15	10.18±0.16	19.0 ±1.4	ST	1	
1213033-043243	11044		14.672	0.995	1.669	L5	13.55±0.24	11.89±0.24	16.7 ±1.8	ST	1	
1224522-123835	11068	BR 1222-1221	12.564	0.733	1.193	M9	11.40±0.14	10.21±0.14	17.06±1.11	Parallax	19, 35	5
1246517+314811	11095	LHS 2632	12.255	0.667	1.022	M7.5	10.96±0.21	9.94±0.21	18.1 ±1.8	ST	3, 19, 36	
1253124+403403	11109	LHS 2645	12.177	0.620	1.004	M7.5	10.96±0.21	9.96±0.22	17.5 ±1.7	ST	3, 37	
1300425+191235	11115		12.710	0.641	1.105	L1 <sup>k</sup>	12.00±0.14	10.90±0.15	13.9 ±0.9	ST	7	
1305401-254106A	11122	Kelu-1A	13.417	1.030	1.691	L2:	12.54±0.09	10.84±0.26	18.66±0.70	Parallax	38	4
1305401-254106B		Kelu-1B				L4:	13.17±0.09	11.50±0.52	18.66±0.70	Parallax	39, 40	4

Table 9—Continued

2MASS Designation <sup>a</sup>	2MUCD #	Other Names	2MASS <i>J</i>	2MASS <i>J - H</i>	2MASS <i>J - K<sub>S</sub></i>	Optical Sp. Type <sup>b</sup>	<i>M<sub>J</sub></i>	<i>M<sub>K<sub>S</sub></sub></i>	<i>d</i> (pc) <sup>c</sup>	<i>d</i> source <sup>c</sup>	Discovery Refs.	Parallax Refs.
1309218–233035	11127	CE 303	11.769	0.682	1.103	M8	11.16±0.18	10.05±0.18	13.3 ±1.1	ST	1, 32, 41	
1332244–044112	11153		12.342	0.591	1.046	M7.5	10.96±0.21	9.92±0.21	18.9 ±1.8	ST	1	
1356414+434258	11177	LP 220- 13	11.704	0.673	1.070	M7	10.73±0.25	9.66±0.25	15.6 ±1.8	ST	1, 6	
1403223+300754	11188		12.691	0.683	1.065	M8.5	11.32±0.15	10.25±0.16	18.8 ±1.4	ST	7	
1411213–211950	11194		12.442	0.619	1.122	M9	11.47±0.14	10.34±0.14	15.7 ±1.0	ST	1	
1438082+640836	11224		12.923	0.895	1.350	M9.5	11.60±0.13	10.25±0.14	18.4 ±1.1	ST	1	
1440229+133923	11230	LSPM J1440+1339	12.379	0.635	1.088	M8	11.16±0.18	10.07±0.18	17.6 ±1.5	ST	10, 42	
1456383–280947	11264	LHS 3003	9.957	0.630	1.040	M7	10.83±0.05	9.79±0.05	6.37±0.12	Parallax	3, 19, 43, 44, 45	3, 5
1506544+132106	11291		13.414	1.002	1.666	L3	12.67±0.20	11.01±0.20	14.1 ±1.3	ST	7	
1507277–200043	11294		11.718	0.668	1.064	M7.5	10.96±0.21	9.90±0.21	14.2 ±1.4	ST	1	
1507476–162738	11296		12.822	0.920	1.520	L5	13.50±0.03	11.98±0.03	7.33±0.03	Parallax	29	4
1515009+484739	11314		14.060	0.991	1.495	L6	14.01±0.30	12.53±0.30	10.2 ±1.4	ST	1, 16	
1521010+505323	11323		11.997	0.655	1.075	M7.5	10.96±0.21	9.89±0.21	16.1 ±1.6	ST	1	
1534570–141848	11346		11.390	0.659	1.079	M7	10.73±0.25	9.65±0.26	13.5 ±1.6	ST	10, 33	
1546054+374946	11439		12.437	0.644	1.018	M7.5	10.96±0.21	9.95±0.22	19.7 ±1.9	ST	7	
1658037+702701	11668		13.309	0.766	1.390	L1	11.97±0.04	10.58±0.04	18.55±0.24	Parallax	7	4
1721039+334415	11694		13.584	0.662	1.110	L3 <sup>k</sup>	12.67±0.20	11.56±0.20	15.2 ±1.4	ST	1	
1757154+704201	11735	LP 44-162	11.446	0.604	1.073	M7.5	10.96±0.21	9.89±0.21	12.5 ±1.2	ST	6, 7	
1807159+501531	11756		12.963	0.814	1.356	L1.5	12.15±0.15	10.79±0.16	14.6 ±1.1	ST	1, 16	
1835379+325954	11792	LSR J1835+3259	10.273	0.691	1.119	M8.5	11.51±0.03	10.39±0.04	5.67±0.02	Parallax	46, 47	9
1843221+404021 <sup>m</sup>	11800	LHS 3406	11.299	0.632	1.030	M8 <sup>l</sup>	10.55±0.04	9.52±0.04	14.14±0.16	Parallax	1, 3	8
2002507–052152	11946		15.320	1.093	1.959	L6	14.02±0.30	12.06±0.31	18.2 ±2.6	ST	10	
2037071–113756	12027		12.284	0.665	1.024	M8	11.16±0.18	10.13±0.18	16.8 ±1.4	ST	1	
2057540–025230	12054		13.123	0.850	1.375	L1.5	12.15±0.15	10.77±0.16	15.7 ±1.1	ST	1	
2104149–103736	12059		13.846	0.887	1.491	L2.5	12.48±0.18	10.99±0.19	18.7 ±1.6	ST	1, 18	
2224438–015852	12128		14.052	1.249	2.035	L4.5	13.75±0.04	11.72±0.04	11.35±0.14	Parallax	29	4, 6
2237325+392239	12145	G 216-7B	13.346	0.664	1.192	M9.5	11.96±0.09	10.77±0.09	18.89±0.69	Parallax	48	10
2306292–050227	12171		11.372	0.654	1.084	M8	11.16±0.18	10.07±0.18	11.0 ±0.9	ST	7	
2325453+425148	13227		15.512	1.052	1.705	L8	14.77±0.30	13.06±0.31	14.1 ±2.0	ST	10	
2349489+122438	12217	LP 523- 55	12.615	0.663	1.053	M8	11.16±0.18	10.10±0.18	19.6 ±1.6	ST	6, 7	
2351504–253736	12220		12.458	0.731	1.170	M8	11.16±0.18	9.99±0.18	18.2 ±1.5	ST	10	

<sup>a</sup>The 2MASS designation is 2MASS Jhhmmss[.]s±ddmmss.<sup>b</sup>A single or double colon indicates an uncertainty on the spectral type of ±1 or ±2 types respectively due to a low signal-to-noise spectrum. A single colon is also used

to indicate uncertainty on the spectral type of individual objects in multiple systems where resolved spectroscopy has not been obtained.

<sup>c</sup>Distance are spectrophotometric ( $d_{\text{source}} = ST$ ) except where a trigonometric parallax is available ( $d_{\text{source}} = \text{Parallax}$ ).

<sup>d</sup>Henry et al. (1999) reported the possible existence of a fourth component, LHS 1070D, at a separation of 50 mas; further observations have shown the original apparent detection to be spurious (T. Henry 2006, priv. comm.).

<sup>e</sup>Bouy et al. (2005) report a T dwarf as a possible third component to the system. The T dwarf is not included in the luminosity function estimate.

<sup>f</sup>Variable and/or flaring object that will be discussed in detail in Schmidt et al. (2006, in prep.).

<sup>g</sup>The absolute magnitude for this object, based on a trigonometric parallax, is brighter than our brightest  $M_J$  bin and is not included in our space density per magnitude analysis. However, it is included in our estimates of the total space densities of ultracool dwarfs. It is also a suspected unresolved binary as discussed in § 5.6.

<sup>h</sup>This object has been resolved into an L/T binary by Burgasser et al. (2005b). The T dwarf is not included in the luminosity function estimate.

<sup>i</sup>This object displays features of low gravity and a spectral type of M9: was used to estimate  $M_J$ .

<sup>j</sup>Change in spectral type from Paper V.

<sup>k</sup>Suspected low-metallicity dwarf as discussed in § 5.4.

<sup>l</sup>Suspected unresolved binary as discussed in § 5.6.

References. — Discovery: (1) Paper V; (2) Irwin et al. (1991); (3) Luyten (1979a, LHS); (4) Leinert et al. (1994); (5) Leinert et al. (2000), Ratzka et al., in prep.; (6) Luyten (1979b, NLTT); (7) Gizis et al. (2000); (8) Forveille et al. (2005); (9) Cruz et al. (2003, Paper III); (10) This Paper; (11) Kendall et al. (2003); (12) Liebert et al. (2003); (13) Delfosse et al. (1997); (14) Koerner et al. (1999); (15) Kirkpatrick et al. (1997); (16) Wilson (2002); (17) Martín et al. (1999); (18) Kirkpatrick et al., in prep.; (19) Kirkpatrick et al. (1995); (20) Reid et al. (1995); (21) Schneider et al. (2002); (22) Siegler et al. (2005); (23) Reid et al. (2006b); (24) Hawley et al. (2002); (25) Phan-Bao et al. (2003); (26) Thorstensen & Kirkpatrick (2003); (27) Gizis & Reid (1997); (28) Kirkpatrick et al. (2000); (29) Reid et al. (2001); (30) Hawkins & Bessell (1988); (31) Knapp et al. (2004); (32) Gizis (2002); (33) Liebert et al. (1984); (34) Freed et al. (2003); (35) Tinney et al. (1993); (36) Hartwick et al. (1984); (37) Kirkpatrick et al. (1991); (38) Ruiz et al. (1997); (39) Liu & Leggett (2005); (40) Gelino et al. (2006); (41) Ruiz et al. (2001); (42) Lépine (2005); (43) Bessell (1991); (44) Hartwick et al. (1984); (45) Ruiz et al. (1990); (46) Reid et al. (2003b, Paper IV); (47) Lépine et al. (2003b); (48) Kirkpatrick et al. (2001b).

References. — Parallax: (1) Tinney et al. (1995); (2) van Altena et al. (1995); (3) Costa et al. (2005); (4) Dahn et al. (2002); (5) Tinney (1996); (6) Vrba et al. (2004); (7) Thorstensen & Kirkpatrick (2003); (8) Monet et al. (1992); (9) Reid et al. (2003b, Paper4); (10) Perryman & ESA (1997, Hipparcos).

Table 10. Objects with distance estimates within  $1\sigma$  of 20 parsecs

2MASS Designation <sup>a</sup>	2MUCD #	Other Names	2MASS $J$	2MASS $J - H$	2MASS $J - K_S$	Optical Sp. Type <sup>b</sup>	$M_J$	$d$ (pc) <sup>c</sup>	d source <sup>c</sup>	Refs.
0050244-153818	10045	SIPS 0050-1538	13.765	0.673	1.126	L1	12.00±0.29	22.5±3.0	ST	1, 2
0120491-074103	10076		12.976	0.684	1.122	M8	11.16±0.35	23.1±3.8	ST	3
0131183+380155	13061		14.694	1.022	1.666	L4	13.09±0.44	20.9±4.3	ST	2
0240295+283257	10138		12.679	0.701	1.103	M7.5	10.96±0.21	22.0±2.2	ST	4
0314401-045031	10172		12.656	0.653	1.035	M7.5	10.96±0.21	21.8±2.1	ST	3
0428509-225322	10286		13.579	0.882	1.459	L1	12.00±0.14	20.7±1.4	ST	5
0614528+453655	10529		13.003	0.755	1.234	M9	11.47±0.14	20.3±1.3	ST	3
0810586+142039	10699		12.714	0.669	1.104	M8	11.16±0.18	20.5±1.7	ST	3
0850017-192418	10768		12.816	0.682	1.189	M8	11.16±0.18	21.5±1.8	ST	3
0952219-192431B	10855		11.877	0.595	1.031	M7:	10.73±0.50	25.6±7.2	ST	3, 4, 6
1003191-010507	10873	LHS 5165/DENIS-P J1003-0105	12.352	0.667	1.085	M7	10.73±0.25	21.1±2.5	ST	7, 8, 9
1017075+130839	10893		14.111	0.879	1.435	L2	12.31±0.34	22.9±3.6	ST	3
1019568+732408	10900		12.884	0.637	1.100	M8.5	11.32±0.15	20.6±1.5	ST	3
1141440-223215	11005		12.651	0.657	1.090	M7.5	10.96±0.21	21.8±2.1	ST	3
1152426+243807	11018		13.033	0.766	1.286	M9	11.47±0.14	20.6±1.4	ST	3
1228152-154734A	11073	DENIS-P J1228.2-1547A	14.375	1.012	1.570	L5:	13.60±0.10	20.2±0.8	Parallax	10, 11
1228152-154734B	11073	DENIS-P J1228.2-1547B				L5:	13.60±0.10	20.2±0.8	Parallax	12, 13
1326298-003831	11143	SDSS 1326-0038	16.110	1.066	1.879	L8:	14.60±0.29	20.0±2.5	Parallax	14, 15, 16
1448033+155414	11248	LHS 2980	12.481	0.629	1.010	M7	10.73±0.25	22.4±2.6	ST	17
1553199+140033	11462		13.019	0.750	1.172	M9	11.47±0.14	20.5±1.3	ST	4
1627279+810507	11595		13.042	0.709	1.168	M9	11.47±0.14	20.7±1.4	ST	4
1733189+463359	11712		13.214	0.806	1.357	M9.5	11.60±0.13	21.0±1.3	ST	4
1847034+552243A	11803		11.919	0.641	1.021	M7:	10.73±0.50	23.2±5.4	ST	3
1847034+552243B	11803		11.919	0.641	1.021	M7.5:	10.96±0.42	23.2±5.4	ST	18
2014035-201621	11977		12.527	0.664	1.092	M7.5	10.96±0.21	20.5±2.0	ST	3
2132114+134158	13177		15.785	1.201	1.951	L6	14.02±0.30	22.5±3.2	ST	2
2158045-155009	12101		14.949	1.033	1.801	L4:	13.09±0.44	23.5±4.8	ST	2, 19
2234139+235955	12139		13.176	0.823	1.341	M9.5	11.60±0.13	20.7±1.3	ST	4
2235490+184029	12142	LP 460- 44	12.458	0.632	1.125	M7	10.73±0.25	22.1±2.6	ST	4, 20
2331016-040619A	12191		12.937	0.648	1.007	M8:	11.16±0.35	23.3±3.8	ST	4
2331016-040619B	12191					L7:	14.45±0.50	23.3±3.8	ST	21, 22
2334394+193304	12194		12.769	0.695	1.128	M8	11.16±0.18	21.0±1.8	ST	4
2344062-073328	12212		14.850	0.985	1.621	L4.5	13.32±0.23	20.2±2.2	ST	2

<sup>a</sup>The 2MASS designation is 2MASSI Jhhmmss[.]s±ddmmss.

<sup>b</sup>A single or double colon indicates an uncertainty on the spectral type of  $\pm 1$  or  $\pm 2$  types respectively due to a low signal-to-noise spectrum. A single colon is also used to indicate uncertainty on the spectral type of individual objects in multiple systems where resolved spectroscopy has not been obtained.

<sup>c</sup>Distance are spectrophotometric (d source = ST) except where a trigonometric parallax is available (d source = Parallax).

References. — (1) Deacon et al. (2005); (2) This Paper; (3) Paper V; (4) Gizis et al. (2000); (5) Kendall et al. (2003); (6) Reid et al. (2002c); (7) Luyten (1979a); (8) Phan-Bao et al. (2001); (9) Gizis (2002); (10) Delfosse et al. (1997); (11) Dahn et al. (2002); (12) Koerner et al. (1999); (13) Martin et al. (1999); (14) Fan et al. (2000); (15) Geballe et al. (2002); (16) Vrba et al. (2004); (17) Kirkpatrick (1992); (18) Siegler et al. (2005); (19) Kirkpatrick et al., in prep.; (20) Luyten (1979b); (21) Close et al. (2002); (22) Close et al. (2003).

Table 11. The 20-pc Ultracool Dwarf  $J$ - and  $K_S$ -band Luminosity Functions

$M_J$	$N_{tot}$	$\rho_{tot}$ ( $10^{-3}$ dwarfs $\text{pc}^{-3}$ )	$M_{K_S}$	$N_{tot}$	$\rho_{tot}$ ( $10^{-3}$ dwarfs $\text{pc}^{-3}$ )
10.75	28.7 <sup>a</sup>	$2.38 \pm 0.64^a$	9.75	30.7 <sup>a</sup>	$2.55 \pm 0.41^a$
11.25	20	$1.66 \pm 0.37$	10.25	25	$2.07 \pm 0.41$
11.75	14	$1.16 \pm 0.31$	10.75	17	$1.41 \pm 0.34$
12.25	10	$0.83 \pm 0.26$	11.25	7	$0.58 \pm 0.22$
12.75	6	$0.50 \pm 0.20$	11.75	9	$0.75 \pm 0.25$
13.25	7	$0.58 \pm 0.22$	12.25	9	$0.75 \pm 0.25$
13.75	6	$0.50 \pm 0.20$	12.75	6	$>0.50 \pm 0.20$
14.25	8	$>0.66 \pm 0.23$			
14.75	4	$>0.33 \pm 0.17$			

Note. — Values for the space densities plotted in Figure 16. The absolute magnitudes listed are the center of 0.5 magnitude wide bin.

<sup>a</sup>Corrected value as discussed in § 6.2.2.



Table 12. The 8-pc  $J$ -band Luminosity Function

$M_J$	$N_{sys}$	$N_{sec}$	$\rho_{sys}$ ( $10^{-3}$ dwarfs $\text{pc}^{-3}$ )	$\rho_{tot}$ ( $10^{-3}$ dwarfs $\text{pc}^{-3}$ )
(1)	(2)	(3)	(4)	(5)
0.75	1	0	0.62	0.62
1.25	1	0	0.62	0.62
1.75	3	0	1.87	1.87
2.25	0	0	...	...
2.75	0	0	...	...
3.25	1	0	0.62	0.62
3.75	2	0	1.24	1.24
4.25	6	1	3.73	4.35
4.75	6	0	3.73	3.73
5.25	3	1	1.87	2.49
5.75	3	5	1.87	4.97
6.25	6	0	3.73	3.73
6.75	5	0	3.11	3.11
7.25	15	4	9.33	11.81
7.75	10	4	6.22	8.70
8.25	12	4	7.46	9.95
8.75	6	2	3.73	4.97
9.25	11	2	5.60	6.84
9.75	6	5	3.11	6.22
10.25	3	5	1.87	4.97
10.75	3	2	1.87	3.11
11.25	1	2	0.62	1.87

Note. — Column 2 lists the number of systems (single stars and primaries) and column 3 gives the number of secondary components; column 4 lists the corresponding system space density, and column 5 lists the total space density, including the contribution

from secondaries. The resulting  $\Phi(M_J)$  (total space density) is shown in Figure 17.